THE POTENTIAL OF MUSCLE-DERIVED PROGENITORS ON TITANIUM SCAFFOLDS IN BONE REGENERATIVE APPLICATIONS

A thesis submitted by

Karin Helena Carlqvist

For the degree of Doctor of Philosophy to

University College London

2011

Division of Biomaterial and Tissue Engineering

Department of UCL Eastman Dental Institute

Faculty of Biomedical Science

University College London

STATEMENT

I, Karin Helena Carlqvist confirm that the work presented in this thesis is my own. Where information has been derived from other sources, I confirm that this has been indicated in the thesis.

ABSTRACT

Muscle-derived cells (MDCs) are a heterogeneous population consisting of cells that can undergo myogenic differentiation; however, it has emerged that not all MDCs are restricted to the myogenic lineage. This discovery may have many implications; for example, MDCs may be a suitable alternative source of osteogenic cells for bone repair. The currently accepted treatment for bone repair, bone grafting, is often associated with small amount of obtainable bone. Much of the work published regarding the differential potential of MDCs has not, to date, focused on the osteogenic pathway and even fewer studies have been performed on human cells. In this thesis osteogenic MDCs were isolated by differential adhesion to fibronectin (Fn) *i.e.* MDCsFn and compared with mesenchymal stem cells (MSCs) in relation to their osteogenic potential. The osteogenic potential was assessed by measuring mineralization and relevant gene- and protein- expression. MSCs and MDCsFn had a similar pattern of ALP activity and expression. Furthermore, MSCs and MDCsFn both showed mineralization after 3 weeks measured by Alizarin Red S. A qPCR Array measuring the activity of 46 osteogenic genes also showed similarities in gene expression between the two cell types; however, the MSCs showed a more consistent pattern between patients, compared to MDCsFn. Titanium (Ti) has previously been used as a bone repair scaffold in humans due to its osteoconductivity. The interaction between Ti, of various roughness and hydrophilicity, and the two cell types, *i.e.* MSCs and MDCsFn, were assessed with relation to biocompatibility. Interestingly, the hydrophilic, rough surface, which has been described as superior in bone formation applications, showed higher levels of cell death, both apoptosis and necrosis, compared to the other tested surfaces for both cell types. In conclusion, due to the similarities between MDCsFn and MSCs there might be possibilities to use the osteogenic fraction in future bone regenerative applications.

TABLE OF CONTENT

LIST OF FIGURES

CHAPTER 1

CHAPTER 2

CHAPTER 3

CHAPTER 4

CHAPTER 5

CHAPTER 6

CHAPTER 7

No figures in chapter 7.

CHAPTER 8

No figures in chapter 8.

CHAPTER 9

No figures in chapter 9.

LIST OF TABLES

CHAPTER 1

CHAPTER 2

CHAPTER 3

CHAPTER 4

CHAPTER 5

CHAPTER 6

CHAPTER 7

CHAPTER 8

No tables in chapter 8.

CHAPTER 9

LIST OF ABBREVIATIONS

ABBREVIATION	FULL LENGTH
ALP	Alkaline phoshatase
AMBN	Ameloblastin enamel matrix protein
AMELY	Amelogenin Y-chromosomal
α-MEM	Minimum Essential Medium Alpha Medium
ARSE	Arylsulfatase E
ASCs	Adipogenic stem cells
β-GP	β-glycerophosphate
BMP1	Bone morphogenic protein 1
BMP2	Bone morphogenic protein 2
BMP4	Bone morphogenic protein 4
BMP7	Bone morphogenic protein 7
BMPs	Bone morphogenic proteins
BMPR-1	Bone morphogenic protein receptor 1
BMPR-II	Bone morphogenic protein receptor 2
BSP	Bone sialoprotein
BTE	Division of biomaterial and tissue engineering
Ca2+	Calcium ion
CALCR	Calcitonin receptor
CASR	Calcium-sensing receptor
CDH11	Cadherin-11
CI	Confidence interval
COL1A1	Collagen, type 1 α 1
COL1A2	Collagen, type 1 α 2
COMP	Cartilage oligomeric matrix protein
DAPI	4, 6-diamidino-2-phenylindole
Dex	Dexamethasone
DMEM	Dulbecco’s modified Eagle's minimal essential medium

DMP1	Dentin matrix acidic phosphoprotein 1
DSPP	Dentin sialophosphoprotein
ECM	Extracellular matrix
EDTA	Ethylenediaminetetraacetic acid
EDI	Eastman dental institute
EtOH	Ethanol
FBS	Fetal bovine serum
FGFR1	Fibroblast growth factor receptor 1
FGFR2	Fibroblast growth factor receptor 2
FGFR3	Fibroblast growth factor receptor 3
FITC	Fluorescein isothiocyanate
FLT1	Fms-related tyrosine kinase
Fn	Fibronectin
GAPDH	Glyceraldehyde-3-phosphate dehydrogenase
GDF10	Growth differentiation factor 10
Gel	Gelatin
HCl	Hydrogen chloride
HSC	Hematopoietic stem cells
IGF-1	Insulin-like growth factor 1
MACS	Magnetic-activated cell sorting
MDCs	Muscle-derived cells
MDCsFn	Muscle-derived cells adherent to fibronectin within 20 min
MDCsGel	Muscle-derived cells adherent to gelatin within 20 min
MDCsPP	Parental population of muscle-derived cells i.e. MDCs
MDCsTCP	Muscle-derived cells adherent to tissue culture plastic within 20 min
MDSCs	Muscle-derived stem cells
MeOH	Methanol
MMPs	Matrix metalloproteinase groups
MMP13	Matrix metalloproteinase 13
MMP2	Matrix metalloproteinase 2
MPCs	Muscle precursor cells

MRF4	Muscle regulatory factor 4
MSCs	Mesenchymal stem cells
MSX1	Muscle segment homeobox 1
MTT	3-(4,5-Dimethylthiazol-2-yl)-2,5-diphenyltetrazolium bromide
Myf	Myogenic factor family
Myf5	Myogenic factor 5
MyoD	Myogenic differentiation antigen 1
N	Number of patients used in an experiment
NaN3	Sodium azide
NaOH	Sodium hydroxide
OP	Osteopontin
Pax7	Paired box transcription factor 7
PBS	Phosphate-buffered saline
PCM	Phase contrast microscopy
PCR	Polymerase chain reaction
PD	Population doubling
PFA	Paraformaldehyde
PI	Propidium iodide
PICs	$PW1^{+}/Pax7^{-}$ interstitial cells
p-NPP	p-nitrophenyl phosphate
PPAR-γ2	Peroxisome proliferator-activated receptors-γ2
P/S	Penicillin Streptomycin
PTH	Parathyroid hormone
PTH1R	Parathyroid hormone receptor 1
Q-PCR	Quantitative polymerase chain reaction
Ra	Surface roughness
R-PE	R-Phycoerythrin
Runx2	Runt-related transcription factor 2
Std	Standard deviation
SDS	Sodium dodecyl sulfate
Sem	Standard error of the mean

SIBLING	Small integrin binding ligand N-linked glycoprotein
SLA	Sand acid treated hydrophobic titanium surface
SLActive	Hydrophilic SLA surface
Smad1	Sma- and mad-related protein 1
Smad2	Sma- and mad-related protein 2
Smad3	Sma- and mad-related protein 3
Smad4	Sma- and mad-related protein 4
Smad7	Sma- and mad-related protein 7
Smad9	Sma- and mad-related protein 8
SMO	Smooth titanium surface
SOX9	Sry-box 9
SPARC	Secreted protein, acidic, cysteine-rich
Sd	Standard deviation
TCP	Tissue culture plastic
TGFBR1	Transforming growth factor-β receptor, type 1
TGFBR2	Transforming growth factor-β receptor, type 2
TGFβ1	Transforming growth factor-β 1
TGFβ3	Transforming growth factor-β 3
Ti	Titanium
Tris	tris(hydroxymethyl)aminomethane
Trypsin	Trypsin-ethylenediaminetetraacetic acid solution
TUFT1	Tuftelin
VDR	Vitamin D receptor
VEGF	Vascular endothelial growth factor
VEGFA	Vascular endothelial growth factor A
VEGFB	Vascular endothelial growth factor B
WNT5A	Wingless-type MMTV integration site family member 5a

PUBLICATIONS

Carlqvist KH, Lewis MP, Hunt NP, Shah R, 2010, Regeneration of jaw muscle-potential cellular mechanisms, Seminars in Orthodontics, 16(2):147-152

Wall I, Donos N, Carlqvist K, Jones F, Brett P, 2009, Modified titanium surfaces promote accelerated osteogenic differentiation of mesenchymal stromal cells *in vitro*, Bone 45(1):17-26

Carlqvist KH, Brett PM, Shah R, Lewis MP, A novel and rapid method to isolate human muscle-derived subpopulation with osteogenic potential, *In preparation*

Carlqvist KH, Lewis MP, Brett PM, "A comparison study of the osteogenic potential of human mesenchymal stromal cells and human muscle-derived cells, *In preparation*

PUBLISHED ABSTRACTS AND/OR CONFERENCE TALKS

Carlqvist K, Brett P, Lewis MP, 2009, Novel and rapid method to isolate human muscle-derived subpopulations, TCES, Glasgow, UK

Carlqvist K, Brett P, Lewis MP, Craniofacial MDPCs could be used in clinical bone regeneration applications, 2008, PEF-IADR, Journal of Dental Research, 87:1, London, UK

Carlqvist K, Al-qahtani K, Sinanan ACM, Aggrewal S, Mudera V, Lewis MP, 2008 Craniofacial Muscle Derived Stem Cells, Symposium PEF-IADR, London, UK

Lewis MP, Smith A, Shah R, Al-qahtani K, Carlqvist K, Sinanan AC, Mudera V, 2009, A little bit of this and a little bit of that! 3D tissue engineered skeletal muscle-Generating basic mechanisms in maintenance and turnover, Comparative Biochemistry and Physiology A- Molecular & Integrative Physiology 153(2):73

TITLE OF POSTER PRESENTATIONS

Carlqvist K, Shah R, Lewis MP, Brett PM, 2010, Masseter Muscle-derived Stem Cell Behaviour on Ti Implant Surfaces, PEF-IADR, Barcelona, Spain

Carlqvist K, Brett P, Lewis MP, 2009, Isolating various muscle-derived subpopulations by adhesion to substrate, NC3Rs conference, London, UK

Carlqvist K, Lewis MP, Brett PM, 2009, The impact of various titanium surfaces on mesenchymal stem cells, 3rd UK Mesenchymal Stem Cell Meeting, Sheffield, UK

Carlqvist K, Sinanan A, Shah R, Lewis MP, Brett PM, 2008, Human craniofacial MDPC might be an alternative to MSC for bone regeneration on titanium implants, EASTMAN 60, London, UK

Carlqvist K, Sinanan A, Shah R, Lewis MP, Brett PM, 2007, A comparison of the differential potential between mesenchymal stem cells and muscle derived precursor cells, UCL STEM CELL DAY, London, UK

ACKNOWLEDGEMENT

There are many people I would like to acknowledge in this section. First of all I would like to thank my supervisors Dr Peter Brett and Professor Mark Lewis for their support and guidance during these years. I am very grateful for all their time and the dedication they have shown. I also want to thank my sponsors, EPSRC, EFFORT and Straumann AG, for funding this project.

I have really enjoyed the time in the division of Biomaterial and Tissue Engineering and I would like to thank all staff and students, past and present, especially Dr Rishma Shah, Dr Batool Kazmi, Dr Kris Gellynck, (very, very soon-to be Dr) Hayley Mulhall and (one day you will become a Dr) Alec Smith. Thank you for all the bright and happy memories.

I also would like to acknowledge Aviva Petrie and Allan Hackshaw for their assistance with the statistical analysis and Dr Nicky Mordan for her assistance with the microscopy.

Finally, I would like to thank my family for supporting my decision to do a PhD and their faith in me.

DEDICATION

This thesis is dedicated to you, Jim, for always being by my side. This is a thank you for all meals you have cooked, all plates you have washed, for all the cleaning you have done during these years, but most importantly, it is for all love and trust you have in me. Thank you!

&

To our son, Aaron, who literally, always has been with me whilst I have been writing this thesis.

CHAPTER 1:

INTRODUCTION

1.1 TISSUE ENGINEERING

Tissue engineering is a form of regenerative medicine where the focus is on using both living cells and biomaterial together to engineer new tissue to restore or improve lost or damaged biological function. Much focus has been on the use of stem cells to achieve this desired goal (Corsi *et al*, 2007). By using stem cells, tissues have been synthesized *in vitro* or in bioreactors where matrices, synthetic or natural, were used to produce precisely shaped constructs to replace diseased or damaged tissue (Schonmeyr *et al*, 2010). There have been attempts to engineer a variety of tissues; for example, breast tissue has been engineered from human epithelial and pre-adipocyte cells derived from breast biopsies (Huss & Kratz, 2000).

Scaffolds are considered to be important if not essential in tissue engineering, especially in orthopaedic applications (Corsi *et al*, 2007). For example, Alhadlaq and Mao (2005) used polyethylene glycol-based hydrogel to engineer an articular condyle of MSCs in the shape and dimensions of the adult human mandibular bone. To achieve the desired outcome they added 15 million pre-differentiated cells to the gel and left them for a 12-week long incubation time *in vivo*.

When stem cells are used in the tissue engineering process, it is generally accepted that before introducing the cells into patients they need to be differentiated into the desired lineage. There are concerns that clinical use of undifferentiated stem cells may lead to a situation of uncontrolled proliferation *i.e.* cancer (Abdullah & Kassem, 2008). The great advantage of using adult stem cells in tissue engineering applications is that it is easier to expand MSCs and other adult stem cells, than mature cell types *e.g.* osteoblasts (Alhadlaq & Mao, 2005)

1.1.1 STEM CELLS

In general stem cells are divided into two groups; embryonic and adult stem cells. Embryonic stem cells are reported to have unlimited self-renewal capacity, but there are ethical concerns regarding the sourcing and use of these cells. There are no ethical concerns regarding the usage of adult stem cells; however, they have limited differential potential and self-renewal *in vitro*, so the amount of stem cells that can be cultured sometimes limits their clinical usage especially in the repair of larger defects (Davis & zur Nieden, 2008).

1.1.2 BONE ENGINEERING

Scaffolds will most likely play a central role in the development of engineered orthopaedic applications. One promising biomaterial for the scaffold is Ti; Warnke *et al* (2004) used a Ti scaffold to engineer a new mandible for a patient who had his jaw removed due to a tumour. In this case they used the patient's own body as a bioreactor and used his blood vessels to create a natural bone environment. After 7 weeks they detected active osteoblasts within the scaffold.

It is considered that one of the major challenges facing the bone engineering field is to combine the knowledge in material science, tissue engineering and biology. Knowledge in these areas are important to design implant surfaces providing biological signals to cells that favour bone healing and osseointegration (Ellingsen *et al*, 2000). In order to achieve this it is especially important to study the interaction of implant surfaces and precursor cells with bone forming capacity, such as MSCs since bone marrow-derived MSCs are believed to be the cells that migrate on implant *in vivo*, not committed osteoblasts (Schwartz *et al*, 1999).

1.1.3 ALLOGENEIC OR AUTOLOGOUS TRANSPLANTATION

In autologous transplantation the donor and the recipient is the same person and in allogeneic transplantation the donor and the recipient are two separate people. Both allogeneic and autologous bone marrow transplantations are performed on patients regularly (Chinen & Buckley, 2010); however, autografts are considered to be the safer option, since it has a minimised risk of rejection (Thibodeau & Patton, 2007). Another advantage of using autografts, it is that autografts, but not allografts, are considered osteoinductive *i.e.* are able to drive cells along the osteogenic lineage (Khan *et al*, 2005). However, even if autografts are considered the preferable alternative in terms of efficiency and safety, there are problems associated with this technique. Harvest of the autograft can result in donor site pain and often the grafted amount is not sufficient for the desired clinical application (Korda *et al*, 2009).

1.1.4 DEFINITION OF STEM CELL AND OSTEOGENIC TERMINOLOGY

Various research groups are using slightly different stem cell terminology (Collins *et al*, 2005; Sinanan *et al*, 2006). In this section following stem cell and osteogenic terminology has been defined (Table 1.1; Table 1.2).

Table 1.1 Stem cell terminology

TERM	DEFINITION
Totipotent	-Cells that can differentiate into any cell type.
Pluripotent	-Cells that can differentiate along lineages belonging to different germ layers.
Multipotent	-Cells that can differentiate along various lineages within the same germ layer.

Table 1.2. Osteogenic terminology

TERM	DEFINITION
Endochondral ossification	-The formation of bone in which a bone matrix gradually replaces a cartilage template. This is the bone formation process of long bones *e.g.* arm or leg bones.
Intramembraneous ossification	-The formation of bone without using a cartilage template. This is the bone formation process of flat bones *e.g.* skull bones.
Osseoconductivity	-A passive process where a scaffold or a matrix facilitate bone growth.
Osseoinductivity	-An active process where bone formation is induced.
Osseointegration	-Creation of a structural and functional connection between living bone and a loading surface.

1.2 BONE

Bone tissue might be the most distinctive form of connective tissue in the body, since its extracellular matrix (ECM) is calcified and therefore hard (Thibodeau & Patton, 2007). The ECM of the bone is much more abundant than the cells and can be subdivided into inorganic salts and organic matrix (Thibodeau & Patton, 2007). The adult human skeleton is comprised of 213 bones (Dempster, 2006) and its principal role is to provide structural support for the body (Sommerfeldt & Rubin, 2001); nevertheless, it also serves as the mineral reservoir of the body. The mineral, often referred to as hydroxyapatite, $Ca_{10}(PO_4)_6(OH)_2$, is the basis of the skeleton; it resists loads caused by the body, protects internal organs and opposes muscle contraction that results in motion (Sommerfeldt & Rubin, 2001).

Bone can, in general, be divided into two types; long bone, *e.g.* femur and tibia, or flat bone, *e.g.* skull and mandible (Dempster, 2006). Both bone types consist of both compact and spongy bone. Spongy bone is mainly located in the edges of the long bone but also in the wall surrounding the medullary cavity. In long bone the compact bone is located in the part between the spongy bones (Figure 1.1).

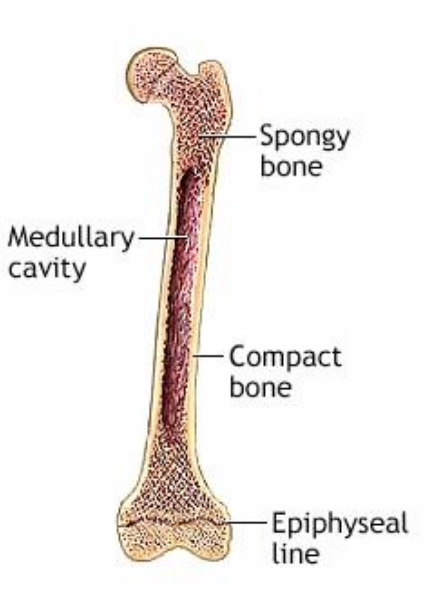

Figure 1.1. Long bone with medullary cavity. The bone marrow resides in the medullary cavity**.** Long bones have most of their spongy bone in the ends and compact bone in the middle surrounding the medullary cavity; however, the walls around the medullary cavity also consist of spongy bone. The epiphyseal line is the remaining of an area of growth in childhood where the bones lengthen. Adapted picture from www.nlm.nih.gov

Compact bone is built up by osteons or haversian system that contains nerves-, blood- and lymphatic- vessels (Thibodeau & Patton, 2007). Terminally differentiated bone cells, *i.e.* osteocytes, are located in lacunae, which are arranged in concentric layers of bone matrix called lamellae. Each lacuna, with its osteocytes is supplied with nutrient by blood vessels or canaliculi from the haversian canal; the haversian canals are connected to each other by Volkmann's canals. Around the bone tissue, apart from around the joints, there is a dense, white fibrous membrane called the periosteum (Figure 1.2; Thibodeau & Patton, 2007).

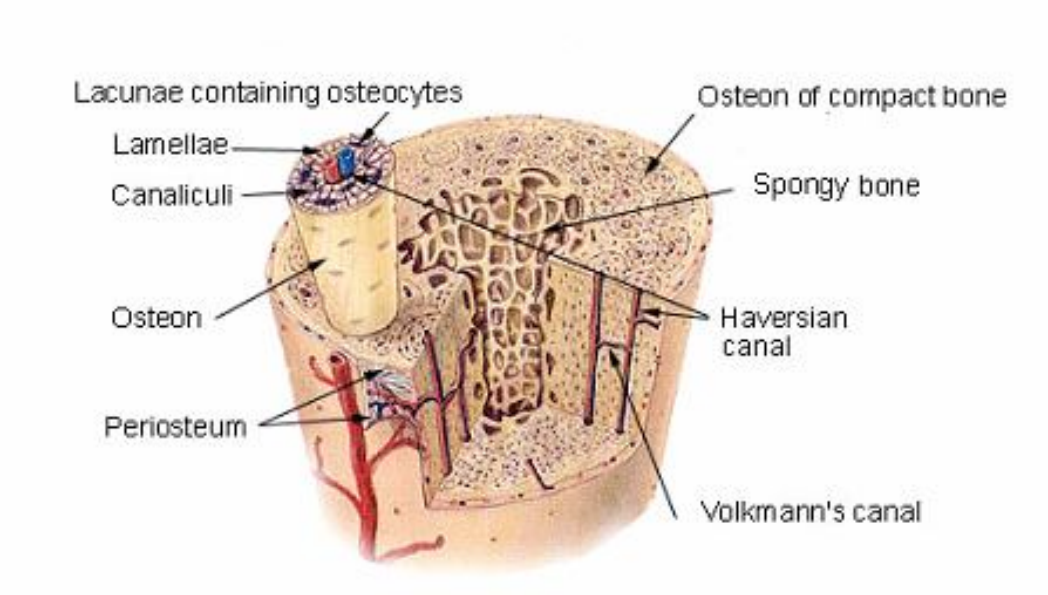

Figure 1.2. Bone structure. Bone consists of compact and spongy bone. The compact bone is built up by osteons or haversian system that contains nerve-, blood- and lymphatic- vessels. The osteocytes are located in the lacunae, which forms the lamellae. Canaliculi supply each lacuna with nutrients via the blood vessels from haversian canal that are connected to each other by Volkmann's canals. The periosteum is the white fibrous membrane that covers the bone (Thibodeau & Patton, 2007). Adapted picture from http://training.seer.cancer.gov/index.html

There are three major bone cell types; osteoblast, osteocytes and osteoclasts that are all involved in the remodelling process of bone (Dempster, 2006; Thibodeau & Patton, 2007). Osteoblasts, which build up bone and can be either active or inactive, are derived from MSCs. The inactive osteoblasts are called bone lining cells and these have a more

flattened morphology than (active) osteoblasts. Osteoblasts (active) have a cuboidal morphology, where their nucleus is towards the upper part of the cell and their protein synthetic apparatus towards the extra cellular matrix (Figure 1.3). They synthesise and secrete a specialised organic matrix, osteoid, where collagen fibrils line up in regular arrays. The osteoid serves as a framework for the deposition of calcium and phosphate *i.e.* mineralised bone (Thibodeau & Patton, 2007). Osteoblasts will eventually be trapped in their own mineralization, which will differentiate them into non-dividing terminally differentiated osteocytes (Schwartz *et al*, 1999; Thibodeau & Patton, 2007). Osteoclasts, which are the third type of bone cells, are derived from haematopoietic stem cells (HSCs); their main function is to direct the new bone formation by degrading the old mineral matrix (Schwartz *et al,* 1999).

1.2.1 BONE MARROW

Bone marrow is a specialized type of soft connective tissue also called myeloid tissue. It serves as the site for production of blood cells and is located in the medullary cavities or in the spongy part of certain long and flat bones (Figure 1.1; Thibodeau & Patton, 2007). There are two types of bone marrow; red bone marrow, which produces red blood cells, and yellow bone marrow, where the cells have become saturated with fat and are inactive in blood cell production (Thibodeau & Patton, 2007). Infants have only red bone marrow, but with age the red bone marrow transforms to yellow; however, there are several bones in an adult that still contain red marrow including ribs, pelvis, femur and thigh bone (Thibodeau & Patton, 2007) and it is from these bones the bone marrow is aspirated for bone marrow donations.

Most types of blood cells in adult mammals are generated in the bone marrow (Thibodeau & Patton, 2007), but there are many other cell types that reside within the bone marrow, such as stromal cells (Alberts *et al*, 2002). Bone marrow stroma includes MSCs, endothelial cells, osteoblasts and adipocytes (Tokoyoda *et al*, 2010). The

different types of cells and their precursors are intermingled with one-another, which produce a supporting meshwork of ECM components (Thibodeau & Patton, 2007).
At bone trauma, there is immediately vascular damage and subsequently hematoma due to the blood vessels located in the bone. The fracture hematoma develops a fibrin mesh and transforms into a soft mass of granulation tissue containing inflammatory cells, fibroblast, bone- and cartilage-forming cells, *i.e.* MSCs. Procallus, an early form of cartilage tissue, anchor the ends of the fractured bone together. Osteoblasts derived from MSCs continue the healing process with formation of calcified tissue. (Thibodeau & Patton, 2007).

1.2.2 GENETIC COORDINATION OF OSTEOGENIC DIFFERENTIATION

The osteogenic differentiation of MSCs is characterized by cell proliferation, differentiation and production of a specific ECM (Figure 1.3). The osteogenic ECM can be divided in two parts, an organic part, which is composed of mostly type 1 collagen and bone matrix proteins, and an inorganic part *i.e.* hydroxyapatite (Marie & Fromigue, 2006). The osteogenic differentiation of human MSCs can be initiated by dexamethasone (dex), L-ascorbic acid and inorganic phosphate (Muraglia *et al*, 2000; Marie & Fromigue, 2006). During the osteogenic differentiation several genes are sequentially upregulated *in vitro*, such as Alkaline phosphatase (ALP), Collagen 1α1 (Col1A1), Osteopontin (OP) and Bone sialoprotein (BSP; Marie & Fromigue, 2006).

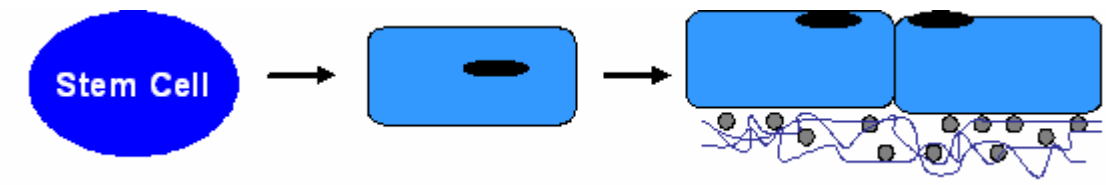

Figure 1.3. Osteogenic differentiation. Stem cells differentiate into osteogenic precursor cell that differentiate into osteoblasts expressing mineralised, osteogenic ECM.

Runt-related transcription factor 2 (Runx2) is the main known transcription factor required for osteoblastic differentiation and the most commonly used marker for osteogenic commitment (Jonason *et al*, 2009). It is an early marker and regulates cell proliferation; furthermore, it interacts with various signalling pathways to control the expression of many genes *e.g.* Vascular endothelial cell growth factor (VEGF) and Dentin matrix protein-1 (DMP1; Khosla *et al*, 2008; Table A9.3). However, it has been noted that in some human MSCs the activity but not the expression of Runx2 increases with osteogenic differentiation (Marom *et al*, 2005).

Lately there have been studies suggesting that osteogenic differentiation is regulated by an interactive process between the two Twist proteins, Twist1 and Twist2, and Runx2 (Bialek *et al*, 2004; Isenmann *et al*, 2009). Twist1 and Twist2 are expressed in Runx2 expressing cells throughout the skeleton during early development and osteoblast specific differentiation only occurs after their expression decreases (Bialek *et al*, 2004). It is believed that the expression of Twist1 and Twist2 maintains cells in an osteo-progenitor or preosteoblast-like state (Figure 1.4) in order to prevent premature or ectopic osteoblast differentiation (Lee *et al*, 2000; Bialek *et al*, 2004).

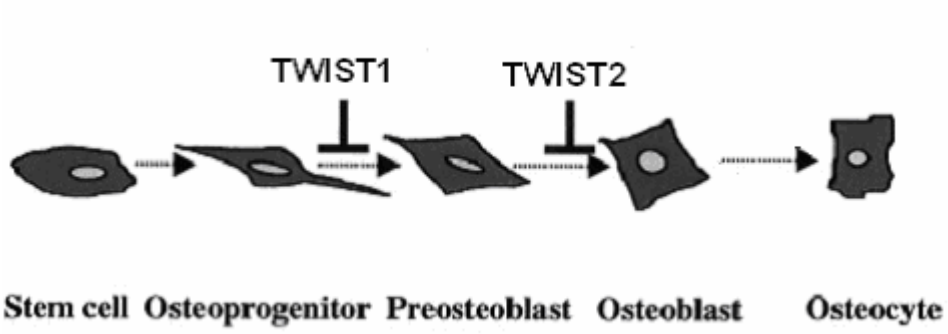

Figure 1.4. Importance of TWIST 1 and 2 in osteogenic differentiation. Stem cells start to differentiate along the osteogenic lineage, but before they can become osteoblasts there is an interaction between Runx2 and Twist 1 and 2 to prevent premature osteogenic differentiation. When the cells are ready, the levels of Twist 1 and 2 decrease and Runx2 levels increase and the cells can differentiate into osteoblast and eventually osteocytes. Adapted from Lee *et al* (2000).

As previously mentioned, Runx2 interacts with and controls the expression levels of several osteogenic genes, including the early osteogenic marker ALP (Weiss *et al*, 1986) and the late marker OP. Runx2 deficient mice showed no expression or severely decreased levels of ALP and OP. These mice completely lacked mature osteoblast and could not mineralize their skeleton (Jonason *et al*, 2009).

ALP is a commonly used osteogenic marker; mature ALP is glycosylated and anchored to the cells plasma membrane but its exact osteogenic role is not yet known. However, ALP is expressed in high levels within mineralized tissue (Gosike-Sone *et al*, 1998) and its importance for osteogenic differentiation is well established. For example, ALP is essential for expression of necessary genes to produce osteogenic ECM (van der Dolder & Jansen, 2007) and Khosla *et al* (2008) showed that the expression of ALP and type 1 collagen are essential for mineralization.

Type 1 collagen is the major protein component in many tissues, including bone, skin, ligaments and tendons. As mentioned earlier, in bone it functions as the template for mineral deposit. Procollagen is its soluble precursor molecule and compromises two pro-α1 and one pro-α2 chains that are encoded by Col1A1 and Collagen 1A2 (Col1A2) genes. The formation of the heterotrimer starts in the rough endoplasmic reticulum, as a propeptide, and is thereafter transferred to the ECM where it forms mature collagen (Pace *et al*, 2001).

Several Bone morphogenic proteins (BMPs), which all apart from BMP-1 belong to Transcription growth factor-beta (TGF-β) superfamily, are capable of acting as potent bone inducing factors, including BMP-2, -4, -7 (Wang *et al*, 1990; Canalis *et al*, 2003; Ito & Miyazono, 2003; Cheng *et al*, 2003; Farhadieh *et al*, 2004). BMP-7 is considered to be a weaker bone inducer than BMP-2 and -4 (Cheng *et al*, 2003). The BMPs initiate their signalling pathway by binding to BMP receptors, such as BMPR-I and BMPR-II. The activated receptors phosphorylate Sma- and mad- related protein (Smad) transcription factors, *e.g.* Smad1 (Cheng *et al*, 2003; Ito & Miyazono, 2003). The phosphorylated Smads then form a complex with Smad4 in the nucleus and activate the

expression of target genes together with other co-activators (Cheng *et al*, 2003). Runx2 is also involved in this signalling cascade mediating the osteogenic differentiation initiated by BMPs (Cheng *et al*, 2003).

Parathyroid hormone (PTH) is produced by the parathyroid glands in humans and is consider to be the most important regulator of calcium ion homeostasis *in vivo* (Mannstadt *et al*, 1999; Pioszak & Xu, 2008) together with its receptor PTH1R (Huang *et al*, 2001). Its synthesis and secretion are largely regulated by the extracellular concentration of calcium and phosphate, which is monitored by the Calcium sensing receptor (CASR) of the parathyroid glands (Mannstadt *et al*, 1999; Pioszak & Xu, 2008). PTH mediates actions in both kidney and bone; in this study only its interaction with bone tissue will be discussed. In response to low blood calcium or high phosphate levels, PTH is secreted into the circulation and acts with PTH1R on osteoblasts (Mannstadt *et al*, 1999; Pioszak & Xu, 2008). PTH increases bone mass and has been used clinically to enhance bone formation and increase bone density in patients with osteoporosis (Pioszak & Xu, 2008). Interestingly, the expression of PTH1R is regulated by the osteoblast-specific Col1A1 promotor (Ono *et al*, 2007).

Modulated vitamin D or 1,25-$(OH)_2$D can both positively and negatively regulate the expression of osteoblastic phenotype markers. In early osteogenic cultures, 1,25-$(OH)_2$D treatment inhibit type 1 collagen and ALP mRNA levels; in contrast, the expression of both genes was stimulated by the hormone in late-stage cultures (St-Arnaud, 2008). This can also explain the finding that BSP expression is suppressed by Vitamin D (Oldberg *et al*, 1990).

Another protein group that regulates the osteoblastic differentiation is TGF-β; TGF-β1 stimulates development and proliferation of osteogenic precursor cells, but it inhibits their maturation (Alliston *et al*, 2001; Tang *et al*, 2009). When TGF-β activates, it binds to receptor TGF-BRII, which initiate the recruitment of receptor TGF-BRI. Subsequent phosphorylation of TGF-BRI by TGF-BRII enables activation of Smad 2 and 3, which propagate the TGF-β signals (Hao *et al*, 2008). Although all isoforms of TGF-β signal

through the same cell surface receptors and have similar cellular targets, they demonstrate different or opposing effects *in vivo* (Hao *et al*, 2008).

1.2.3 BONE MARROW-DERIVED MSCs

MSCs are a heterogeneous multipotent cell population of mesoderm origin that can differentiate along several lineages including chondrogenic, osteogenic and adipogenic (Marie & Fromigue, 2006). Researchers have also reported that MSCs can differentiate along the myogenic lineage by fusing with myoblasts (Lee *et al*, 2005). There have been reports that they can also differentiate along non-mesoderm lineages, for example, neuronal cells and hepatocytes (Abdallah & Kassem, 2008); however, these findings are more controversial. MSCs are in general derived from the bone marrow, but researchers have also derived MSCs-like cells from other tissues, such as umbilical cord blood, adipogenic and connective tissue (Young *et al*, 1995; Lee *et al*, 2004; Romanov *et al*, 2005). There is no single cell marker to define the MSC population; therefore, a whole range of the presence or absence of markers define the MSCs *e.g.* they are $CD29^+$, $CD73^+$, $CD90^+$, $CD105^+$, $CD166^+$, $CD44^+$, $CD34^-$, $CD45^-$ and $CD14^-$ (Abdallah & Kassem, 2008). However, only approximately 30% of the cells in a MSCs population are truly multipotent *i.e.* can differentiate along at least three lineages (Abdallah & Kassem, 2008).

Recently, Stro-1, an uncharacterized cell surface epitope expressed by human MSCs and erythrocytic cells (Gronthos *et al*, 1994), has been used as a marker for osteogenic progenitor cells (Marie & Fromigue, 2006). However, bone marrow cells expressing Stro-1 can also give rise to cells with the phenotype of fibroblasts, adipocytes and smooth muscle cells (Gronthos *et al*, 1994). Furthermore, MSCs can change their morphology and cell surface expression between different *in vitro* processes (Abdallah & Kassem, 2008). Cell surface expression could also be due to time in culture (Alhadlaq & Mao, 2004).

The mechanism by which MSCs regenerate tissues or organs *in vivo* is not very well understood but it has been suggested that it is a process by tissue-specific progenitor cells, which are renewed by MSCs from bone marrow (Sethe *et al*, 2006). It appears that injured mature cells are able to secrete not only homing signals but also differentiation signals. Uninjured cells can also induce differentiation when direct contact is allowed (Kolf *et al*, 2007). MSCs are considered to be the reason why bone can repair itself without scaring (Sommerfeldt & Rubin, 2001).

1.3 MUSCLE

Muscle can be divided into three groups; smooth muscle, cardiac muscle and skeletal muscle. In this study, craniofacial skeletal muscle from the masseter muscle has been used and from now on skeletal muscle will be referred as 'muscle' or 'muscle tissue'.

Muscles have a very particular structure (Figure 1.5) that distinguishes them from other cell types. Muscle tissue consists of bundles of multi-nuclei muscle fibres, *i.e.* fasicles, where individual fibres can vary considerably in diameter, 10-100 um, and length, 1- 4 cm (Thibodeau & Patton, 2007). The muscle fibre is composed by myofibrils *i.e.* they have in their cytoskeleton bundles of fine fibrils, myofibrils. A muscle fibre may have 1000 myofibrils tightly packed inside it (Thibodeau & Patton, 2007).

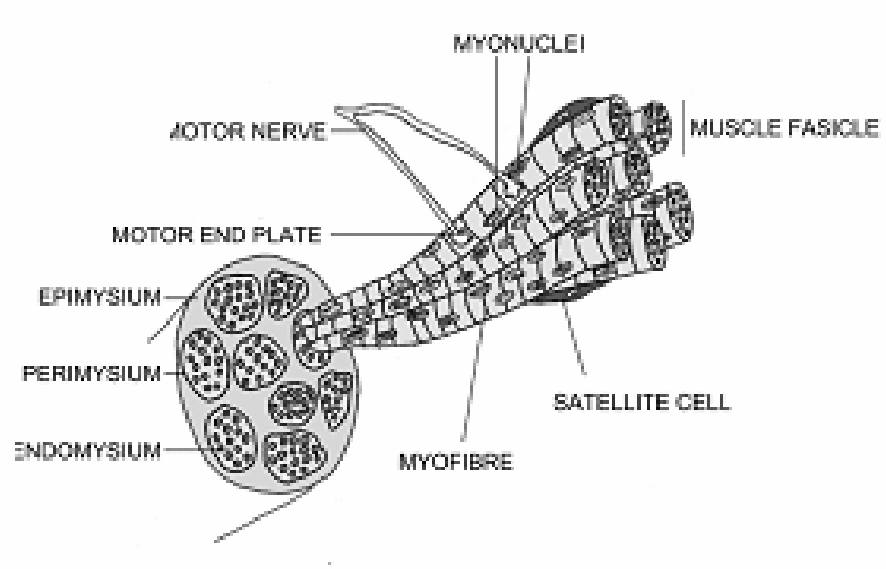

Figure 1.5. Structure of skeletal muscle. Muscle fibres are organised by three layers of connective tissue. Endomysium surrounds the muscle fibre, and bundles of muscle fibres, fasicles, are surrounded by perimysium. Bundles of fasicles are surrounded by epimysium. Picture adapted from Sinanan *et al* (2006).

The myofibrils are made up of even finer filaments called myofilaments. There are two types of myofilaments thin and thick filaments (Thibodeau & Patton, 2007). Four proteins make up these myofilaments. The thin myofilaments consist of three proteins actin, tropomyosin and troponin, and the thick myofilament consists of myosin. Within a myofibril the thick and thin myofilaments alternate (Stewart & Rittweger, 2006) and this particular structure makes it possible for muscle to contract and relax.

Calcium ions also play an important role in muscle contraction. They are concentrated within the sarcoplasmic reticulum and when the calcium ions are released from sarcoplasmic reticulum into the sarcoplasm surrounding the myofilaments this activates the sliding filament mechanism resulting in muscle contraction (Thibodeau & Patton, 2007).

However, it is important to know that apart from muscle fibres, muscle tissue consists of a heterogeneous population of cells (Beauchamp *et al*, 2000). Hence, if you isolate cells from muscle tissue by the explant method (Chapter 2.1.2) the amount of myogenic cells are estimated to be 5-45% (Lewis *et al*, 2000).

1.3.1 MYOGENIC DIFFERERNTIATION

The myogenic differentiation pathway has been investigated to find a successful therapy for muscle diseases *e.g.* muscular dystrophy. The cells responsible for the muscle regeneration are named satellite cells. They are considered to be myogenic stem cells and are small, flattened, quiescent, mononucleated cells situated beneath the same basal lamina as the multinucleated muscle fibre (Sinanan *et al*, 2006). Satellite cells are defined by their location and their main known function is to act as reserve cells for muscle growth and repair (Seale & Rudnicki, 2000; Sinanan *et al*, 2006). Skeletal muscle fibres are unable to divide: the only way they can increase in number is by muscle precursor cells (MPCs) fusion (Cornelison & Wold, 1997). When satellite cells become activated, *e.g.* by injury, they start to proliferate and become MPCs that express

specific muscle markers *e.g.* desmin (Seale & Rudnicki, 2000) before they fuse with damaged muscle fibres to restore the damage or with each other to create new muscle fibres (Ambrosio *et al*, 2009; Figure 1.6). This process is helped *in vivo* by Insulin-like growth factor-1 (IGF-1; Table 1.3), which is synthesized and secreted by muscle cells to enhance the proliferation and myogenic differentiation (Stewart & Rittweger, 2006; Clemmons, 2009).

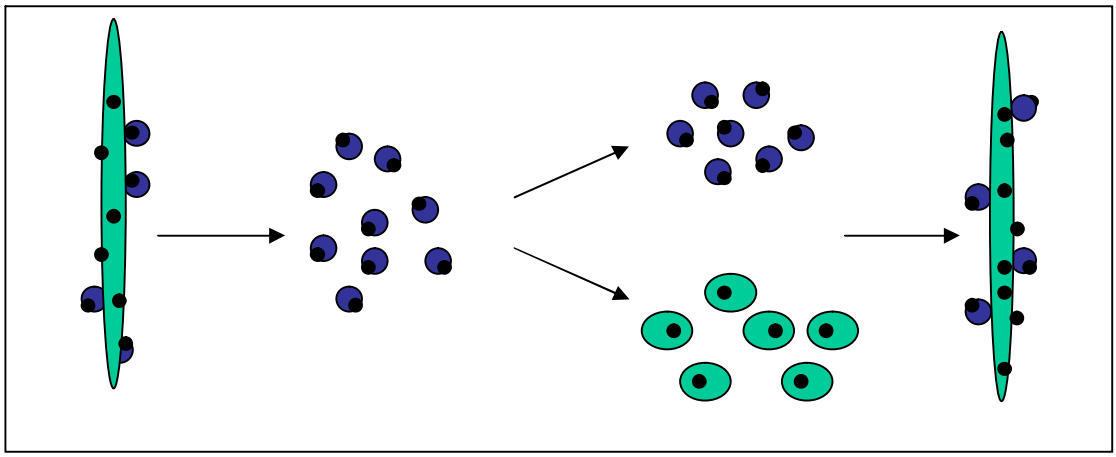

Figure 1.6. Scheme over regeneration of muscle fibre by satellite cells. Signals released by muscle injury to activate satellite cells, which start to proliferate, and their progeny, MPCs, can either self-renew, restoring the satellite cell pool, or differentiate along the myogenic lineage and fuse to repair damaged muscle fibres or fuse to form new ones. Picture taken from Carlqvist *et al* (2010).

This transition from mono-nuclear MPCs to multinucleic myotubes is regulated by various factors including a transcription factor family, the Myogenic factor (Myf) family, where Myogenic differentiation antigen 1 (MyoD) and Myogenic factor 5 (Myf5) are required for the commitment of stem cells to the myogenic lineage, whereas myogenin and Muscle regulatory factor 4 (MRF4) regulate the transition of these committed cells to multinucleated myofibres (Table 1.3; Stewart & Rittweger, 2006). If the myogenic differentiation is disturbed the precursor cells can form myosacs, which are rounded multi-nuclei structures (Kang *et al*, 1995).

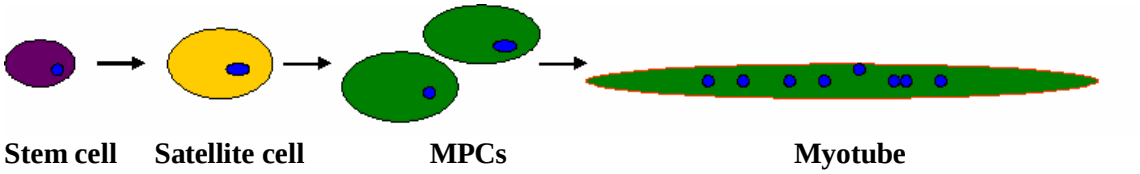

Figure 1.7. Adult muscle-derived stem cells are hypothesised to be precursor cells to satellite cells. According to this theory the myogenic differentiation pathway would go from stem cells to satellite cells to MPCs that proliferate and fuse to myotubes.

Furthermore, there have been several reports about adult stem cells (Figure 1.7) residing in the skeletal muscle *i.e.* cells that are not restricted to the myogenic lineage (Qu-Petersen *et al*, 2002; Sinanan *et al*, 2004). Most researchers agree that the cell population that is able to differentiate along non-myogenic lineages is distinct from satellite cells (Jankowski *et al*, 2002); there have been suggestions that muscle-derived stem cells are precursors to satellite cells (Figure 1.7; Jankowski *et al*, 2002).

Table 1.3 Myogenic markers and growth factors used in this study. Markers and growth factors are listed in an alphabetical order.

MARKER	DESCRIPTION	MYOGENIC FUNCTION
α-sarcomeric actin	- Contractile protein	-The most abundant actin in terminally differentiated myofibres (Lancioni *et al*, 2007)
CD56	- Cell surface receptor	- Used as a satellite cell marker (Mackey *et al*, 2009)
Desmin	-Cytoplastic intermediate filament	- Links the z-lines of adjacent myofibrils - Maintaining sarcomere adhesion and structure (Stewart & Rittweger, 2006). - Expressed by myoblasts and myotubes (Lewis *et al*, 2000).
IGF-1	-Growth factor	-Stimulate MPCs to proliferate and differentiate (Clemmons, 2009)
Myogenin	-Transcription factor -Belong to Myf family	- Regulates the fusion of myoblasts to myotubes (Stewart & Rittweger, 2006)

1.4 ISOLATION OF CELLS

1.4.1 MDCs

Muscle tissue contains several different cell types (Lewis *et al*, 2000), so in order to improve the regenerative capacity of the muscle researchers have tested various isolation methods to obtain different subpopulations for study. Most researchers have focused on the isolation of the more myogenic population to use in muscle regeneration applications to treat diseases, such as muscular dystrophy. However, when it was discovered that MDCs contain cells that are not restricted to the myogenic lineage, attempts to develop methods to isolate other MDC-derived subpopulations have been made. Qu-Petersen *et al* (2002) developed an isolation method for MDCs derived from mice where the muscle was first enzymatically digested before the cells were isolated by differential adhesion to collagen. The main aim for this method was to isolate the more myogenic cells, however, they also isolated one population they named to muscle-derived stem cells (MDSCs), that showed increased expression of neuronal (*ca* 1-2%) and endothelial markers (*ca* 15-20 %) after they had been treated with either neuronal or endothelial stimuli (Qu-Petersen *et al*, 2002).

This pre-plate technique has not been thoroughly studied nor employed successfully for isolating human muscle stem cells (Ozeki *et al*, 2006). Therefore, other strategies have used cell surface markers of human MDCs to isolate specific cell types. The two markers that have been used are CD56, which has been used as a satellite cell marker (Mackey *et al*, 2009) and α7 (Ozeki *et al*, 2006), which has been used as a myoblast marker (Blanco-Bose *et al*, 2001). It was concluded that the $MDCs^{CD56+}$ population consisted of both cells committed to the myogenic lineage and cells that are not able to express osteogenic and adipogenic genes when stimulated accordingly (Sinanan *et al*, 2004). However, it was suggested that the cells with highest differentiation potential were the ones with either low expression of CD56 or lacking CD56 (Sinanan *et al*, 2004), since CD56 is a marker for satellite cells.

Support for the theory that the more stem cell-like cells could reside in both the $MDCs^{CD56+}$ and $MDCs^{CD56-}$ population was given by Andriamanalijaona *et al* (2008) who managed to induce chondrogenic differentiation in both subpopulations.

Recently, Mitchell *et al* (2010) identified a novel cell population resident within the muscle interstitium by selecting the $CD34^{+}/Sca1^{+}$ population. When this cell population was freshly isolated, the cells expressed PW1, a stress mediator marker, but not Paired box transcription factor 7 (Pax7), which is expressed in satellite cells. Thus, the cell population was named $PW1^{+}/Pax7^{-}$ interstitial cells (PICs). It was shown that PICs could differentiate into both smooth and skeletal muscle; however, PICs started to express Pax7, which is required for postnatal myogenic differentiation, before they formed skeletal muscle *in vitro* (Mitchell *et al* 2010).

1.4.2 BONE MARROW-DERIVED MSCs

The common approach to isolate MSCs from bone marrow is to let the cells adhere to tissue culture plastic (TCP). Bone marrow derived-cells adherent to TCP are considered more MSC-like, than other cells from the bone marrow, such as adipocytes, macrophages HSC and plasma cells (Alhadlaq & Mao, 2004). To confirm that the isolated population are MSCs, they are analysed by flow cytometry for a range of cell surface markers (Chapter 1.2.3; Alhadlaq & Mao, 2004). But it should be kept in mind that also *in vivo* MSCs express a heterogeneous set of cell surface markers and secreted matrix molecules (Tokoyoda *et al*, 2010).

1.4.3 OTHER STEM CELL-LIKE POPULATIONS

Researchers have also isolated stem cell-like populations from other tissues than muscle and bone marrow, for example from neonatal foreskin (Jones & Watt, 1993), cartilage

(Dowthwaite *et al*, 2004) and oral mucosa (Davies *et al*, 2010). All these researchers have used the cells adhesion properties to fibronectin (Fn). For all these cell types the early adherent cells have been shown to belong to the more stem cell-like population (Jones & Watt, 1993; Dowthwaite *et al*, 2004; Davies *et al*, 2010).

1.5 DEVELOPMENTAL ORIGIN OF BONE AND MUSCLE

Development of an organism starts with the fertilized egg cell divides to form the germ layers. Firstly, a layer facing the external medium is formed. A large part of this layer remains external, forming the ectoderm *i.e.* the precursor of epidermis and the nervous system. The interior part of the layer forms the endoderm *i.e.* the precursor of gut and its appendages, such as lung and liver. These are the primary germ layers (Hall, 2009). Thereafter, another group of cells move into the space between the ectoderm and the endoderm, and form the mesoderm *i.e.* the precursors of muscle and connective tissue (Alberts *et al*, 2002). The mesoderm arises by activation of genes following interactions between ectoderm and endoderm germ layer (Hall, 2009). According to the classical germ layer theory the ectoderm, endoderm and mesoderm, all belong to the primary germ layers; however, according to a modification of the theory, the mesoderm belongs to the secondary germ layer together with the neural crest (Hall, 2009). As mesoderm, neural crest arises early in the development and gives rise to divergent cell and tissue types and is formed by induction of primary germ layer (Hall, 2009).

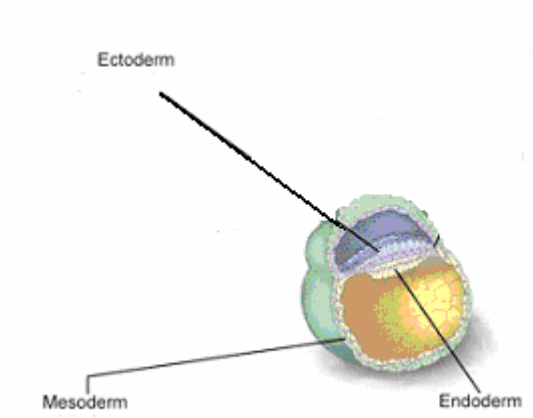

Figure 1.8. Classical view of the three germ layers; endoderm, ectoderm and mesoderm. The primary germ layers are the ectoderm, the outer layer, and the endoderm, the inner layer; the secondary germ layer is mesoderm, the middle layer. Picture adapted from http://www.ncbi.nlm.nih.gov/About/primer/genetics_cell.html

The developmental origin of skeleton is dependant on its anatomical location. The craniofacial bone and connective tissue originate from the neural crest, while the associated muscles derive from cranial mesoderm (Dupin *et al*, 2007; Grenier *et al*, 2009). In the rest of the human body, the muscles and the skeleton, including the iliac crest, have the same developmental origin *i.e.* mesoderm (Alberts *et al*, 2002).

1.6 TI SCAFFOLDS

Metal implants have the structure and the mechanical strength necessary to function in heavily loaded positions, such as jaws and joints (Ellingsen *et al*, 2000) and especially Ti and Ti alloys are commonly used in dental and orthopaedic implants (Brett *et al*, 2004). Ti has apart from its mechanical strength and high degree of biocompatibility (Brett *et al*, 2004), also capacity to osseointegrate *i.e.* to create 'a direct structural and functional connection between living bone and the surface of load' (Granström, 2007).

The osseointegration properties of Ti was originally used to anchor dental prostheses or bridges in the jaws to replace lost teeth (Granström, 2007) but Ti has also been used in various applications *e.g.* attachment of bone hearing aid, rehabilitation of patients with defects from cancer therapy and traumatic amputations (Granström, 2007). When a Ti implant is anchored, areas of bone are interspersed with regions of thicker fibroblastic tissue and regions of bone marrow (Schwartz *et al*, 2008). In fact, bone marrow-derived MSCs are believed to be the cells that migrate on an implant *in vivo*, not committed osteoblasts (Schwartz *et al*, 1999). Hence, it is important that the surface coating gives the wanted signals to cells for successful osseointegration (Ellingsen *et al*, 2000). The aim for bone implant researchers is to manipulate the surface to make it more acceptable to bone cells for a rapid integration (Ellingsen *et al*, 2000).

Ellingsen *et al* (2000) stated that successful osseointegration of an implant was dependent on both the physiology of the bone and the implant *e.g.* surface structure and chemistry. For example, the microstructure of the implant is known to affect osseointegration; a very smooth surface will result in poor integration, but with minor contraction. A very rough surface will result in rapid integration, but can cause secondary inflammation and contraction that can jeopardize integration later on (Ellingsen *et al*, 2000). However, there is a consensus in the dental world that rough surfaces have enhanced bone-to-implant shear strength and also osseous contact area compared with their smooth counterparts (Brett *et al*, 2004). A fibrous capsule of poorly vascularised collagen is developed around most of smooth surfaces (Ellingsen *et*

al, 2000). Implants with rough surface have shown a reduction of fibrous encapsulation and an increment of the biomechanical properties of the implant-bone interface (Ellingsen *et al*, 2000).

Polishing and blasting techniques are in general used to modify the topography of the Ti surface. During the process of polishing the surface is polished by a hard abrasive medium while using a lubricant. Sandblasting and acid etching are often used to increase the surface roughness (Ellingsen *et al*, 2000). Cells on Ti surfaces treated by sandblasting and acid etching have shown enhanced osteogenic properties compared to cells on polished Ti surfaces (Rupp *et al*, 2006).

Lately, there have been suggestions that hydrophilic rough surfaces increase the rate and extent of bone formation compared to hydrophobic rough surfaces (Table 1.4; Zhao *et al*, 2005; Rupp *et al*, 2006). Straumann AG, has developed a hydrophilic rough surface for their dental Ti implant screws called SLActive, which Schwartz *et al* (2008) showed enhanced the amount of formed bone around its site compared to its hydrophobic counterpart, SLA. Used in clinic, Ti screws with SLActive surface significantly reduces the healing time; for standard screws the healing time recommended before loading is 12 weeks, for screws with SLActive surface this time is reduced to between immediate or early loading *i.e.* 4 weeks (Zöller *et al*, 2008; Morton *et al*, 2010). There are several benefits of reducing the healing time of implants, such as simplifying the clinical procedure, lowering the cost and improved appearance for the patients (Morton *et al*, 2010).

Table 1.4. Definition of hydrophilicity/hydrophobicity depending on the water contact angle. The water contact angel is the angle which a droplet of water meets the solid surface.

WATER CONTACT ANGLE (°)	HYDROPHILIC OR HYDROPHOBIC
0	Very strongly hydrophilic
0-30	Strongly hydrophilic
30-90	Less hydrophilic
> 90	Hydrophobic
Ca 120	Strongly hydrophobic
> 150	Superhydrophobic

1.6.1 SURFACE ROUGHNESS (Ra)

The surface roughness or the Ra value of the material is defined as the peak-to-valley measurement of a surface. However, it is important to remember that differences in the topography of a surface could also affect how the cells perceive its surface. In addition, the cells different differential stages and morphology could influence how they interact with the surface (Schwarts *et al*, 1999).

1.7 CELL DEATH

In general, researchers divide cell death into two groups: apoptosis and necrosis. In healthy cells, phospholipids are asymmetrically distributed, with the anionic phospholipids *e.g.* phosphatidylserine situated on the cytoplasmic side of the plasma membrane. This asymmetrically distribution is disturbed by apoptosis; thus, AnnexinV, a natural human phosphatidylserine-binding protein can, and is often, used as a marker for apoptosis (Tait, 2008).

In necrosis, the cell and its organelles start to swell, whilst in apoptosis the cell shrinks together with its nucleus. This distinction is due to the plasma membranes different roles in the two processes. In necrosis, the plasma membrane looses its coherence, which allows an influx of extracellular ions and fluid. Thus, the cell and its organelles start to swell. In apoptosis on the other hand, plasma-membrane coherence persists until later in the process (Hotchkiss *et al*, 2009).

It has long been known that apoptosis is genetically controlled *i.e.* programmed cell death (Hotchkiss *et al*, 2009). However, there is now evidence that necrosis, which was considered as being an accidental form of cell death, can be initiated or modulated by programmed mechanisms. It has also been shown that there can be cross-talk between the two forms of cell death pathways (Goldspink *et al*, 2004; Hotchkiss *et al*, 2009).

1.8 APPLICATION OF RESEARCH

This thesis has compared the osteogenic differentiation potential between bone marrow-derived MSCs and MDCs, or an osteogenic subpopulation of MDCs, and their interaction with Ti.

The idea of using MDCs in bone regenerative applications originate in the discovery that muscle tissue contained cells that could differentiate along the osteogenic lineage (Bosch *et al*, 2000). There could be various advantages of using osteogenic MDCs instead of bone marrow-derived MSCs in bone regeneration applications. One could be that using osteogenic MDCs would lower the risks associated with bone marrow transplantation; the bone marrow containing MSCs also contains white blood cells and by removing white blood cells the patient's immune system is decreased. Taking muscle biopsies is not associated with a decreased immune system and muscle tissue, especially masseter muscle, is considered to be easy accessible.

If a patient is in need of bone material for repair and regeration as a result of a bone related disease, such as osteoporosis, it might be possible to use an expanded culture of their own osteogenic MDCs for transplantation into the affected sites. This would possibly have the advantage over the use of MSCs in a patient with osteoporosis who might suffer extra morbidity from the cell harvesting procedures. The possibility of using osteogenic MDCs in autologous transplantations is important since there is always a risk in allogenic transplantations that the patient will reject the donor's bone marrow or contract an infection (Thibodeau & Patton, 2007).

Osteogenic cells seeded onto Ti could be used as enhancers of osseointegration for implants used throughout the body. Using the osseointegrational properties of Ti is very common in dental industry, but has also been used in bone conducting hearing aids, implants after defects from cancer therapy and traumatic amputations (Granström, 2007).

MSCs have already shown promising results to improve the bone regeneration around Ti knee implants in sheep (Frosch *et al*, 2006). Frosch *et al* (2006) coated Ti knee implants with autologous MSCs and inserted the implants back *in vivo* (Frosch *et al*, 2006). Defects treated with MSC-coated implants demonstrated a complete regeneration of the subchondral bone in 50% of the cases. When uncoated implants were inserted, it resulted in incomplete healing in 50% of the cases. In 50% of the cases both uncoated and MSC-coated implants failed to osseointegrate (Frosch *et al*, 2006).

Another application could be the use of osteogenic cells to regenerate new bone; in this case, Ti would function as a permanent scaffold that will be integrated in the newly formed or old bone structure. Promising results have already been shown in humans where autologous MSCs have been used. Warnke *et al* (2004) constructed a Ti scaffold to regenerate a new mandibular. They filled the scaffold with bone mineral blocks and bone marrow, including MSCs, and after 7 weeks found new osteoblast activity (Warnke *et al*, 2004).

In both of these applications, it is considered necessary to culture the cells *in vitro* prior to transplantation in order to increase the cell number and differentiate the cells along the osteogenic pathway (Sikavitsas *et al*, 2001). A way to enhance the osteogenic differentiation of the cells *in vivo* could be to incorporate BMP-2 into the Ti coating (Liu *et al*, 2004). Implant failure in the clinic could have several causes, such as infections, impaired healing or overloading. If the rate of osseointegration between the implant and bone could increase by coating the implants with osteogenic cells the success rate could increase.

1.9 AIM OF RESEARCH

The main aim for this research is to investigate the potential to use MDCs in bone engineering applications, where Ti is used as the scaffold. To achieve the aim of this project the research had to be divided into three parts with their own objectives:

a) Develop an isolation method for the more osteogenic fraction of MDCs.

b) Study the osteogenic differentiation of the more osteogenic fraction of MDCs and compare it with MSCs

c) Comparison of the interaction of the more osteogenic fraction of MDCs with Ti and compare it with MSCs

CHAPTER 2:

METHODS

2.1 ISOLATION

2.1.1 MSCs DERIVED FROM BONE MARROW*

***Performed by Tulane Center for Gene Therapy, US, thanks to grant from NCRR of the NIH # P40RR017447**

The MSCs were isolated from iliac crest bone marrow from 5 male patients in the age range of 22-28 years old. In order to separate the mononuclear cells from erythrocytes density centrifugation was performed. Thereafter, the cells were plated on TCP so the MSCs could adhere and cultured in α-MEM based culture media. The MSCs were harvested when they reached 60%-80% confluency and named passage 0 cells.

The isolated MSCs were expanded and tested for a range of cell surface markers at passage 2. The MSCs were positive for markers known to be expressed on MSCs *i.e.* > 90% of the cells expressed, for CD29, CD49c, CD59, CD73a, CD90, CD105, CD147, CD166 and HLA-I. The cells were also negative for blood cell markers *i.e.* < 1 % of the cells expressed, for CD11b, CD19, CD34, CD36, and CD45.

The MSCs were aliquoted in vials, $1x10^6$ cells/vial, and delivered to UCL Eastman Dental Institute (EDI) in liquid nitrogen, where they were transferred directly to their permanent liquid nitrogen storage.

Table 2.1. Cell surface markers for which the MSCs were tested positive or negative.

The table is an adapted version of the information sheet from Tulane Center for Gene Therapy

CELL SURFACE MARKER	DESCRIPTION
CD11b	Mediates adhesion to substrates
CD19	Early B-cell antigen in fetal tissue and regulates cell development
CD29	Fn receptor
CD34	Cell-cell adhesion and molecule and cell surface glycoprotein
CD45	Leukocyte antigen
CD49c	Receptor for laminin, collagen, Fn, thrombospondin
CD59	Regulates mediated cell lysis
CD73a	Catalyzes dephosphorylation
CD90	Marker for HSCs, neurons and connective tissue
CD105	Mediates cellular response to TGF-β1
CD147	Induces MMPs
CD166	Is an activated leukocyte cell adhesion molecule
HLA-I	Is associated with β-2 microglobulin

2.1.2 MDCs DERIVED FROM MASSETER MUSCLE TISSUE

The MDCs were derived from masseter muscle biopsies from 3 healthy, adult, informed and consenting patients undergoing wisdom tooth removal at EDI. The procedure was approved by the ethical committee. Biopsies from three patients were used in this study; the sexes and ages of the donors were kept unknown.

The biopsies were washed with 1% antibiotic (penicillin/streptomycin)-supplemented Dulbecco's modified eagle's essential medium (DMEM) and minced with sterile scalpels. The tissue fragments were plated onto 0.2%-gelatin-coated T25 cm^2 flasks with culture media *i.e.* DMEM, low glucose, in the presence of 20 % Fetal bovine serum (FBS) and antibiotics, and incubated at 37 °C in 5 % CO_2.

The culture media was changed every 4 days and after 2-4 weeks cells started to migrate from the biopsies. The first wave of migration of mononuclear cells from the explant was named 'α-wave', and this population was used throughout this study. The harvested 'α-wave' cells were named MDCs passage 1 cells. This isolation protocol has previously been developed and used in laboratories at EDI (Sinanan *et al,* 2004).

2.2 CELL CULTURE

2.2.1 MDCs

The MDCs were cultured on 0.2% gelatin (Gel)-coated TCP in DMEM, low glucose, supplemented with 20% FBS and 1% P/S if not otherwise stated. Before the MDCs reached confluency they were enzymatically harvested using Trypsin/EDTA (Trypsin), unless otherwise stated. All experiments were performed using cells in passage range 3-7.

2.2.2 MSCs

The MSCs were cultured on TCP in alpha-minimal essential medium (α-MEM), supplemented with 20% FBS and 1 % P/S unless otherwise stated. Before the MSCs reached confluency they were enzymatically harvested using Trypsin unless otherwise stated. All experiments were performed using cells in passage range 2-5.

2.3 DIFFERENTIATION

At differentiation experiments, the cells were seeded at 5000 cells/cm^2, and left in culture media until they became confluent approximately at 10000 cells/cm^2. Confluency is a subjective term and Figure 2.1 demonstrates the degree of confluency that is defined confluence in this thesis. This degree of confluency was chosen since it is important for cells to have cell contact for differentiation purposes; however, the differentiation should be directed by the differentiation media and not by cell-to-cell contact.

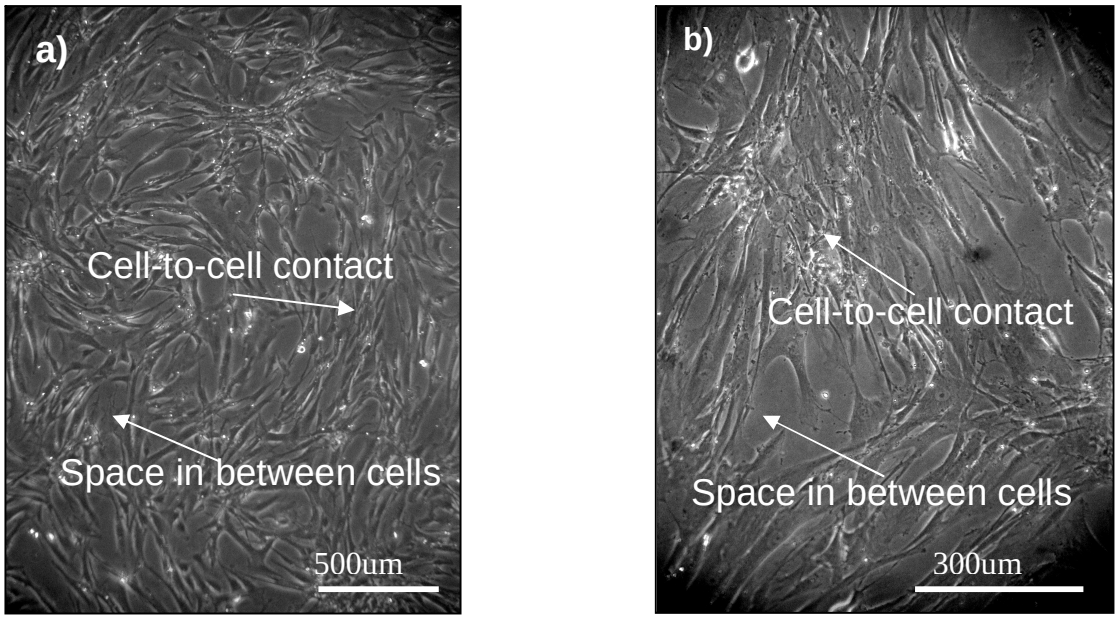

Figure 2.1. Level of confluency for when differentiation medium is added to the cells. These photographs by Phase contrast microscopy (PCM) show MSCs of a) x4 and b) x10 magnification.

2.3.1 OSTEOGENIC MEDIA

The osteogenic media was titrated to find the optimal concentration of dex and β-glycerophosphate (β-GP) in chapter 3, Result section 1. If nothing else is stated 'osteogenic media' consisted of DMEM (low glucose), 20 % FBS, 100nM dex, 50ug/ml L-ascorbic acid, 2 mM β-GP and 1 % P/S (Table 2.2). The osteogenic media in the literature has had various concentrations of dex (Ahdjoudi *et al*, 2001; van den Dolder & Jansen, 2007) and β-GP (Aslan *et al*, 2006; Ozeki *et al*, 2006).

2.3.2 MYOGENIC MEDIA

The optimal myogenic media has been determined earlier by Allen & Boxhorn (1989) and consisted of 10 ng/ml IGF-1(E3R), DMEM (high glucose), 2 % FBS, and 1 % P/S (Table 2.2).

2.3.3 ADIPOGENIC MEDIA

The adipogenic media consisted of DMEM (low glucose), 20 % FBS, 0.5uM dex, 0.5 uM isobutylmethylxanthine, 50 uM indomethacin and 1 % P/S (protocol taken from information sheet from Tulane Center for Gene Therapy; Table 2.2).

Table 2.2. Summary of types of cell media used in this project. All media were supplemented with 20% FBS apart from myogenic media that was supplemented with 2 % FBS. All media were supplemented with 1 % P/S. Media presented in alphabetical order.

MEDIA	**BASAL MEDIA**	**SUPPLEMENT**
Adipogenic media	DMEM, low glucose	0.5uM dex 0.5 uM iso-butylmethylxanthine 50 uM indomethacin
Control media	DMEM, low glucose	-
Culture media for MSCs	α-MEM, low glucose	-
Culture media for MDCs	DMEM, low glucose	-
Myogenic media	DMEM, high glucose	2% FBS 10 ng/ml IGF-1 (E3R)
Osteogenic media	DMEM, low glucose	100nM dex 50ug/ml L-ascorbic acid 2 mM β-GP
Tulane's osteogenic media	α-MEM, low glucose	1 nM dex 50 uM L-ascorbic acid 20 mM β-GP

2.4 METABOLIC ACTIVITY

In this thesis two methods have been used to assess metabolic activity of the cells: Alamar Blue and 3-(4,5-Dimethylthiazol-2-yl)-2,5-diphenyltetrazolium bromide (MTT).

2.4.1 ALAMAR BLUE

Alamar Blue is a dye that assesses the metabolic activity of cells by functioning as an oxidation-reduction indicator. Blue coloured non-fluorescent Alamar Blue dye is reduced to pink coloured fluorescence by live cells. The oxidation-reduction process is based on the detection of metabolic activity or on the level of oxidation during respiration. The level of fluorescence is monitored at 530 nm excitation wavelength and 590 nm emission wavelength. The fluorescence is proportional with cell number (Figure 2.2), but the results are in general presented as percentage reduction of Alamar blue dye compared to maximal reduction (see equation below).

Following formula gives reduction of Alamar Blue in percentage:

$$\mathrm{Re}\,ductionAlamarBlue(\%) = \frac{(Fl_{Sample} - Fl_{Blank})}{(Fl_{100\%\,\mathrm{Re}\,dAB} - Fl_{Blank})} x100$$

where; Fl_{Sample} = Fluorescence in sample
Fl_{Blank} = Fluorescence in an acellular sample
$Fl_{100\%}$ = Fluorescence in an autoclaved sample

2.4.1.1 PROTOCOL

The cell media were first removed and exactly 900 ul of fresh culture media was pipetted into each well, in a 24-well plate, with cells plus an acellular well, which was used as a blank control. Thereafter, 100 ul of Alamar Blue was added to each well and incubated for exactly 4 h in incubator at 37 °C. In order to assess the maximal reduction, an acellular sample with Alamar Blue/culture media mixture was autoclaved.

After 4 h incubation, 2x100 ul was taken from each well, the acellular and the autoclaved control and pipetted to a black 96-well plate. The fluorescence was measured immediately in a fluoroscan (Ascent, Labsystems) at 530 nm excitation wavelength and 590 nm emission wavelength using software Ascent version 2.4. One important feature of Almar Blue is that is not cytotoxic, so the cell cultures can be used over many time periods. In order to control that the incubation time, 4 h, gave a linear relationship between fluorescent intensity and number of cells control standard curves were performed (Figure 2.2).

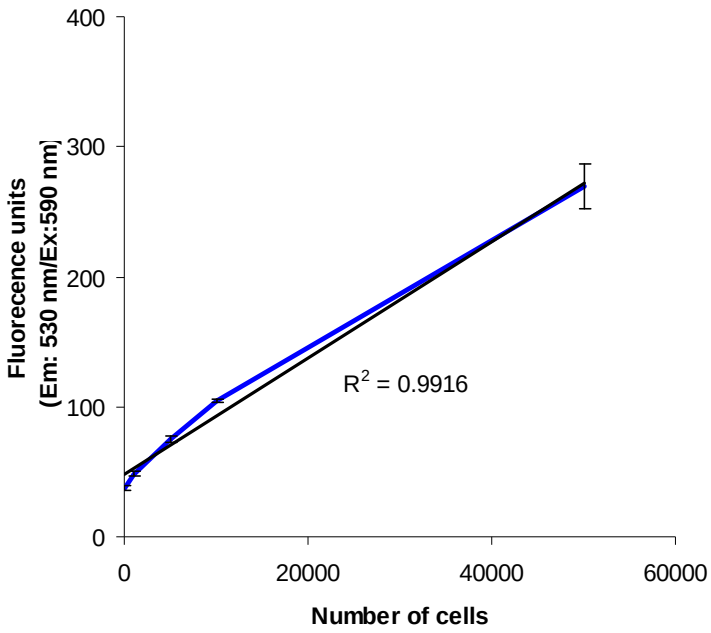

Figure 2.2. Standard curve of fluorescence *v.s.* number of cells after 4 h incuabtion with Alamar Blue. Graph shows the result of different seeding densities of MSCs incubated with Alamar Blue. Result presented as mean± 1sd.

2.4.2 MTT ASSAY

MTT assay is a colorimetric method for measuring cell metabolic activity. Yellow MTT is reduced to form purple formazan in the mitochondria of live cells. The reduction from yellow MTT to purple formazan takes place when mitochondrial reductase enzymes are active, and is directly related to the number of viable cells.

2.4.2.1 GENERAL PROTOCOL

The 250 ul/ml culture media of the MTT dye, stock concentration 5mg/ml, was added to the cells in culture media before the cells are incubated 4 h in 37 ºC. After 4 h, the

medium was removed and an 1 ml/well, in a 24 well plate, extraction buffer, 0.5 M DMF in 20-% Sodium dodecyl sulfate (SDS) solution (w/v, SDS/dd-H_2O) was added to dissolve the formed formazan over night in 37 ºC.

When the formazan was extracted, 2x 100 ul aliquotes per sample were transferred to a 96 well plate. The absorbance was measured using a plate reader at 590 nm where extraction buffer was used as a blank control.

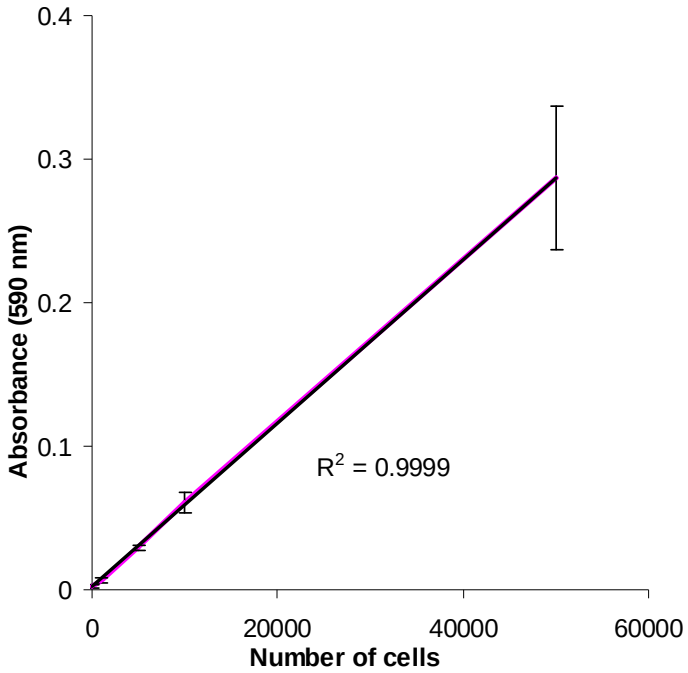

Figure 2.3. Standard curve of absorbance at 590 nm *v.s.* number of cells after MTT Assay. Graph shows the result of different seeding densities of MDCs incubated with MTT. Result presented as mean± 1sd.

2.4.2.1.1 PROTOCOL TO DETERMINE POPULATION DOUBLING (PD)

Cells were seeded at a density of 100cells/cm^2 in 6-well plates in triplicates. A reference plate was analysed, to measure the absorbance at time point 0. A theoretical standard curve was calculated with PD as a function of absorbance. This standard curve gave a

logarithmic equation (see equation below), which was used to calculate the PD values from the assessed absorbance.

$$y = k\ln(x) + m$$

where; y = PD
k = slope constant
x = absorbance
m = constant

2.4.2.1.2 PROTOCOL FOR ATTACHMENT

In order to assess the level of attachment in different cell subpopulations the MTT assay was used (Chapter 4.3.2). Immediately after the wanted cell population was isolated MTT was added to the cells in culture media. This was done to minimise the bias of proliferation that might occur differently in different cell subpopulations. The MTT assay was performed as described in Chapter 2.4.2.1.

2.5 SIZE ASSESSMENT

2.5.1 MEASURING BY IMAGE ANALYSIS

In order to assess the average size of MDCsFn and MDCsPP the cells were isolated in triplicates and the area of the two populations were assessed by image analysis. The images were captured using Leica FW4000 on an inverted light microscope Leica DMIRB, 48 hours after isolation. Photographs of 30 cells of each triplicate were taken. First the photographs were calibrated by a micrometer graticule; thereafter, by using calibrated photographs of the cells and software Image-pro the cell size could be assessed.

2.5.2 MEASURING BY FLOW CYTOMETRY

In order to confirm the differences in size of the two cell populations, MDCsFn and MDCsPP, they were also studied by flow cytometry. Light scattering detects cells in flow cytometery where Forward scattering measures size and Side scattering measures granularity. The Forward scattering was used to compare the size of the cells in the two populations.

2.6 STAINING

2.6.1 HISTOLOGICAL

2.6.1.1 ALP

ALP expression was analysed as it is known to initiate one of the earliest phases of osteogenesis (Weiss *et al*, 1986) as well as being involved in bone mineralization (Miyake *et al*, 1997).

Cells were placed in osteogenic media or culture media, as a control, for various time points. For ALP expression analysis, the cells were fixed by 4% paraformaldehyde (PFA) for 10 min before they were washed by phosphate buffered saline (PBS). Thereafter, the freshly prepared ALP staining mixture (Figure 2.4), 0.5 ml/cm^2, was added onto the cells. After 45 min incubation the ALP staining mixture was removed and the cells were washed three times with PBS. The cells were left in PBS and images were captured immediately.

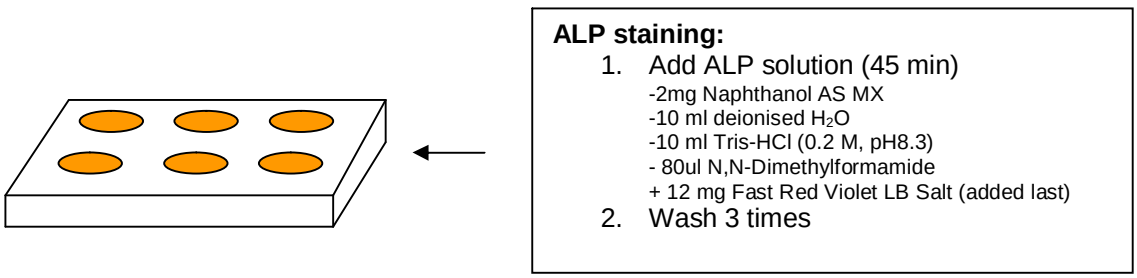

Figure 2.4. Protocol of ALP staining. The ALP solution was prepared fresh and added straight onto the cells and incubated for 45 min in room temperature.

2.6.1.2 SIRIUS RED

Collagen expression was analysed by Sirius Red S staining. Collagen is the major component in the specialised organic matrix of bone tissue (Thibodeau & Patton, 2007).

The cells were incubated in osteogenic media for 3 weeks before they were fixed in 4% PFA for 15 min. After fixation the cells were washed with PBS and air dried. The Sirius Red dye, 100mg/ml, was freshly prepared in saturated picric acid. The cells were stained for 1 h under mild shaking on a microplate shaker. Thereafter, the dye solution was removed and the stained layer was washed by 0.01 M hydrogen chloride (HCl) to remove excess dye. The stained material was extracted by 0.1 M sodium hydroxide (NaOH) in 1 ml/well (in a 24-well plate) on a microplate shaker for 30 min at room temperature. The extracted dye solution was measured using a spectrophotometer to detect absorbance at 550 nm where 0.1 M NaOH was used as reference. The protocol was adapted from Tullbert-Reinert & Jundt (1999).

2.6.1.3 ALIZARIN RED S

In order to measure mineralization by cells, Alizarin Red S staining and quantification was performed. Alizarin Red S forms a complex with the Ca^{2+} in the hydroxyapatite (see Chapter 1.2).

The cells were washed in Ca^{2+} free PBS before being fixed for 10 min in 4% PFA. After a rinse with deionised water, Alizarin Red S solution 1 ml/well, in 24-well plate, (2 w/v-% in deionised water, pH 4.1-4.2) was added to the cells. After 10 min, the Alizarin Red S solution was removed and the cells were washed four times with deionised water to remove any excess dye. The dye was dried before images were captured of the cells using CoolSnap-Pro camera through an Olympus BX50 microscope using Image-Pro Plus 4.5 software.

2.6.1.3.1 PROTOCOL QUANTIFICATION

The Alizarin Red S-calcium complexes were extracted by 10 % cetylpyridium chloride in 10 mM sodium phosphate (w/v, pH 7.0) for 2 h. The result was analysed with spectrophotometer at 562 nm (Stanford *et al,* 1995). Extraction buffer was used as reference.

2.6.2 IMMUNOCYTOCHEMICAL

Desmin is an early myogenic marker (Lewis *et al*, 2000) and α-sarcomeric actin a myotube marker (Lancioni *et al*, 2007). In order to visualise terminal myogenic differentiation, cells were stained for the presence of these two markers (Table 1.1). The cells were stained using primary antibodies, specific for desmin or α-sarcomeric actin and thereafter specific secondary antibodies (see Table A9.4). The cells were imaged by either inverted flourescent microscopy or confocal microscopy.

The cells were seeded onto glass cover slips and cultured to confluency; thereafter, myogenic media or control media was added onto the cells for 4 days. After 4 days the cells were lightly fixed for 5 min with 2 % PFA and, after 2 washes with PBS, with ice-cold Metanol (MeOH) for 10 min. If the staining was not performed directly, the cells were stored in PBS with 0.0625 % Sodium azide (NaN_3) in 4 ºC until stained.

Before the start of the staining the cells on the cover slips were washed five times in freshly prepared PBS before they were placed on home-made stands (Figure 2.5). The cells were permeabilised by a solution containing 0.25 % Triton-X (v/v) and 0.0625 % NaN_3 in PBS for 15 min. Meanwhile the primary antibodies were diluted in antibody diluent *i.e.* PBS, 10 % heat-inactivated FBS, 0.0625 % (w/v) NaN_3 and 0.1 M lysine; the desmin specific antibody was diluted 1:200 and the α-sarcomeric actin 1:500. The primary antibody was added onto the cells and incubated for 1h. Thereafter the cells

were washed 5 times in freshly prepared PBS, before the specific secondary antibodies and 4, 6-diamidino-2-phenylindole (DAPI), diluted in antibody diluent, were added and incubated with the cells for 30 min. The secondary antibody for desmin staining was diluted 1:200, and for α-sarcomeric actin diluted 1:800 (see Table A9.4 for antibody details).

After the incubation with the secondary antibodies the cells were mounted onto glass slides with Citiflour and sealed with nail varnish. Example of the staining can be seen in Figure 2.6.

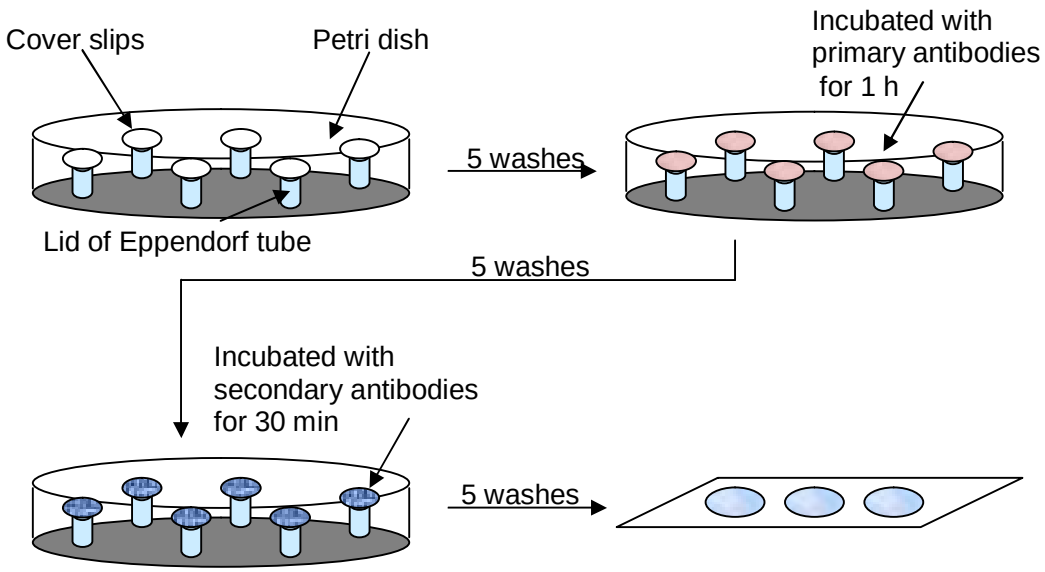

Figure 2.5. Staining procedure. The cover slips with the cells were first washed five times in PBS before placed on stands made of Petri dishes and eppendorf lids. First the cells were permeabilised by 0.25 Triton-X for 15 min before they were washed five times in PBS. Therafter the primary antibodies in antibody diluent were added to the cover slips for 1 h. After the 1h incubation the cover slips were washed again five times, before the secondary antibodies in antibody diluent were added for 30 min. Finally, the cover slips were washed five times before being mounted onto glass slides.

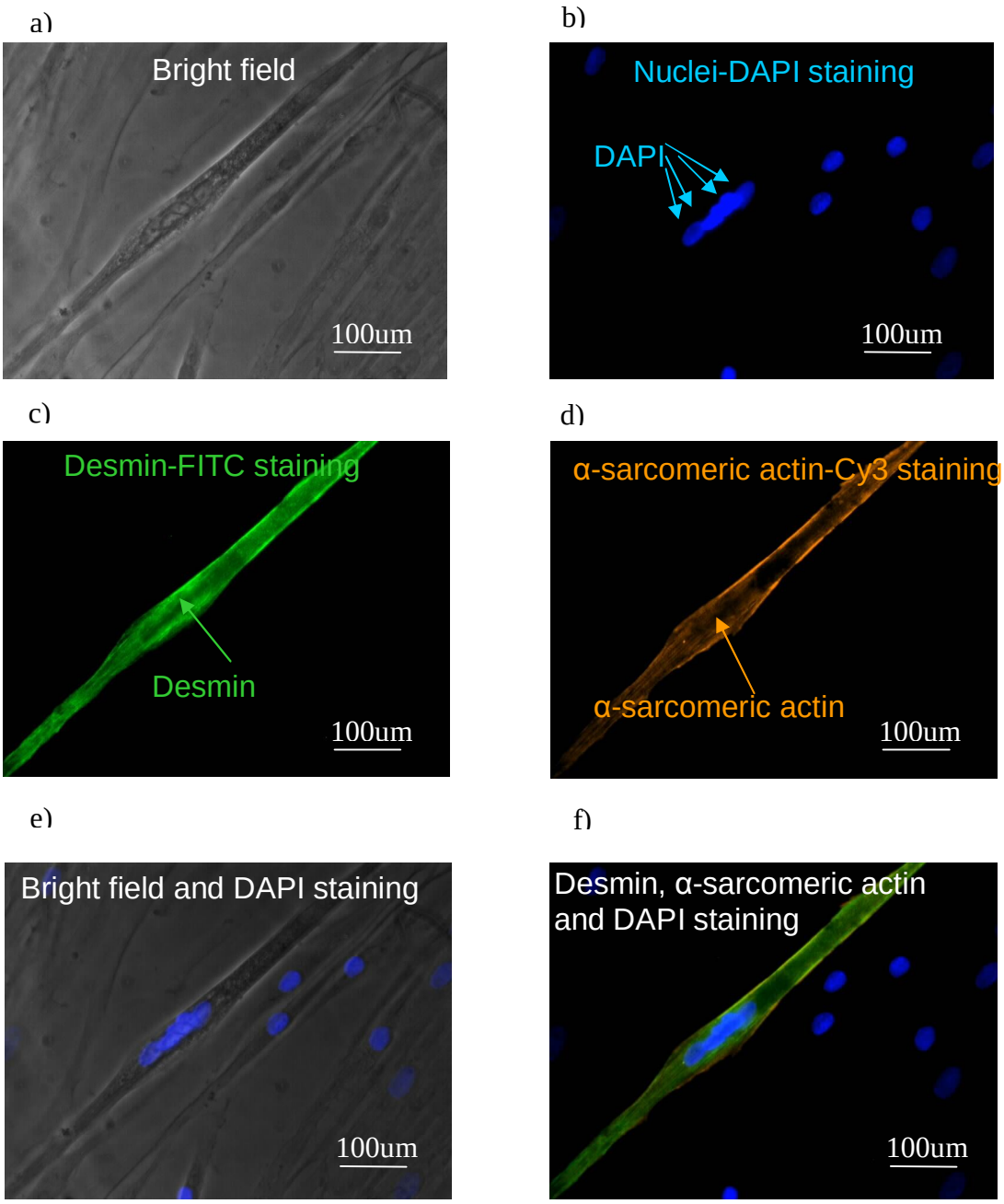

Figure 2.6. Example staining of MDCs in myogenic media. MDCs in a) bright field, b) nuclei stained by DAPI, c) desmin stained by FITC, d) α-sarcomeric actin stained by Cy3, e) merged photograph of a and b, f) merged photograph of b, c, and d.

2.7 ENZYME IMMUNOASSAY-ALP ACTIVITY

The ALP activity was measured by p-nitrophenyl phosphate (p-NPP) kit according to the manufacturer's guidelines. The cells in the 24-well plate were first washed by PBS then 200ul of 1%Triton-X/PBS (v/v) was added to each well (24-well plate) while they were shaken for 20 min on a microplate shaker (Biometra WY16). An aliquot of 50 ul of the Triton-X/ALP/PBS mixture was transferred in duplicates to a 96-well plate for exactly 30 min of incubation in the dark at room temperature with p-NPP solution, consisting of 1.0 mg/ml pNPP, and 0.2 M tris(hydroxymethyl)aminomethane (Tris) buffer. During the incubation following reaction took place.

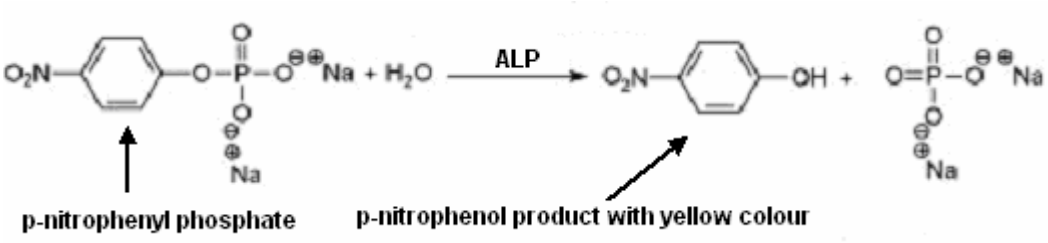

Figure 2.7. ALP catalyzes the reaction to transform p-NPP to p-nitrophenol. The final product of p-nitrophenol has a yellow colour which absorbance can be measured using spectrophotometer at 405 nm.

The reaction was stopped by 150 ul /well 1M NaOH and the ALP activity absorbance was read at 405 nm in a plate reader (MRX-TC, Dynex Technologies) using software Revelation version 4.25. To assess the ALP activity per cell density the ALP activity was normalised to the cell number calculated using the MTT assay (Chapter 2.4.2.1).

2.8 FLOW CYTOMETRY

2.8.1 STRO-1 AND CD56

Flow cytometry was used to study the expression of Stro-1 and CD56 on the cells. The Stro-1 antibody was reconstituted in PBS to 500ug/ml and stored accordingly to manufacturer's recommendation; CD56 was delivered pre-reconstituted to 200 ug/ml (Table A9.4).

Subconfluent cells were washed then detached by 5-10 min incubation in accutase. The effect of accutase was inactivated by culture media and the cell suspension was transferred to flow tubes. The samples were washed twice in PBS by centrifugation for 5 min at 1300 rpm and then resuspended in 200 ul/sample Flow buffer *i.e.* 2% FBS in PBS. To each tube 2ul of Stro-1 or 10 ul of CD56 antibody was added. The cells were incubated with the antibody on ice for 1h before being washed twice in PBS by centrifugation for 5 min at 1300 rpm. The stainings were performed as single-stainings.

For cells incubated with Stro-1, 10 ul of R-Phycoerythrin (R-PE)-conjugated IgM specific, 1 mg/ml, secondary antibody was added together with 190 ul Flow buffer to each sample (see Table A9.4). For cells incubated with antibodies for CD56, 5ul of Alexa Fluor 488-conjugated IgG_1, 2 mg/ml, specific secondary antibody (see Table A9.4) together with 190 ul Flow buffer was added to the cells. For both cells incubated with antibodies Stro-1 or anti-CD56 the incubation period was 30 min on ice. After incubation the cells were washed three times in PBS by centrifugation for 5 min at 1300 rpm and resuspended in Flow buffer.

The cells were analysed in terms of size, granularity and fluorescence using the software CellQuest and FACScanTM (Becton Dickinson). Light scatter identified cells and 10000 cells/sample were counted and gated. Immunopositivity was determined by comparison with cells incubated with only the secondary antibody.

2.8.2 APOPTOSIS AND NECROSIS

The levels of apoptosis and necrosis of cells were analysed by staining with Annexin V-FITC and Propidium iodide (PI). Annexin V-FITC is a fluorescent probe which binds to phosphatidylserine in the presence of calcium. Phosphatidylserine is normally found on the internal part of the plasma membrane. The affinity between Annexin V and phosphatidylserine can be used in apoptosis measurements since the cell membrane, including the phospholipids, start to loose its asymmetry at an early stage of apoptosis (Chapter 1.7). PI is a nucleus stain, for which the cells stain positive when their membrane have been completely compromised as in necrosis.

2.8.2.1 PROTOCOL

The cells were detached by accutase that was later inactivated by culture media before the cells were washed twice in PBS by centrifugation at 1300 rpm. Thereafter, the cells were resuspended in 500 ul binding solution/sample *i.e.* 10X binding buffer in 450 ul deionised water. Finally, 5 ul of Annexin V-FITC and 10 ul of PI were added to each sample. The samples were incubated 10 min in darkness before being analysed by flow cytometry.

In order to avoid superimposition between FITC and PI, the settings on the flow cytometer were adjusted (Figure 2.8).

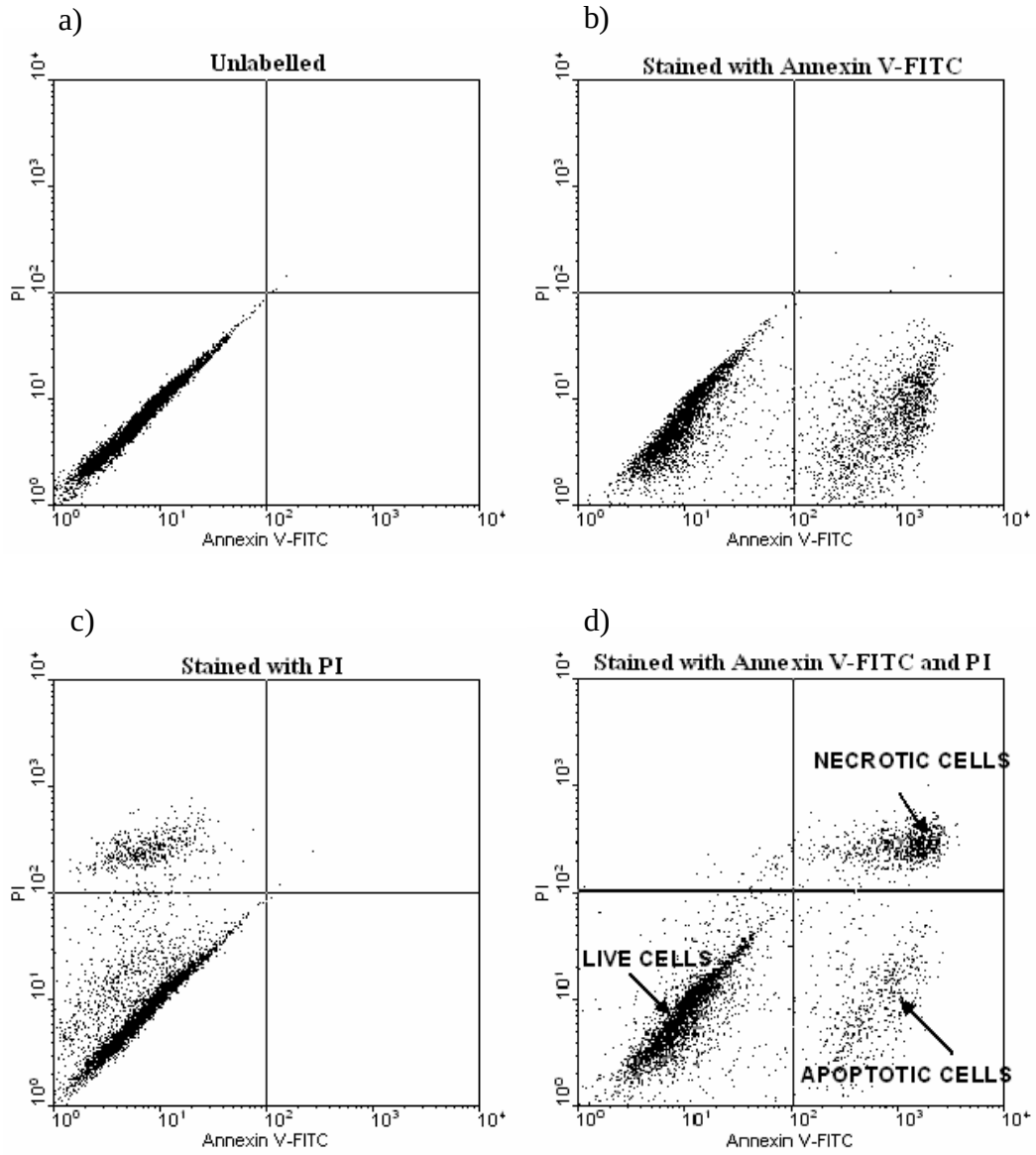

Figure 2.8. Graphs of MSCs stained with either Annexin V-FITC or PI or both or left unlabelled. MSCs a) unlabelled b) labelled with only Annexin V-FITC, c) labelled only with PI and d) labelled with both PI and Annexin V-FITC.

2.9 REAL-TIME/Q-POLYMERASE CHAIN REACTION (PCR)

2.9.1 ISOLATION OF RNA

Isolation of RNA was performed by the TRIzol method according to manufacturer's protocol (Table A9.6). At the desired time point, the samples were lysed in TRIzol, 0.125 ml/cm^2; the samples were first homogenised by pipetting before they were transferred to 1.5 ml eppendorf tubes where they were vortexed to homogenise the sample further. If isolation was not performed immediately, the samples were stored at -80 °C.

Before isolation, the samples were thawed and incubated for 5 min at room temperature; chloroform, 0.2 ml/ml TRIzol, was then added to the samples. The samples were shaken for 15 sec and incubated in room temperature for 2-3 min before centrifuged (Sorvall Legend RT) at 11999 x *g* for 15 min at 4 ºC. This caused a phase separation with an upper aqueous colourless phase, where the RNA remained and a red phenol based lower base.

The aqueous RNA phase was transferred to a fresh 1.5 ml-eppendorf tube and RNAse free glycogen, final concentration of 0.3ug/ul, was added to the samples as a RNA carrier. The RNA was precipitated by iso-propyl alcohol, 0.5 ml/ml TRIzol and incubated for 10 min before the samples were centrifuged for 10 min at 11999 x *g* at 4 ºC.

The supernatant was removed and the RNA was washed by 1ml ethanol (EtOH)/ml TRIzol and mixed by vortexing; thereafter, the samples were centrifuged by 5 min at 7499 x *g* at 4 ºC. After centrifugation, the supernatant was removed and the samples were air dried for 5 min before resuspended in nuclease-free water and dissolved by 10 min at 55 ºC. The quantity and the quality of the RNA sample was assessed by

spectrophotometer. All the RNA samples were diluted by nuclease-free water to 25 ng/ul; the quality, which ranged between 1.6 and 2.0, was measured by the ratio of 260/280 with corrections of absorbance at 320 nm, since dirty cuvettes and dust particles cause light scatter at 320 nm.

2.9.2 RNA TO cDNA CONVERSION

The RNA was converted to cDNA by using the High Capacity cDNA Reverse Transcription kit accordingly the manufacturer's protocol (Table A9.5). The number of desired qPCR reactions was calculated first. Each reaction consisted of equal parts, 1:1, Master Mix (10X RT buffer/ 25X dNTP Mix/ 10X Random Primers/Multiscribe Reverse Transcriptase/ nuclease-free water, 2:0.8:2:1;4.2, v/v/v/v/v) and RNA, 10 ng/reaction, diluted in nuclease-free water. The diluted RNA and Master Mix were added to a tube and mixed well. Before placing the tubes in the thermal cycler (PTC-100, Genetic Research Instrumentation, Ltd), the samples were lightly centrifuged (MSE, Microcentaur, Scotlab) for 5 sec at 1000rpm.

Table 2.3. The program used to convert the Master Mix and RNA mixture to cDNA.

	STEP 1	**STEP 2**	**STEP 3**	**STEP 4**
Temperature (ºC)	25	37	85	4
Time	10 min	120 min	5 sec	∞

2.9.3 Q-PCR

RT-or q-PCR is a method to quantitative analyse the gene expression *i.e.* mRNA in cells. First the mRNA has to be converted to cDNA (Chapter 2.9.2) and thereafter the cDNA is replicated by q-PCR. Sequence-specific DNA oligonucleotide probes, with a fluorescent reporter dye and a quencher, hybridize with the complementary strand of cDNA (Figure 2.9). The fluorescence quenching depends on the proximity of the reporter dye and the quencher. When Taq polymerase adds nucleotides from each primer it also removes the probe from the template DNA (Figure 2.9). This separates the quencher from the reporter dye resulting in fluorescence. The fluorescence is measured continuously over the run of 40 cycles and the gene expression can therefore be quantified.

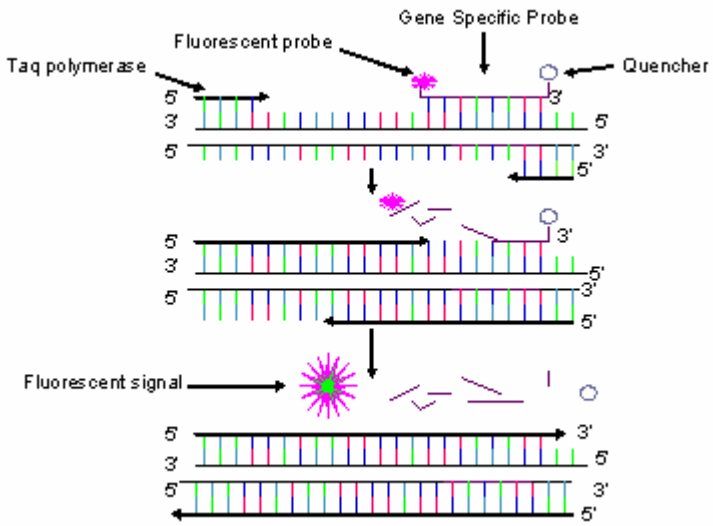

Figure 2.9. Description of q-PCR. Gene specific probes, with a fluorescent reporter dye and a quencher, hybridize with the complementary strand of cDNA. Taq polymerase adds nucleotides from each primer so it removes the probe from the template DNA; this separates the quencher from the reporter dye resulting in fluorescence.

The calculation of the quantification was performed by the Ct method, where Ct is the number of cycles before the fluorescence reached the base line. The house keeping and the gene of interest were amplified in separate wells; the average Ct value of the gene of interested was subtracted from the average value of Ct for the house keeping gene generating a ΔCt value. The ΔCt value was normalised to the control *i.e.* creating a ΔΔCt value and the result was presented as $2^{-\Delta\Delta Ct}$. This equation takes into account the exponential nature of PCR reaction.

2.9.3.1 PROTOCOL

The RT-PCR reaction was set up by adding 1.25ul of gene assay, 2.5 ul of cDNA, 8.75 ul of nuclease-free water and 12.5 ul of TaqMan Universal Master Mix to each well in a special designed qPCR 96-well plate. The gene assays were designed and supplied by Applied Biosystems (see Table A9.2 for more details). The fluorescence was measured after each cycle (Table 2.4) and 40 cycles were performed. GapdH was used as the house keeping gene if not otherwise stated. Ct levels ≥ 37 were considered to be negative.

Table 2.4. The qPCR machine measured the fluorescence continuously during the PCR. Step 1 and 2 are only performed during the first cycle. Total numbers of cycles were 40.

	STEP 1 -only cycle 1	**STEP 2 -only cycle 1**	**STEP 3**	**STEP 4**
Temperature (ºC)	50.0	95.0	95.0	60.0
Time (min)	2.00	10.00	0.15	1.00

2.10 STATISTICAL ANALYSIS

The following section will go through the statistics and the terminology that have been used. The experiments were performed on *n* number of patients in triplicates, if not otherwise were stated. In a few cases the experiment has only been performed on one patient (n=1), then the results have been presented as mean ± 1standard deviation (sd). In these cases an up-or-down regulation is defined as an increase/decrease > 1sd. Sd is a measurement of the average spread of data around the mean and is defined by following equation:

$$Sd = \sqrt{\frac{1}{n}\sum_{i=1}^{n}(x_i - \bar{x})^2}$$

where; n = number of replicates

x_i = data of tested sample

$\bar{x}$ = mean of all tested samples

The majority of experiments were performed on more than 1 patient and then the results were presented as mean±sem. Sem gives a measure of precision of the estimated mean, *i.e.* sem gives an interval within the true mean is expected to lie within. Sem is derived from sd accordingly following equation:

$$Sem = \frac{1sd}{\sqrt{n}}$$

where; n= number of samples

Due to lack of consenting volunteers only three samples of MDCs were used in this thesis. It was considered not sensible to perform any kind of statistical analysis, such as ANOVA or t-test, due to the risk or impact of outliners within the samples. Therefore, in cases n>1 the trends of the data are reported and sample size estimation has been performed. The trends were reported in following form:

$$Samples_{Positive} / Samples_{Total}$$

where the number of samples following the trend ($samples_{Positive}$) are compared with the total number of analysed samples ($samples_{Total}$).

The sample size estimations have calculated the minimum sample size required to accept the outcome of a statistical test at a significance level of 0.05 and power of 80%. Using a significance level of 0.05 is generally accepted as a cut-off point and a power effect of 80% is generally considered to be the lowest power to accept the sample number for statistical analysis. In order to perform sample size estimations software G*Power version 3.1 has been used and the statistical analysis has been performed accordingly a statistician recommendation. Another important parameter, for sample size estimations, is variability *i.e.* sd of the data.

Pearson correlation coefficient, r, is used to measure linear correlation of a set of samples; r has a value between -1 and 1. R^2 gives the proportion of variation of one variable, y, explained by variable, x.

CHAPTER 3:

RESULT SECTION 1

- CULTURE AND DIFFERENTIATION CONDITIONS

3.1 INTRODUCTION SPECIFIC FOR RESULT SECTION 1

In this chapter the cell populations, both MSCs and MDCs, were analysed in terms of their differentiation potential *i.e.* their potential to differentiation along the osteogenic, adipogenic and myogenic lineage. This was done to verify the cells differentiation potential. The importance of CD56 for the myogenic differentiation will also be discussed.

The CD56+ fraction of MDCs, *i.e.* $MDCs^{CD56+}$, has previously been analysed in the laboratories of EDI in terms of their cell surface expression and differentiation potential (see Sinanan *et al*, 2004 for more details). In this thesis the CD56- fraction, *i.e.* $MDCs^{CD56-}$, was analysed in terms of their differentiation potential along the adipogenic, osteogenic and myogenic lineage. This was performed to investigate if the $MDCs^{CD56-}$ contained osteogenic cells and also compare this fraction in terms of their differentiation potential of the already analysed $MDCs^{CD56+}$ (Sinanan *et al*, 2004). Throughout this chapter MDCs will refer to the unsorted parental population of MDCs and $MDCs^{CD56-}$ to the sorted CD56- fraction of MDCs.

Osteogenic differentiation protocols with various concentrations of the osteogenic components have been reported in the literature; thus, the osteogenic media was titrated for both MSCs and MDCs (the unsorted parental population of MDCs) in terms of metabolic activity, ALP activity and mineralization. Furthermore, also the two cell types maximal PD numbers were determined

3.2 METHODS SPECIFIC FOR RESULT SECTION 1

3.2.1 MAGNETIC-ACTIVATED CELL SORTING (MACS)

MACS is an isolation method of cells depending on their surface markers. The cells were incubated for 30 min at 4 °C with magnetic beads that were coated with antibodies to CD56. They were then placed in a column and exposed to a magnetic field. The $CD56^+$ cells where the magnetic beads attached were held within the column due to the magnetic field; the $CD56^-$ cells were washed through by MACS buffer (Figure 3.1). The cells of the negative fraction used in this study had been previously isolated by colleagues at EDI and had been cryopreserved in liquid nitrogen. This fraction was named $MDCs^{CD56-}$ and the parental population *i.e.* the unsorted population of MDCs was named MDCs.

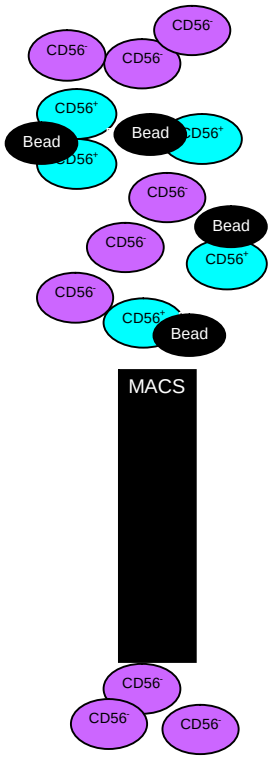

Figure 3.1. Cell isolation by MACS. The cells were incubated with magnetic beads coated with CD56 specific antibodies. The mixture was placed in a column and exposed to a magnetic field so the $CD56^+$ cells (turquoise) *i.e.* $MDCs^{CD56+}$ stayed in the column and the $CD56^-$ cells (purple) *i.e.* $MDCs^{CD56-}$ were washed through by MACS buffer.

3.3 RESULTS FOR RESULT SECTION 1

3.3.1 VERIFICATION OF DIFFERENTIATION POTENTIAL

3.3.1.1 MSCs MULTIPOTENCY

It has been known for many years that MSCs have the potential to differentiate along the osteogenic, adipogenic and chondrogenic lineages (Pittenger *et al*, 1999). Researchers have tried to explore where the limits of MSCs multipotency lay, for example, there have been some reports that MSCs can differentiate along the myogenic lineage (Lee *et al*, 2005). In this section, Chapter 3.3.1.1, MSCs myogenic and adipogenic differentiation potential will be studied, the osteogenic will be discussed in Chapter 3.3.2.2.

3.3.1.1.1 MYOGENIC DIFFERENTIATION

In order to investigate whether the MSCs could differentiate along the myogenic lineage, cells were placed in a well-established *in vitro* myogenic media (Allen & Boxhorn, 1989) for six weeks and their gene expression of desmin and myogenin was studied. Desmin's role *in vivo* is linked to the adjacent myofibrils to maintain sarcomere adhesion and structure (Stewart & Rittweger, 2006) and has been used as early marker for myogenic commitment (Sinanan *et al*, 2004). Myogenin is a transcription factor that is expressed during the terminal myogenic differentiation (Charge & Rudnicki, 2004; Stewart & Rittweger, 2006; Chapter 1.3.1). The cells morphology was also studied by PCM to see if the cells formed myotubes. Desmin expression of a low level was found in the MSCs, but no upregulation of gene expression, defined as an increase > 1sd, could be detected by qPCR (Figure 3.2). Myogenin (data not shown) was neither expressed nor could any myotubes be detected by PCM (Figure 3.3). These results are

consistent, since MPCs start to express myogenin when myoblasts fuse to myotubes (Charge & Rudnicki, 2004; Stewart & Rittweger, 2006). These results clearly show that human MSCs are not able to differentiate along the myogenic lineage, at least, not by using the published protocol. It was concluded that even though researchers have stated that MSCs are able to differentiate along the myogenic lineage, this is still very uncertain with inconsistent results; for example, Lee *et al* (2005), managed to fuse human MSCs with mouse myoblasts but no group has managed to differentiate a pure monoculture of human MSC cultures along the myogenic lineage.

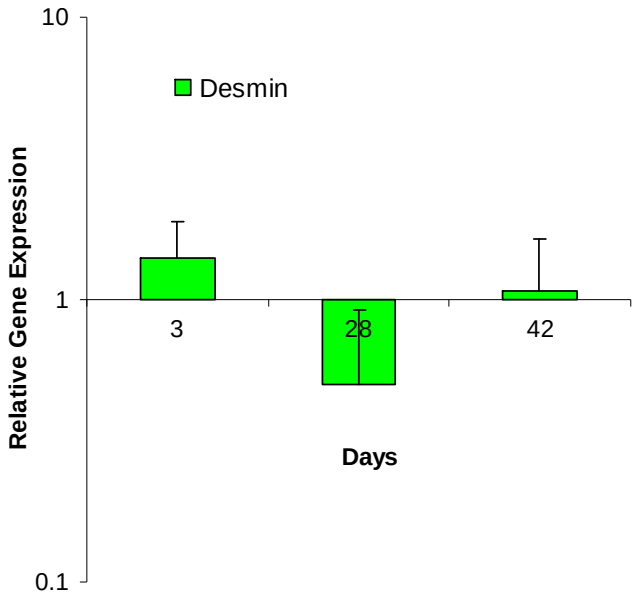

Figure 3.2. MSCs did not upregulate desmin in myogenic media. The MSCs in myogenic media did not upregulate, defined as an increase > 1sd, their gene expression of desmin during six weeks compared to MSCs in culture media. The result (n=1) is presented as mean + 1sd of triplicates.

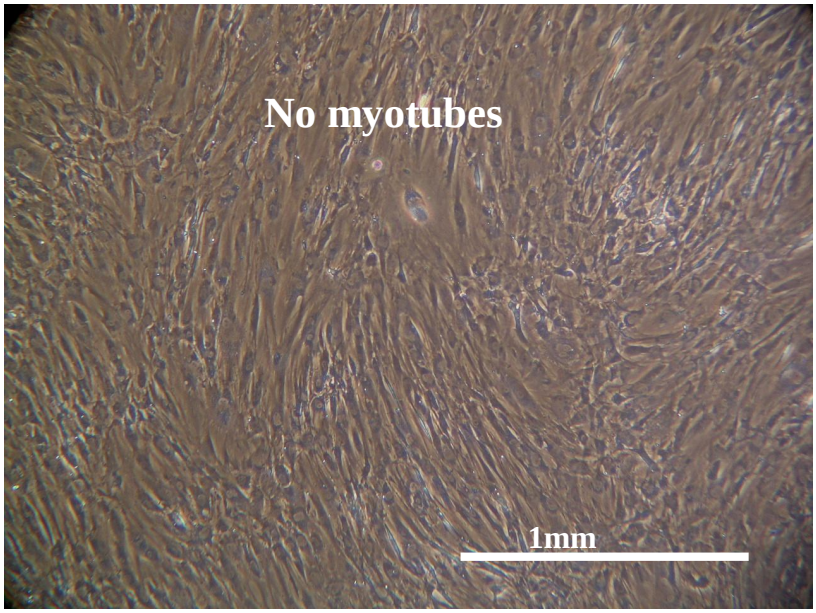

(a)

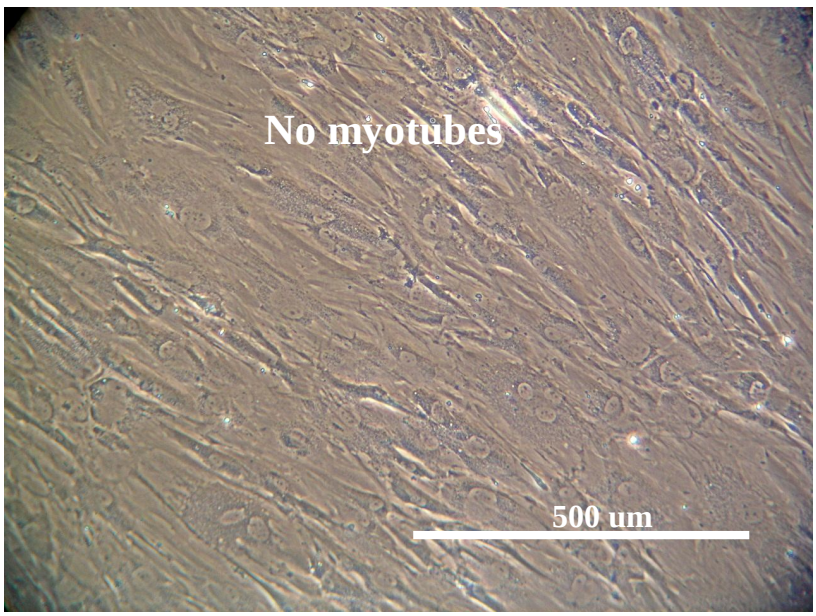

(b)

Figure 3.3. MSCs did not fuse into myotubes *in vitro*. No myotubes were detected throughout the test period of six weeks in myogenic media. The experiments (n=3) were performed in triplicates. Photographs taken through PCM at week 3 have the magnification a) x4 and b) x10.

3.3.1.1.2 ADIPOGENIC DIFFERENTIATION

It is known that MSCs can differentiate along the adipogenic lineage, when placed in adipogenic media (Pittenger *et al*, 1999). In this study, the MSCs upregulated, defined as an increase > 1sd, the adipogenic transcription factor PPAR-γ2 after 3 days (Figure 3.4) and this increased until day 28. The first lipid droplets could be detected by PCM after 2 weeks and the amount of lipid droplets continued to increase throughout the test period of six weeks (Figure 3.5). These experiments (Figure 3.4-3.5) show that MSCs have the potential to differentiate along the adipogenic lineage.

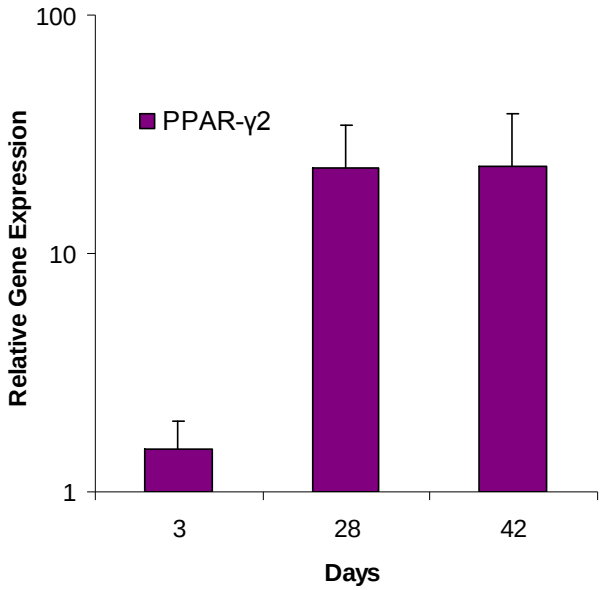

Figure 3.4. MSCs upregulated PPAR-γ2 in adipogenic media. The upregulation, defined as an increase > 1sd, of the adipogenic transcription factor PPAR-γ2 was detected after 3 days and increased to day 28. This showed that MSCs can differentiate along the adipogenic lineage. The experiment was performed in triplicates and the result (n=1) is presented as mean + 1sd of triplicates.

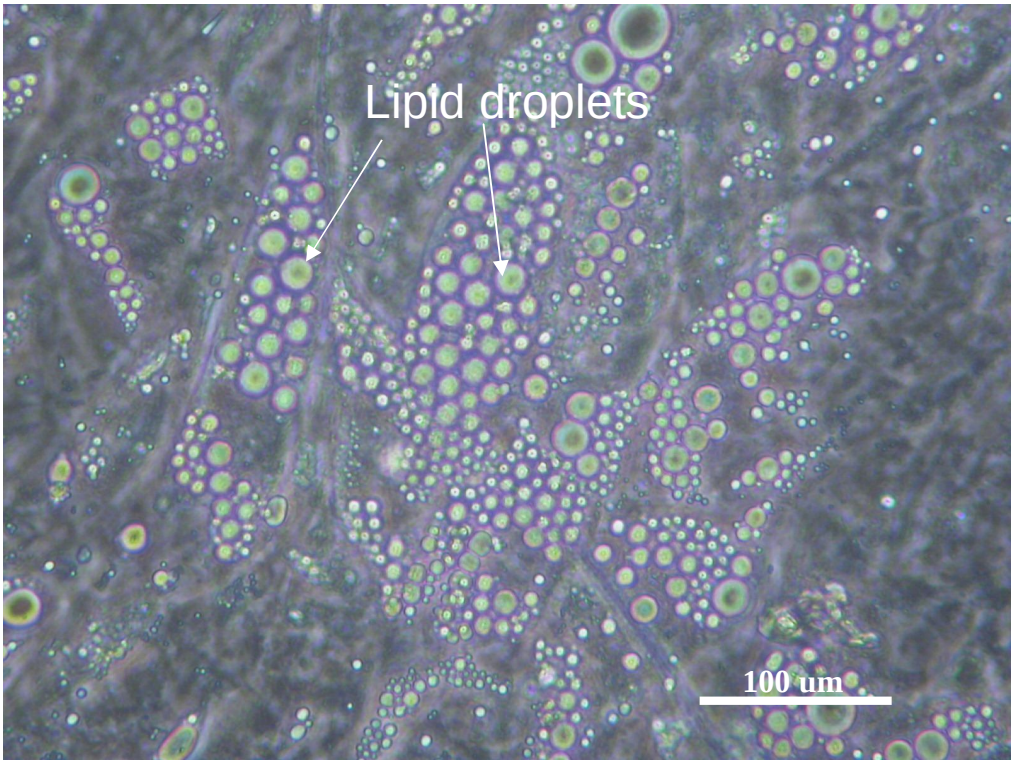

Figure 3.5. MSCs formed lipid droplets in adipogenic media. MSCs could form lipid droplets. Photograph was taken by PCM after 6 weeks in adipogenic media. The experiments were performed on three patients (n=3) in triplicates. Magnification x20.

3.3.1.2 MDCs MULTIPOTENCY

3.3.1.2.1 MYOGENIC DIFFERENTIATION

The MDCs placed in myogenic media could easily differentiate along the myogenic lineage and some of the desmin-expressing myoblasts had fused and formed multinucleated myotubes after 4 days (Figure 3.6).

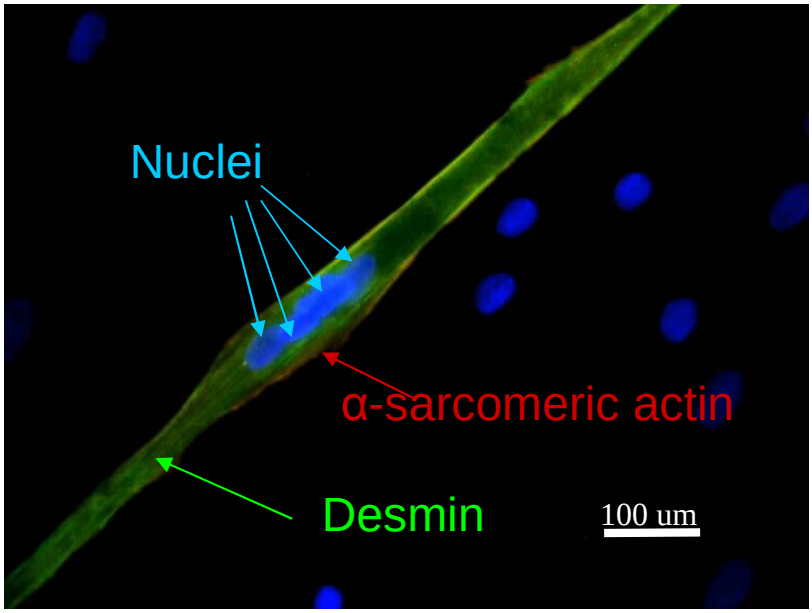

(a)

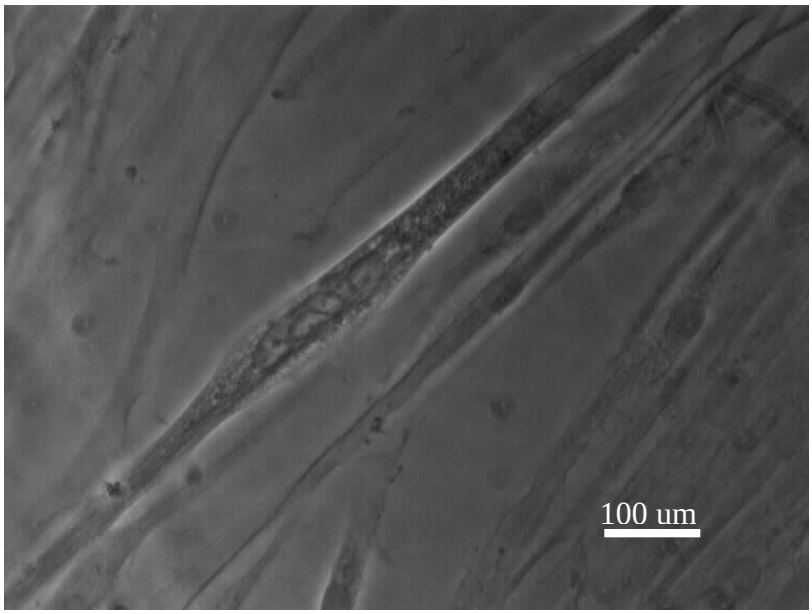

(b)

Figure 3.6. Myogenicity of MDCs. The cells a) were stained for desmin (green) and α-sarcomeric actin (red) and nuclei were stained with DAPI (blue) b) in bright field. All experiments were performed on three patients (n=3) in triplicates. Photographs taken by an inverted fluorescence and bright field microscope. Magnification x40.

3.3.1.2.2 THE IMPORTANCE OF CD56 FOR MYOGENIC DIFFERENTIATION

CD56 has been identified as a satellite cell marker (Mackey *et al*, 2009; see Chapter 1.3.1). In order to study its importance for myogenic differentiation, $MDCs^{CD56+}$ were depleted from the population by MACS. When the $MDCs^{CD56-}$ were placed in myogenic media they could not form myotubes; instead they formed multinucleated, dysmorphic myosacs (Figure 3.7). No myotubes could be detected by PCM in the $MDCs^{CD56-}$ population, and after 2 weeks the cells started to become rounded. When the cells were stained and analysed by confocal microscopy for desmin and α-sarcomeric actin, it became clear that the cells had fused to desmin-expressing myosacs. No α-sarcomeric actin was detected.

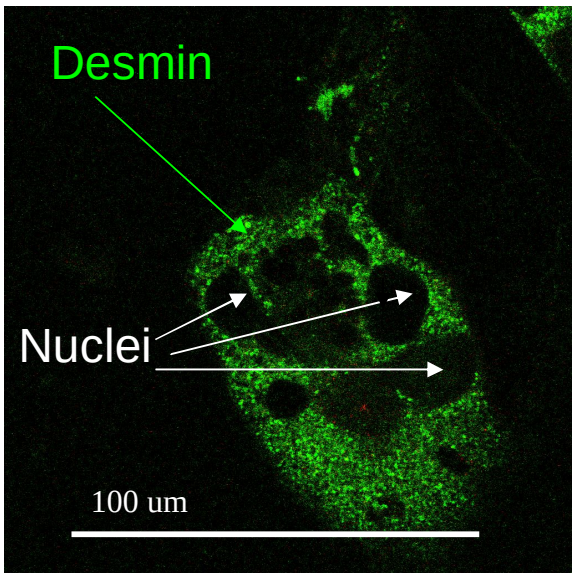

Figure 3.7. $MDCs^{CD56-}$ formed myosacs in myogenic media. $MDCs^{CD56-}$ formed myosacs after 2 weeks in myogenic media. The experiments were performed on two patients (n=2) in triplicates. Magnification x63.

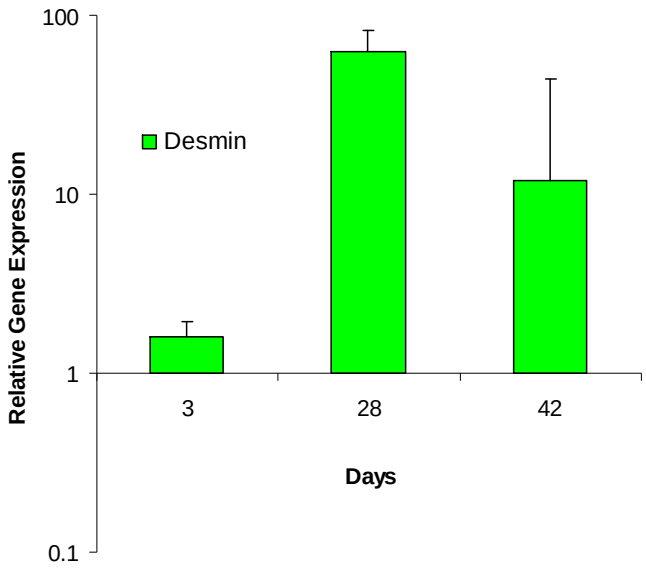

Figure 3.8. MDCs^{CD56-} upregulated desmin in myogenic media. MDCs^{CD56-} upregulated, defined as an increase > 1sd, desmin during six weeks in myogenic media, but did not express myogenin (data not shown). The experiment was performed in triplicates. Results (n=1) presented as mean + 1 sd of the triplicates.

The cells' gene expression was analysed by qPCR for desmin and myogenin and the MDCs^{CD56-} cells did upregulate, defined as an increase > 1sd, desmin expression over the test period of six weeks (Figure 3.8) but did not express myogenin (data not shown). It is known from previous studies that myosacs express desmin (Hill *et al*, 1986).

3.3.1.2.3 ADIPOGENIC DIFFERENTIATION

In order to test if the MDCs^{CD56-} could differentiate along the adipogenic lineage, they were placed in adipogenic media for six weeks. In this study it was clearly shown that MDCs^{CD56-} could upregulate, defined as an increase > 1sd, PPAR-γ2 (Figure 3.9) and form lipid droplets (Figure 3.10) under adipogenic conditions. They started to form lipid droplets after 2.5 weeks and the formation continued during the whole test period (Figure 3.10). Previously, it has been demonstrated by Sinanan *et al* (2004) that the MDCs^{CD56+} could also form lipid droplets. Also Ozeki *et al* (2006) have previously shown that a human derived subpopulation of MDCs, MDCs$^{\alpha 7+}$, could differentiate along the adipogenic lineage.

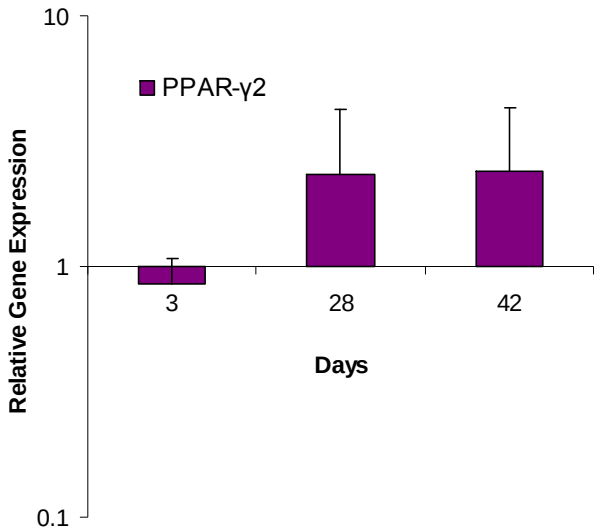

Figure 3.9. Expression of PPAR-γ2 in MDCs^{CD56-} in adipogenic media. The MDCs^{CD56-} showed upregulation, defined as an increase > 1sd, of PPAR-γ2 at day 28 and 42, which demonstrated that they could differentiate along the adipogenic lineage. The experiment was performed in triplicates. Results (n=1) presented as mean +1sd of the triplicates.

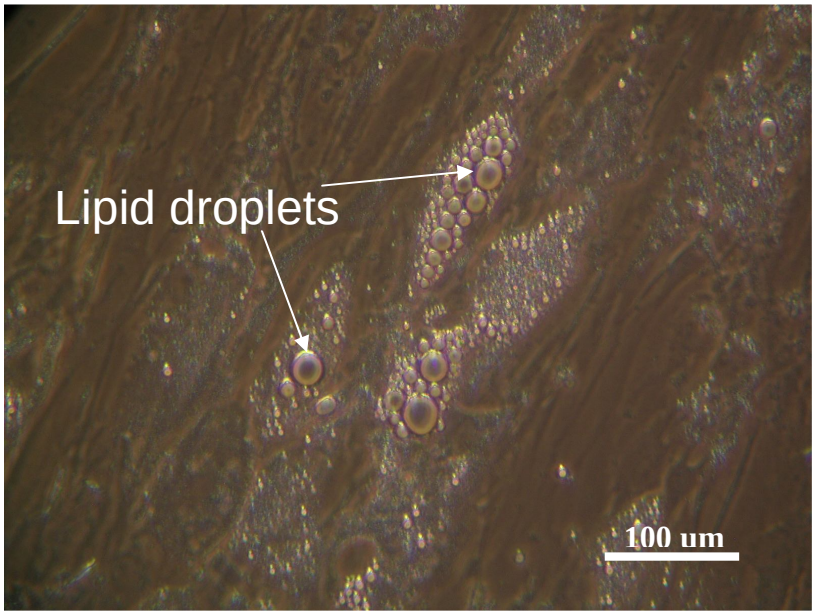

Figure 3.10. MDCs^{CD56-} formed lipid droplets. Picture taken of lipid droplets after six weeks in adipogenic media. The experiments were performed on two patients (n=2) in triplicates. Magnification x20.

3.3.1.2.4 OSTEOGENIC DIFFERENTIATION

In order to analyse if the MDCs^{CD56-} could differentiate along the osteogenic lineage, the cells were placed in osteogenic condition and stained for ALP. However, the results were inconsistent. One out of two patients expressed ALP (Figure 3.11), but the other patient did not (data not shown). The inconsistency in osteogenic response in MDCs^{CD56-} led to the need for the development of a reliable isolation method for osteogenic MDCs described in Chapter 4, result section 2.

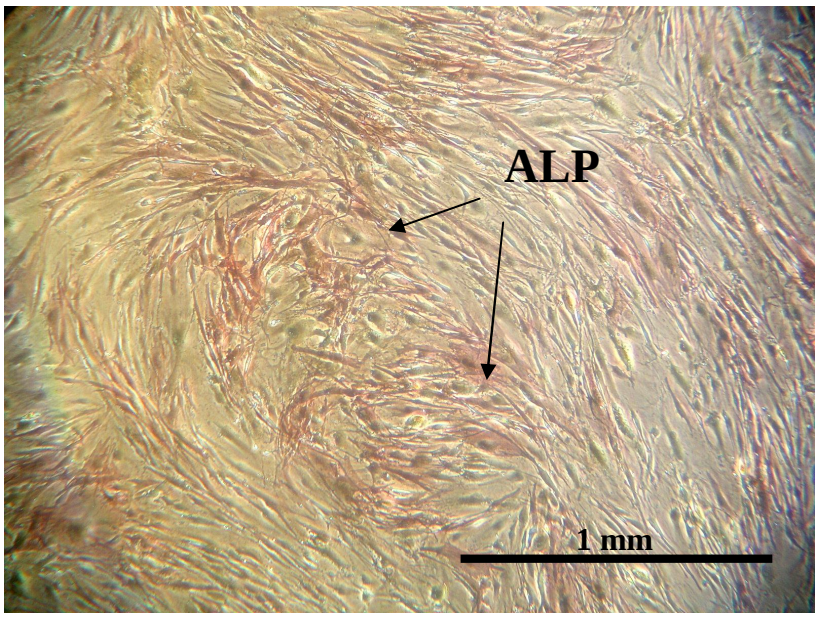

Figure 3.11. The ALP expression in MDCs^{CD56-} was inconsistent. MDCs^{CD56-} from one patient expressed ALP (see picture), but another sample from a different patient did not. Picture taken after two weeks in osteogenic media. Note: In this experiment osteogenic media recommended by Tulane Stem Cell Center was used (Table 2.2).

3.3.2 CULTURE CONDITIONS AND OSTEOGENIC MEDIA TITRATION FOR MSCs

3.3.2.1 OPTIMISING THE CULTURE MEDIA FOR MSCs FOR MAXIMAL CELL NUMBER

There is no general consensus about the optimal culture media for MSCs in the literature (Simmons *et al* 1991; Yu *et al*, 2005; Fox *et al*, 2007); therefore, various culture media with either DMEM or α-MEM as basal media and either 10 or 20% FBS was tested in terms of cell number over time. In order to do this MTT Assay was used; MTT Assay assesses the metabolic activity that correlates with cell number (Figure 2.3). In general, the yield of MSCs was higher, defined as an increase>1sd, when they had been cultured in 20% FBS at day 5 (Figure 3.12). In terms of basal media, the MSCs showed stark differences depending on the patient. Most MSCs had higher metabolic

activity in α-MEM compared to DMEM (Figure 3.12), the metabolic activity of MSCs from one tested patient barely increased in DMEM (Figure 3.12b); however, the metabolic activity of MSCs from one patient did increase in DMEM, but barely in α-MEM (Figure 3.12a). In summary, four out of five, tested MSC batches derived from specific patients had higher MSC number *i.e.* metabolic activity in α-MEM; thus, α-MEM was used in standard culture media for MSCs. Sotiropoulou *et al* (2005) also concluded that α-MEM was the best basal media after testing 8 different basal media for optimal MSC expansion. These results may explain why there are various different culture protocols for MSCs in the literature; as it has been shown here (Figure 3.12) MSCs are very patient dependent in their preferences in culture media.

a)

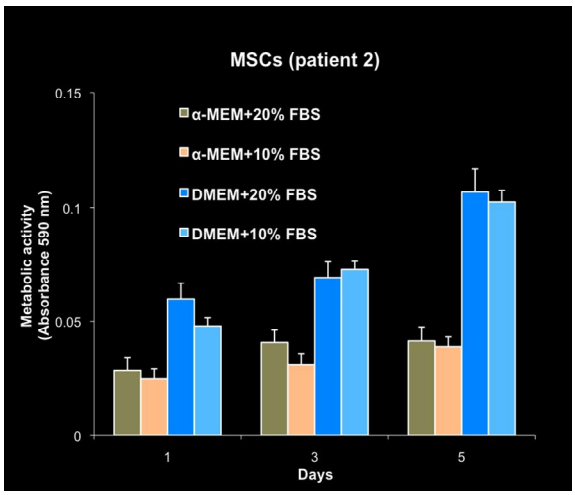

b)

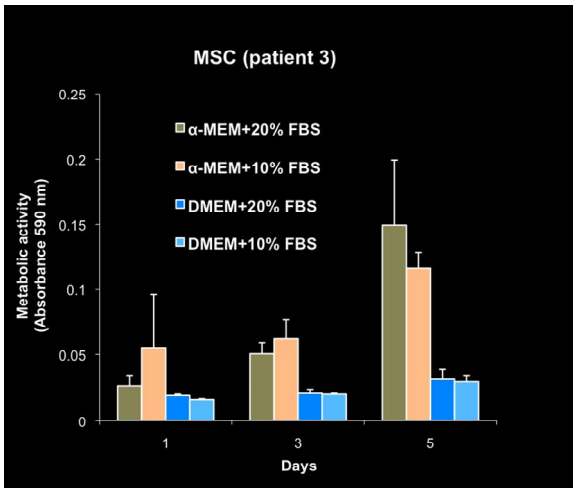

c)

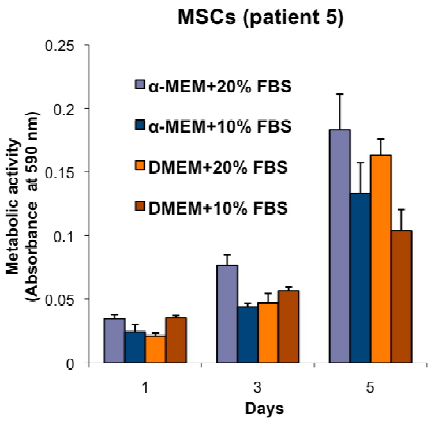

Figure 3.12. Impact of culture media on the metabolic activity of MSCs from three example patients. a) The metabolic activity of MSCs from patient 2 was clearly enhanced by DMEM based culture media. b) The metabolic activity of the MSCs from patient 3 was clearly enhanced by α-MEM based culture media, c) patient 5 appeared to prefer α-MEM as basal media but there was no distinct differences regarding the basal media. All experiments performed in triplicates. The results are presented as mean + 1sd of the triplicates. Difference is defined as an increase/decrease> 1sd.

The patient dependent differences in basal media preferences were consistent over time (Figure 3.13). Using the correct basal media could increase the number of PD before senescence *i.e.* maximal growth.

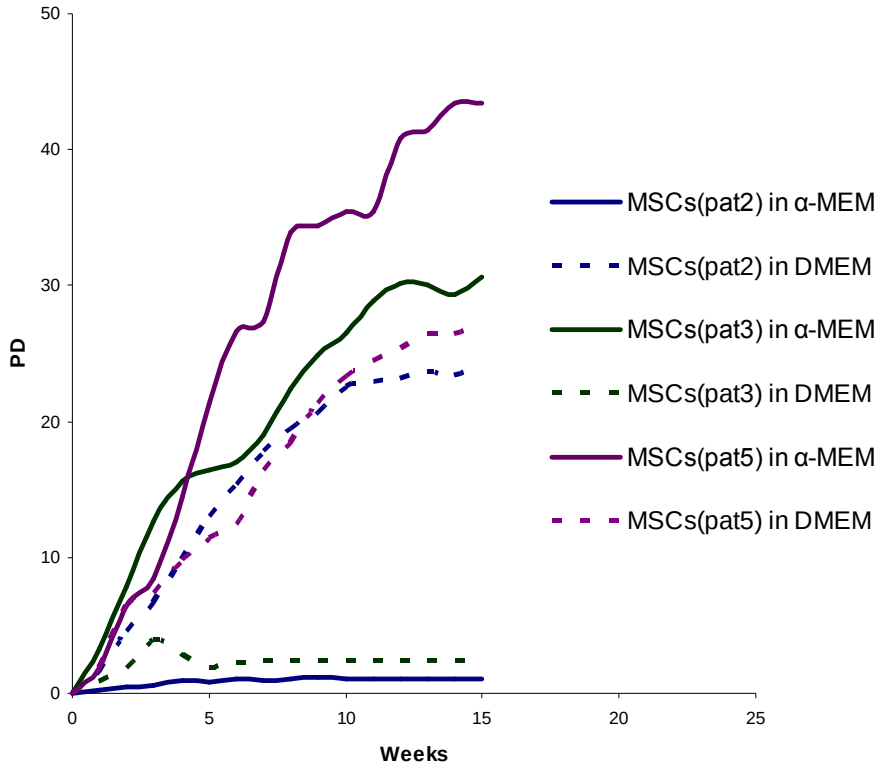

Figure 3.13. Number of PD of MSCs, over 15 weeks, in α-MEM or DMEM based culture media. Using a MSCs-matched basal media could increase the number of PD. All culture media were supplemented with 20% FBS and antibiotics.

In the literature, there have been reports that MSCs have a PD of approximately 20-40, depending on the age of the donor (Pittenger *et al*, 1999; Stenderup *et al*, 2003). MSCs derived from young donors tend to reach a higher PD before senescence compared with older donors (Stenderup *et al*, 2003). Senescent cells have an enlarged, flattened

morphology and an irreversible G1 growth arrest (Sethe *et al*, 2006). The MSCs investigated in this study appear to be able to reach a number of PDs in the same range as Pittenger *et al* (1999); however, all the donors in this study were relative young (Chapter 2.1.1) and only MSCs from patient 5 managed to reach a PD close to 40 (Figure 3.13). This could be explained by natural variations of the MSCs between the donors.

Studies have shown that human cells can divide between 500-5000 times during a life span *in vivo*, depending on the cell type. In addition to this stem cells should have the ability of self-renewal (Phipps *et al*, 2007). These numbers differ greatly from what was seen in this study (Figure 3.13) and in other *in vitro* studies where 20-70 PD are reported (Phipps *et al*, 2007). Rubin (1997) proposed that the decrease in the number of PD was a result of the inability of cells to adapt to the trauma of explant and *in vitro* cell culture.

3.3.2.2 TITRATION OF OSTEOGENIC MEDIA FOR MSCs

The use of varying concentrations of the components of osteogenic media have been reported in the literature, especially for dex (Ahdjoudi *et al*, 2001; van den Dolder & Jansen, 2007) and β-GP (Aslan *et al*, 2006; Ozeki *et al*, 2006). Therefore, in this study we have titrated these components, *i.e.* dex and β-GP, to find the optimal osteogenic differentiation media for MSCs. First, the optimal concentrations of dex and β-GP were established by analysing metabolic activity, ALP activity, mineralization and the gene expression of Runx2, Col1A1 and OP. The tested concentrations of dex were: 1, 10 or 100 nM in either 2 or 10 mM β-GP. The osteogenic differentiation pathway is very pH sensitive (Brandao-Bunch *et al*, 2005) and, thus, DMEM was chosen as basal media for osteogenic differentiation media since it has slightly higher pH than α-MEM.

3.3.2.2.1 METABOLIC ACTIVITY

When the metabolic activity of MSCs was measured in either 2 mM or 10 mM β-GP, it was clear that osteogenic media with 10mM β-GP, for all tested concentration of dex, had a negative impact (trend 2/2) on the metabolic activity of MSCs after 2 weeks compared to MSCs in control media (Figure 3.14). No decrease of metabolic activity was detected when cells were cultured in 2 mM β-GP, for all tested concentration of dex, compared to MSCs in control media. It has earlier been established that concentrations higher than 5 mM β-GP can cause apoptosis in osteoblasts (Meleti *et al*, 2000). This experiment showed that MSCs also start to show decreased metabolic activity, which can indicate cell death, after 2 weeks in osteogenic differentiation media with 10 mM β-GP (Figure 3.14b). Hence, only osteogenic media with 2mM β-GP was used in the following experiments.

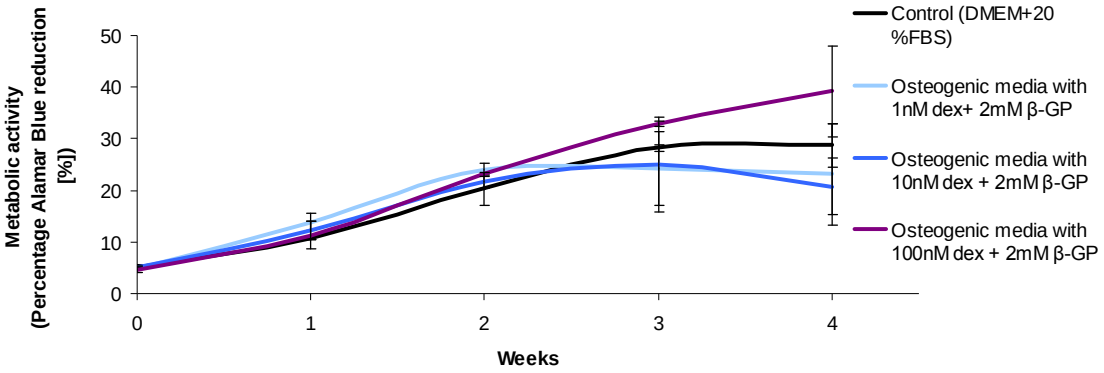

(a)

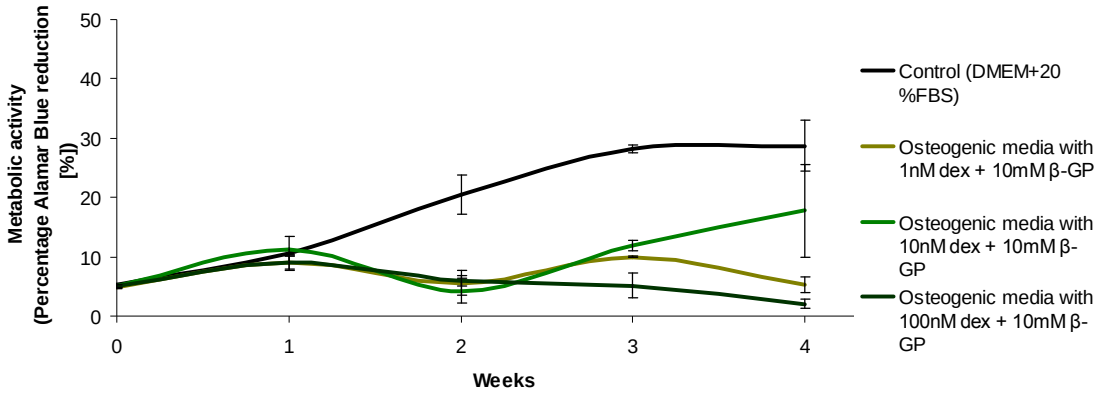

(b)

Figure 3.14. Concentration of β-GP has an impact on metabolic activity. Osteogenic media with a) 2 mM β-GP b) 10 mM β-GP. Alamar Blue assay was performed at day 0, 7, 14, 21 and 28. a) MSCs in osteogenic media with 2 mM β-GP compared with control media, b) MSCs in osteogenic media with 10mM β-GP compared with control media. There was no consistent decrease in metabolic activity between MSCs that had been in osteogenic media with 2 mM β-GP and control media. MSCs in osteogenic media with 10 mM β-GP had lower metabolic activity compared to MSCs in control media at week 2, 3 and 4 (trend 2/2 for all three conditions). The dex concentration did not appear to have a consistent impact on the metabolic activity of MSCs. All osteogenic media consisted of DMEM (low glucose), 20% FBS, 50ug/ml L-ascorbic acid and antibiotics. The experiments were performed on two patients (n= 2) in triplicates. Results presented as mean ± sem. Sample size calculation estimated that 4 samples were required to accept the outcome of a statistical test to see an effect of 10% lower metabolic activity, compared with control, at 2 weeks.

3.3.2.2.2 ALP ACTIVITY

ALP is an enzyme that hydrolyses β-GP; ALP exists in the bone marrow *in vivo* and has been used as a marker of early osteogenic activity (Ozeki *et al*, 2006). To test the impact of dex on the ALP activity of MSCs, the cells were placed in osteogenic media with varying concentrations of dex and ALP activity was assessed after 1 week (Figure 3.15). After 1 week, the highest ALP activity levels were detected in MSCs incubated in osteogenic media with 100 nM dex (trend 3/3) compared to MSCs in osteogenic media with 10 nM or 1 nM dex or control media.

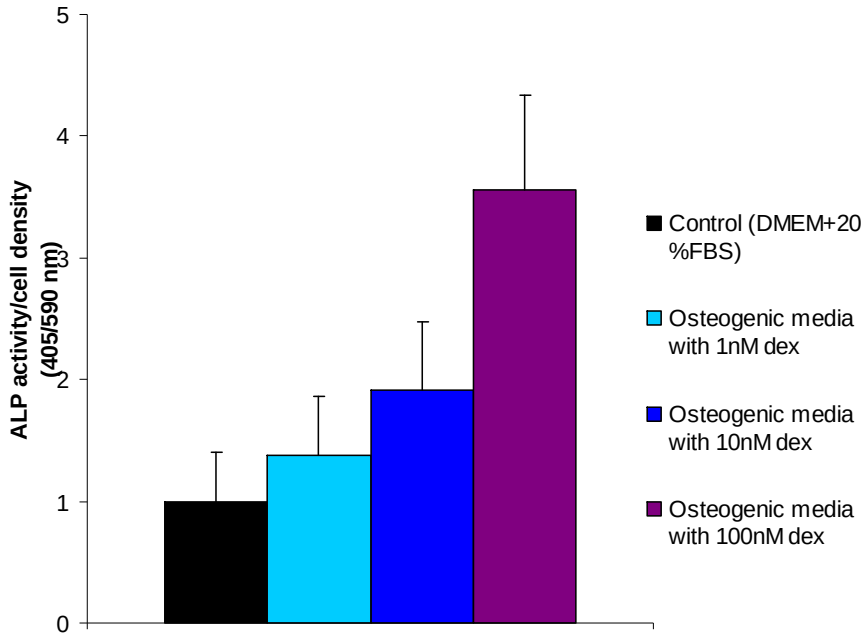

Figure 3.15. Impact of dex on ALP activity of MSCs. Highest levels of ALP activity was detected in MSCs that had been incubated with 100 nM dex (trend 3/3) compared to MSCs in osteogenic media with 10 nM or 1 nM dex or control media. All osteogenic media consisted of DMEM (low glucose), 20% serum, 50ug/ml L-ascorbic acid, 2 mM β-GP and antibiotics. The experiments were performed on three patients (n=3) and in triplicates. Results presented as mean + sem. Sample size calculation estimated that 10 samples were required to accept the outcome of a statistical test to see an effect of 1 unit.

3.3.2.2.3 COLLAGEN

The organic part of the osteogenic ECM consists of collagen, mostly collagen 1 (Mackie, 2003). In order to test the impact of various osteogenic media with different dex concentrations on collagen formation, Sirius Red S quantification was performed after 3 weeks. The highest mean collagen levels were detected on MSCs incubated in 100nM dex (Figure 3.16); however, due to the high variation between replicates it was not possible to determine if dex has a positive impact, defined as an increase > 1sd, on collagen formation on MSCs.

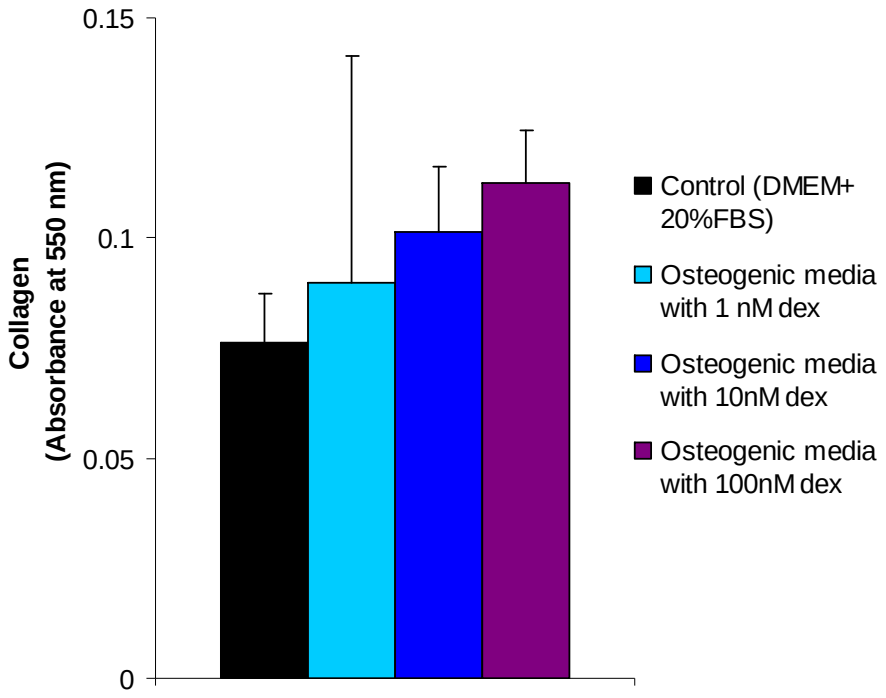

Figure 3.16. Dex might have an impact on collagen secretion after 3 weeks. Collagen secretion was detected by Sirious Red S quantification. All osteogenic media consisted of 50ug/ml L-ascorbic acid, 2mM β-GP and antibiotics. Result (n=1) presented as mean + 1sd of triplicates.

3.3.2.2.4 GENE EXPRESSION OF RUNX2, COL1A1 AND OP

The effect of dex concentrations on osteogenesis was also assessed by their expression of three important osteogenic genes compared to the gene expression of MSCs in control media. The genes analysed were Runx 2, COL1A1 and OP. Runx2 is an osteogenic transcription factor involved in osteogenic differentiation (Jonason *et al*, 2009), Col 1A1 codes for the major component of type 1 collagen and OP protein is involved in bone remodelling (Kazanecki *et al*, 2007; Chapter 1.2.2). The gene expression by the cells was analysed by qPCR when the cells had been incubated for 4 weeks in osteogenic media.

After 4 weeks, all tested osteogenic genes were upregulated in the MSCs that had been in osteogenic media with 100 nM dex (Figure 3.17). The upregulation of Runx2 was higher in MSCs that had been in osteogenic media with 100 nM dex compared to 10 nM dex and 1nM dex (trend 2/2). In the case of Col1A1 only MSCs in 100 nM upregulated this gene (trend 2/2); however, this trend was not detected for OP.

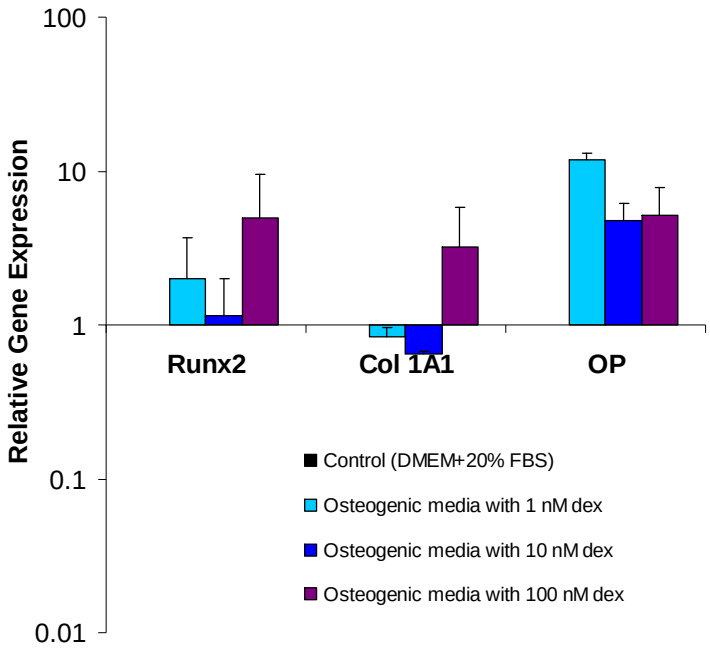

Figure 3.17 Gene expression of Runx2, Col 1A1 and OP in MSCs. MSCs were placed in osteogenic media with 1, 10 or 100 nM dex for 4 weeks. All tested genes were upregulated in MSCs that had been in osteogenic media with 100 nM dex (trend 2/2). All experiments were performed on two patients (n= 2) in triplicates. Results presented as mean+sem. Sample size calculation estimated that 5 samples were required to accept the outcome of a statistical test to see an effect of 2-fold regulation.

3.3.2.2.5 MINERALIZATION

Mineralization was assessed on MSCs by Alizarin Red S quantification after 4 weeks. There was no detected difference, defined as an increase/decrease > 1sd, in mineralization between MSCs in osteogenic media with 10 nM or 100 nM dex after 4 weeks; however, the mean level of mineralization on both MSCs in 10nM and 100 nM was higher than on MSCs in control media or osteogenic media with 1 nM dex, defined as an increase/decrease > 1sd (Figure 3.18).

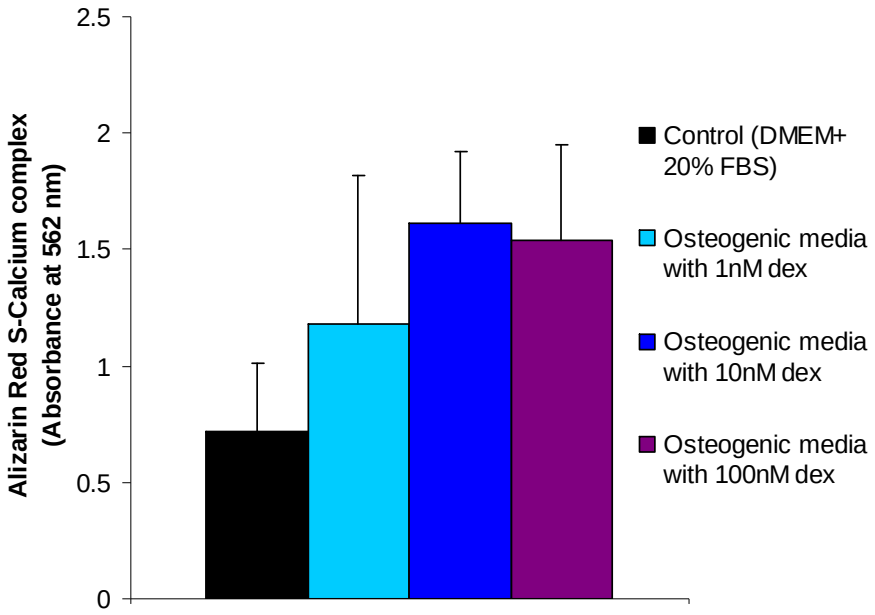

Figure 3.18. Impact of dex on mineralization by MSCs. There was no difference, defined as an increase/decrease > 1sd, between the quantity of mineralization on MSCs in 10nM dex and 100nM dex. All osteogenic media consisted of DMEM (low glucose), 20% serum, 50ug/ml L-ascorbic acid 2 mM β-GP and antibiotics. Results (n=1) presented as mean + 1sd of triplicates.

Taking the results as a whole, it appeared, as the optimal osteogenic media for *in vitro* experiments should be supplemented with 100nM dex, 50ug/ml L-ascorbic acid and 2 mM β-GP.

3.3.3 CULTURE CONDITIONS AND OSTEOGENIC MEDIA TITRATION FOR MDCs

3.3.3.1 PDs OF MDCs

The population doubling of the MDCs was studied by measuring cell number once a week by MTT. The MDCs initial numbers of PD appeared to be relatively consistent between the patients; however, there was a difference in the number of population doublings before senescence *i.e.* maximal growth between the patients (Figure 3.19). This final number of PD of MDCs ranged from *ca* 20-30. According to literature MDCs from mice can divide more than 30 times (Qu-Petersen *et al*, 2002), which appears to be the in same range as human MDCs (Figure 3.19).

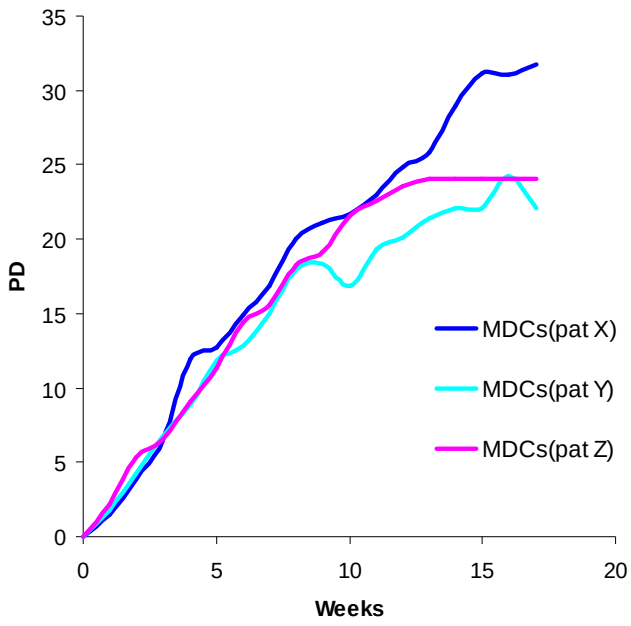

Figure 3.19. Growth curves of MDCs over 15 weeks in culture media. The MDCs appear to initially have same PD rate, but reach senescence *i.e.* maximal growth at different PDs.

3.3.3.2 TITRATION OF OSTEOGENIC MEDIA FOR MDCs

Optimal concentrations of dex and β-GP were established by analysing metabolic activity, ALP activity and mineralization of the MDCs. Dex was tested in concentrations of 1, 10 or 100 nM in either 2 or 10 mM β-GP. It was considered important to investigate if the MDCs behaved similar to MSCs in the various osteogenic media in terms of metabolic activity, ALP activity and mineralization.

3.3.3.2.1 METABOLIC ACTIVITY

The metabolic activity of MDCs was measured in either 2 mM or 10 mM β-GP. It was shown that osteogenic media with 10mM β-GP had a negative impact on the metabolic activity of MDCs after 3 weeks (trend 3/3 for all conditions) compared to MDCs in control media; however, there was no negative impact on MDCs in osteogenic media with 2 mM β-GP compared to cells in control media (Figure 3.20 a). For cells in osteogenic media with 10 mM β-GP there was a negative trend at week 3 and 4 (Figure 3.20 b; trend 3/3 for all conditions at both time points). As previously mentioned, no decrease of metabolic activity was seen when the cells were in 2 mM β-GP compared to MDCs in control media. Hence, only osteogenic media with varying dex concentrations in 2mM β-GP was tested for ALP activity and mineralization.

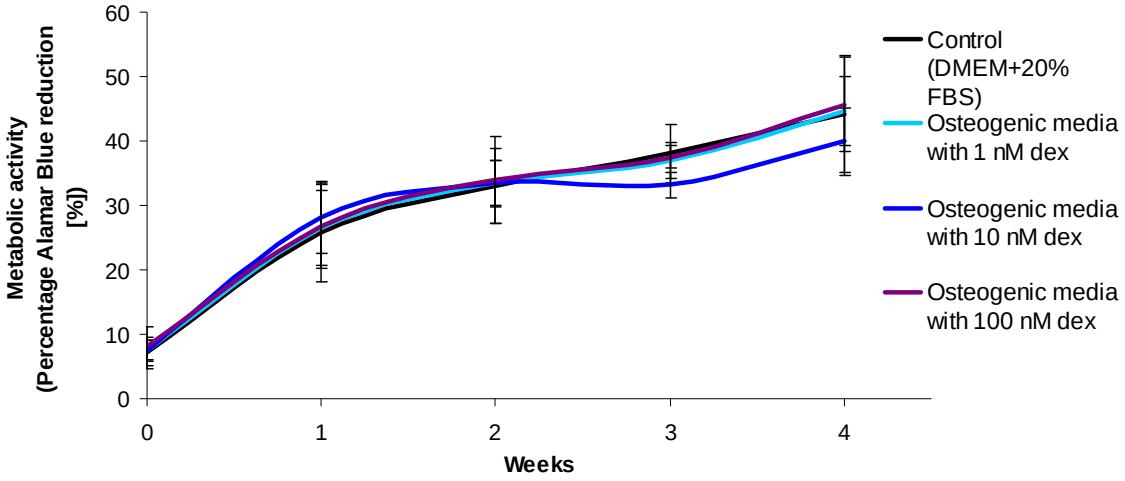

(a)

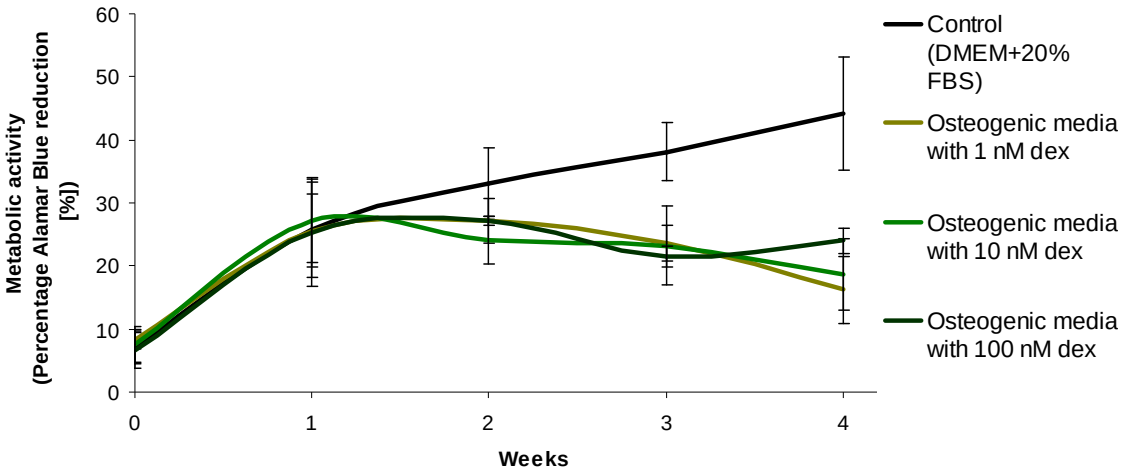

(b)

Figure 3.20. Concentration of β-GP has an impact on metabolic activity of MDCs. a) MDCs in osteogenic media with 2 mM β-GP or control media, b) MDCs in osteogenic media with 10mM β-GP or control media. MDCs cultured in osteogenic media with 10nM β-GP had lower metabolic activity compared to MDCs in control media at week 3 and 4 (trend 3/3 for all conditions). All osteogenic media consisted of DMEM (low glucose), 20% FBS, 50ug/ml L-ascorbic acid, and antibiotics. The experiments were performed on three patients (n=3) in triplicates. Results presented as mean ± sem. Sample size calculation estimated that 4 samples were required to accept the outcome of a statistical test to see an effect of 10% lower metabolic activity, compared with control, at 2 weeks.

3.3.3.2.2 ALP ACTIVITY

ALP activity has previously been used an early marker for osteogenic differentiation (Ozeki *et al*, 2006) and it has been reported that MDCs start to express ALP when they are placed in osteogenic media (Ozeki *et al*, 2006). To decide the more potent osteogenic media, cells were placed in either control media or osteogenic media with 1, 10 or 100nM dex and the ALP activity was assessed after 1 week. The highest mean ALP activity levels were detected in MDCs in osteogenic media with 100nM dex (Figure 3.21): however, the ALP activity differences due to dex concentration were not consistent (trend 2/3).

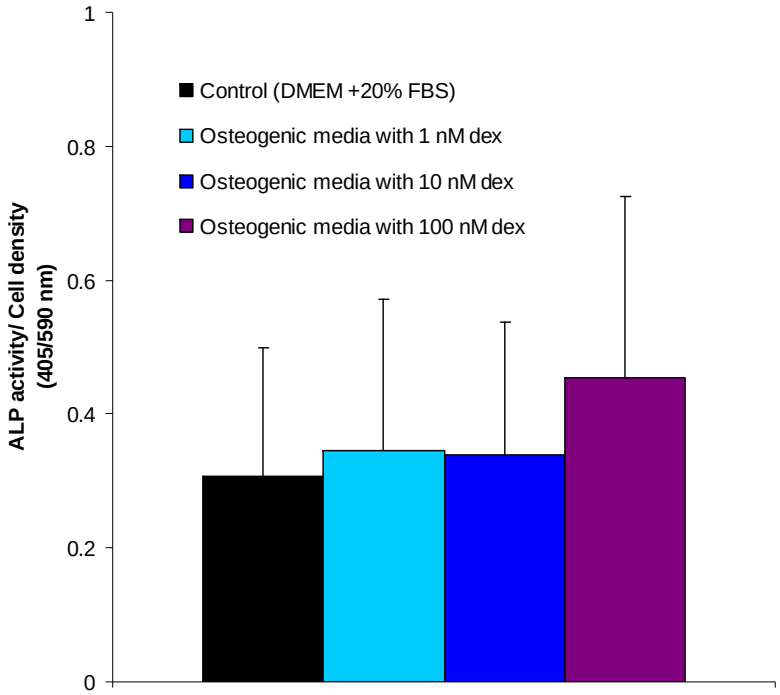

Figure 3.21. Impact of dex concentration on ALP activity in MDCs. There was an increase, in terms of highest mean, of ALP activity in MDCs that had been in osteogenic media with 100 nM dex; however, the ALP activity differences due to dex concentration was not consistent (trend 2/3) since one sample showed highest ALP activity in osteogenic media with 10 nM dex. All osteogenic media consisted of DMEM (low glucose), 20% serum, 50ug/ml L-ascorbic acid, 2 mM β-GP and antibiotics. The experiments were performed on three patients (n=3) in triplicates. Results presented as mean + sem. Sample size calculation estimated that 199 samples were required to accept the outcome of a statistical test to see an effect of 0.2 units.

3.3.3.2.3 MINERALIZATION

The mineralization of MDCs was assessed by Alizarin Red S quantification after 4 weeks. There was no trend in mineralization between cells in osteogenic media with 10 nM or 100 nM dex after 4 weeks; however, the mineralization level on both MDCs in 10nM (trend 3/3) and 100 nM (trend 3/3) were higher than on MDCs in 1nM dex or control media (Figure 3.22).

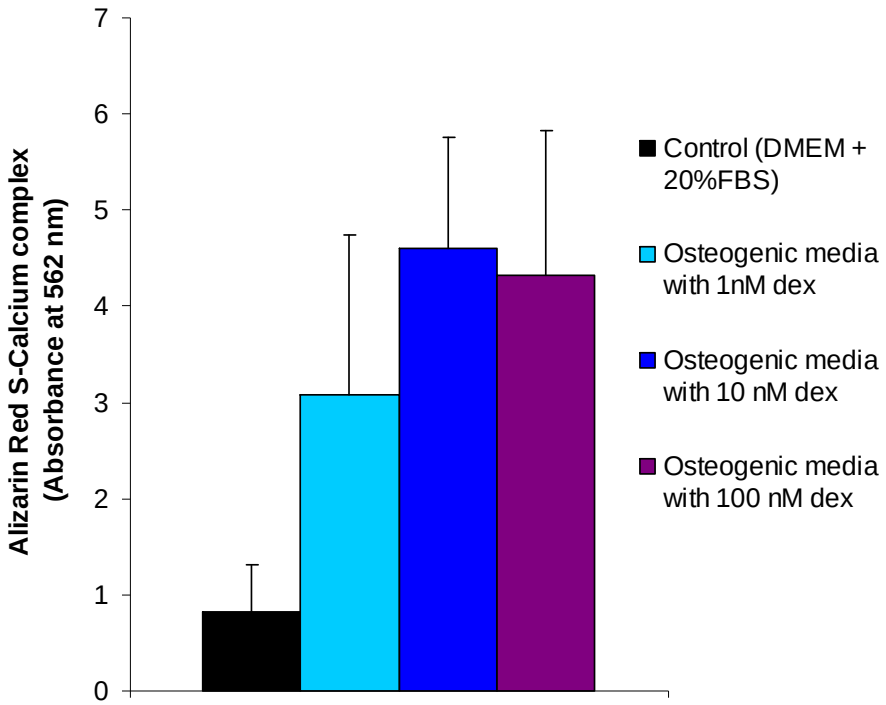

Figure 3.22. Impact of dex concentration on mineralization by MDCs. There was no difference between mineralization by MDCs in osteogenic media with 10 or 100nM dex. However, there was an increase in mineralization between MDCs that had been in osteogenic media supplemented with 1 nM and 10 (trend 3/3) or 100 nM dex (trend 3/3). All osteogenic media consisted of DMEM (low glucose), 20 % serum, 50ug/ml L-ascorbic acid, 2mM β-GP and antibiotics. The experiments were performed on three patients (n=3) in triplicates. Results presented as mean + sem. Sample size calculation estimated that 10 samples were required to accept the outcome of a statistical test to see an effect of 1 unit.

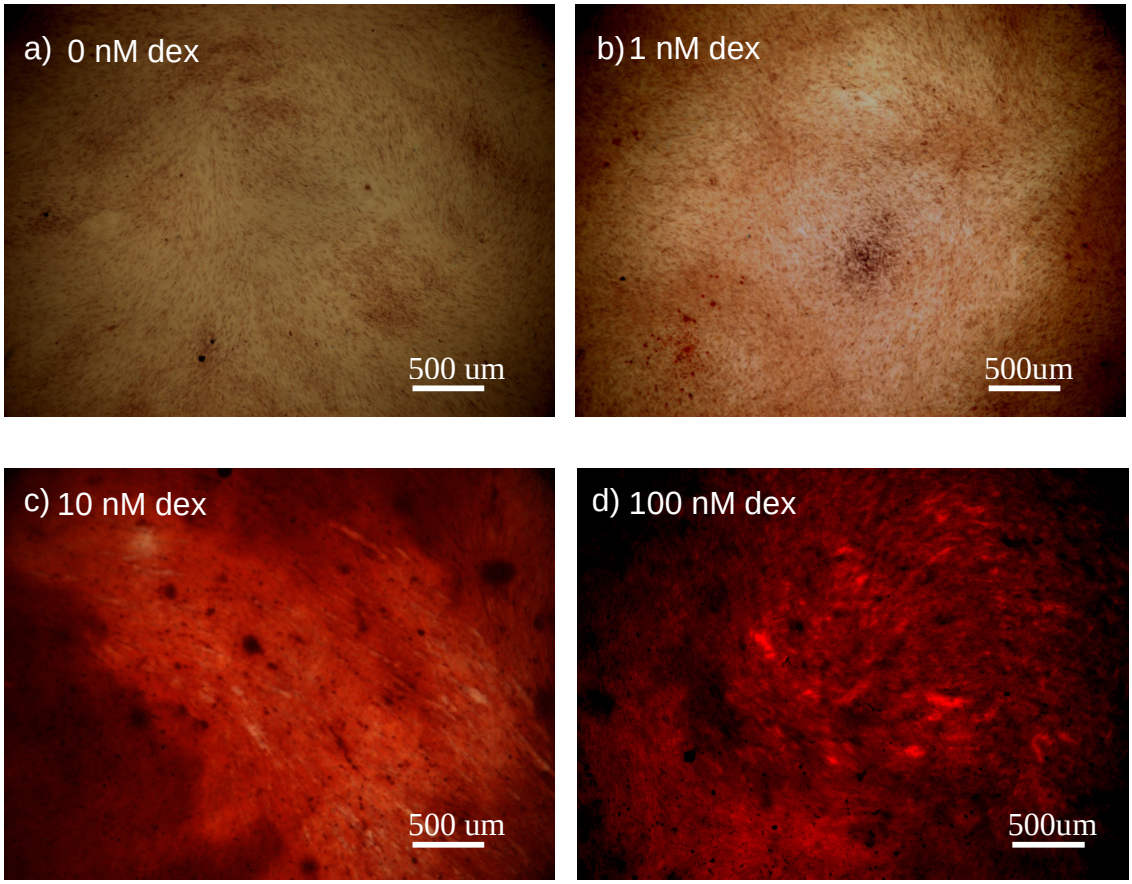

Figure 3.23. Staining of MDCs in various osteogenic media by Alizarin Red S. MDCs in a) control media (DMEM +20% FBS) or osteogenic media supplemented with b) 1 nM dex, c) 10 nM dex and d)100 nM dex after 4 weeks. There is clearly more mineralization on MDCs that have been in osteogenic media complemented with either 10 or 100 nM dex. The experiments were performed on three patients (n=3) in triplicates. Magnification x4.

3.4 SUMMARY

There is a general consensus that MSCs are able to differentiate along the osteogenic and the adipogenic lineage, which also have been verified in Chapter 3.3.1. In this chapter it was also shown that MDCs could differentiate along the myogenic, osteogenic and adipogenic lineage. MDCs that had been depleted of CD56 positive cells *i.e.* $MDCs^{CD56-}$ could not form myotubes. However, it was shown that MSCs do not differentiate along the myogenic lineage *in vitro*, at least not with the myogenic media used in this study.

The MSCs and the MDCs showed similar range of number of PDs; number of PD were for MSCs 33 ± 6 and for MDCs 26 ± 3 (mean±sem). Furthermore, both cell types showed optimal osteogenic response in osteogenic media supplemented with 100 nM dex, 50ug/ml L-ascorbic acid and 2mM β-GP.

It has been suggested that concentrations of 10 mM β-GP could induce apoptosis in osteoblasts (Khouja *et al*, 1990) and in this study it was shown that both MSCs (Figure 3.14b) and MDCs (Figure 3.20b) showed decreased metabolic activity in osteogenic media supplemented with 10 mM β-GP after 2 to 3 weeks. This can be compared with MSCs (Figure 314a) and MDCs (Figure 3.20a) in osteogenic media supplemented with 2 mM β-GP that showed comparable metabolic activity as cells in control media. These results are consistent since reduced metabolic activity can indicate apoptosis. The conclusion was that osteogenic media with 2 mM β-GP was optimal in terms of metabolic activity and would be used in all following experiments.

Both MSCs and MDCs expressed higher levels of ALP in osteogenic media supplemented with 100 nM dex compared to the other media. For both MSCs and MDCs there was no difference between the mineralization in osteogenic media supplemented with 10 or 100 nM dex.

Most importantly, in this chapter it was shown that MDCs and MSCs are able to differentiate along the osteogenic lineage and mineralize. Furthermore, an optimised protocol for the osteogenic media was developed to be used in this study.

Table 3.1. Summary of results from Chapter 3. MDCs are compared with MSCs. *MDC^{CD56-}

	MDCs	**MSCs**
Detected potential to express ALP	Yes	Yes
Detected potential to mineralize	Yes	Yes
Detected potential to form myotubes	Yes	No
Detected potential to form lipid droplets	Yes*	Yes
Metabolic activity response in osteogenic media with 10 mM β-GP compared to control media	Lower	Lower
Metabolic activity response in osteogenic media with 2 mM β-GP compared to control media	Unaffected	Unaffected

CHAPTER 4:

RESULT SECTION 2

- ISOLATION OF THE OSTEOGENIC SUBPOPULATION OF MDCs

4.1 INTRODUCTION SPECIFIC FOR RESULT SECTION 2

In Chapter 3, Result section 1, it was shown that the MDCs were able to express ALP activity and mineralize *i.e.* MDCs showed osteogenic potential. It has previously been shown by several research groups that there is a subpopulation within the skeletal muscles both in humans (Sinanan *et al*, 2004; Jackson *et al*, 2009) and in mice (Lee *et al*, 2000) that have the potential to differentiate along the osteogenic lineage. Even though the researchers have recognised the possibilities of using these cells for bone regenerative applications (Usas & Huard, 2007), no technique has specifically been developed to isolate the subpopulations with the highest osteogenic potential. The majority of the isolation techniques have been developed to isolate myogenic subpopulations of MDCs (Chapter 1.3.1; Sinanan *et al*, 2004) or the isolation of the more stem cell like population in adult tissue (Jones & Watt 1993; Qu-Petersen *et al*, 2002). Hence, there is a gap to fill. In this chapter various subpopulations were isolated by differential adhesion to three different surfaces and their osteogenic potential were tested.

4.2 METHODS SPECIFIC FOR RESULT SECTION 2

4.2.1 DIFFERENTIAL ADHESION TO FN, GEL OR TCP

In order to isolate the subpopulations, the cells adhesion properties, to three different surfaces the plates were coated with Fn, Gel or left uncoated *i.e.* on TCP. Flasks or plates were coated by 1.5ug Fn/cm^2 (see Chapter A9.1.3) and stored in 4°C over night. Gel (see Chapter A9.1.4) was added to flasks/plates, 0.250ul/cm^2, and left at room temperature for 30 minutes. Before the separation the coating excess was removed by pipetting.

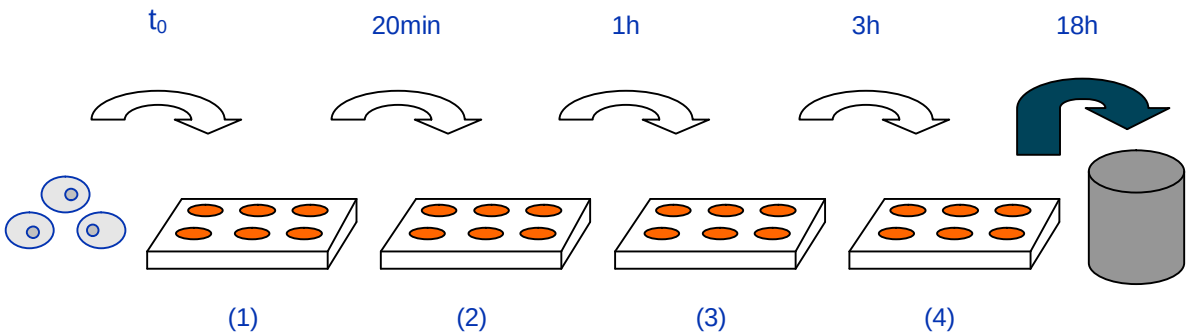

Figure 4.1. Isolation of MDCs subpopulations by differential adhesion. The plates were coated by Fn or Gel, or left uncoated (*i.e.* TCP). The cells were seeded on plate/flask 1(1) at time point 0 (t_0) and left for 20 min. After 20 min the supernatant with unattached cells was removed and plated on (2) and left for 40 min *i.e.* 1h from t_0 then the cells were plated on (3) for 2 h, *i.e.* 3 h from t_0. For the final plate/flask (4) the cells were left over night (15h) *i.e.* 18h from t_0. The differential adhesion was performed under serum-free conditions. Method adapted from Davies *et al*, 2010.

The starting density of the MDCs was 2000 cells/cm^2 and isolation was performed according to Figure 4.1. If the cells did not reach confluency within two weeks, the plate with this isolated population was discarded. After isolation the cells were cultured in standard serum-based culture media.

4.3 RESULTS FOR RESULT SECTION 2

4.3.1 IDENTIFYING THE MORE OSTEOGENIC SUBPOPULATION BY DIFFERENTIAL ADHESION

In order to identify the more osteogenic population, ALP activity of the various subpopulations was measured after 1 week in osteogenic media. The time points, measured from t_0, for the differential adhesion were 20 (plate 1), 60 (plate 2), 180 (plate 3) and 1080 min (plate 4) as previously described (Chapter 4.2.1; Figure 4.1). No subpopulations on plate 4 reached confluency within two weeks in culture and were therefore discarded. The unsorted parental population of MDCs will be called MDCsPP from now on when used in comparison experiments with isolated subpopulations of MDCs.

After the isolated subpopulations reached confluency, the cells were incubated in osteogenic media for 1 week. The subpopulation that was early adherent, within 20 min, to Fn (MDCsFn20) showed higher ALP activity compared to the other isolated populations (trend 3/3). Hence, MDCsFn20 was believed to be the more osteogenic subpopulation (Figure 4.2). Jones &Watt (1993) and Dowthwaite *et al* (2004) had found that the more stem-cell like population from keratinocytes and cartilage belonged to the subpopulation that was early adherent to Fn.

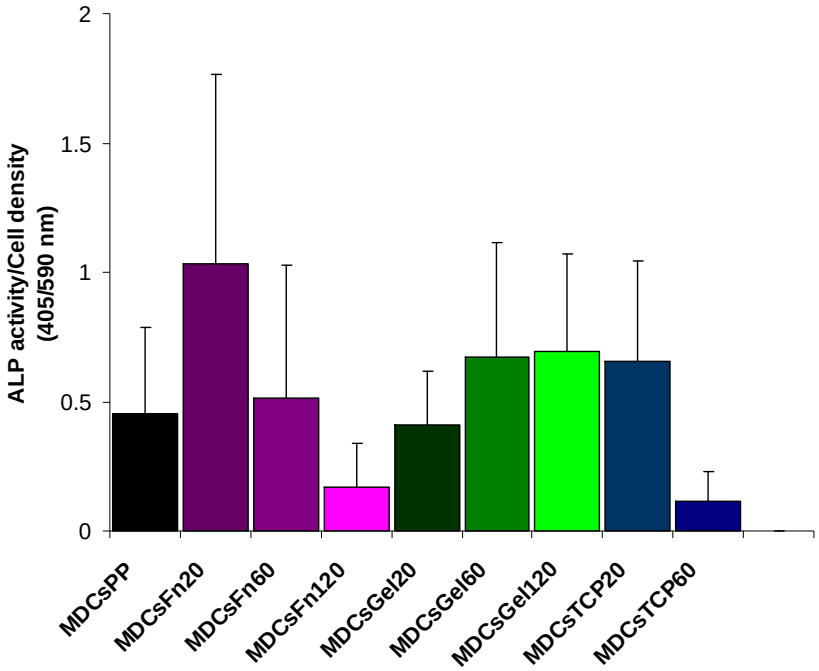

Figure 4.2. ALP activity of the isolated subpopulations. The MDCsFn20 showed the highest level of ALP expression The ALP activity of MDCsFn20 was consistent higher than the other subpopulations (trend 3/3). The experiments were performed on three patients (n=3) in triplicates. The unsorted parental population of MDCs was named MDCsPP. Results presented as mean+sem. Sample size calculation estimated that 34 samples were required to accept the outcome of a statistical test to see an effect of 0.5 units.

In order to check that the ALP activity of the different subpopulations was not caused by the substrate, the cells that were early adherent to the surfaces were harvested and reseeded onto TCP or the same substrate (for experimental details, see Chapter 2.4.2.1.2) and their ALP activity was assessed (Figure 4.3). Since the highest ALP activity was detected on the early adherent MDCs to Fn *i.e.* within 20 min, only the early adherent groups were analysed in this control experiment.

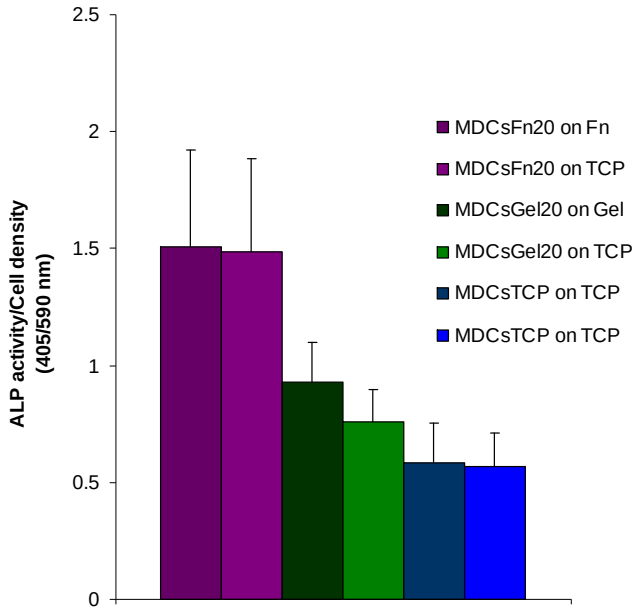

Figure 4.3. The substrates did not alter the ALP activity in MDCsFn. The groups were compared separately. MDCsFn20 on Fn was compared with MDCsFn20 on TCP, and MDCsGel20 on Gel was compared with MDCsGel20 on TCP. All experiments were performed on three patients (n=3) in triplicate. Results presented as mean+sem.

The Fn substrate did not appear to have an impact on the ALP activity, but in order to avoid affecting the results the isolation was performed in coated flasks and thereafter seeded onto TCP for the differentiation experiments.

4.3.2 COMPARISON OF MDCsFN AND MDCsPP

4.3.2.1 MEASUREMENT OF THE SIZE

The average sizes of the cells in the two populations, MDCsFn and MDCsPP, were compared since cell size can be used as an indicator of a cell's maturity and has been used in adult-stem cells isolations (Zuba-Surma *et al*, 2009). Smaller cells tend to indicate that the cells are less differentiated. The MDCsFn were freshly isolated, by early adherence to Fn, and compared with MDCsPP; the sizes of the cells were assessed by photograph image analysis by Image-pro. The isolated MDCsFn population appeared to contain the smaller and more rounded cell population of MDCsPP (Figure 4.4 – 4.6) *i.e.* more homogeneous in terms of size and less mature population.

The average sizes of the cell populations were quantified (Figure 4.4-4.5). The average size of MDCsFn was $4.4x10^{-3}mm^2$ (95% CI: 4.0-$4.8x10^{-3}$ mm^2) and the average size of MDCsPP was 5.7 $x10^{-3}mm^2$ (95% CI: 4.9-6.4 $x10^{-3}$ mm^2).

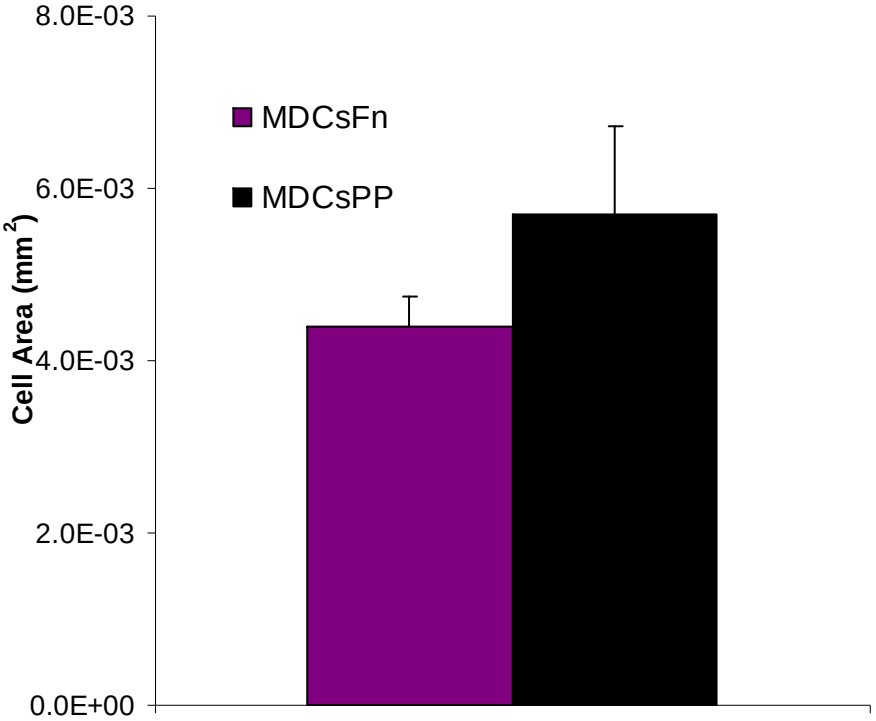

Figure 4.4. Size quantification of MDCsFn and MDCsPP. The different subpopulations of MDCs showed differences in size. The mean size of MDCsFn was consistently smaller than MDCsPP (trend 3/3). The MDCsFn consist of smaller cells compared to the other isolated groups and MDCsPP. The mean cell size of MDCsFn was assessed to be $4.4x10^{-3}mm^2$ (95% CI: $4.0\text{-}4.8x10^{-3}$ mm^2) and the mean for MDCsPP was $5.7x10^{-3}mm^2$. (95% CI: $4.9\text{-}6.4x10^{-3}$ mm^2). Thirty cells per well and three wells per population were photographed and measured. The experiments were performed on three patients (n=3) in triplicate. The confidence interval is of all cells. The results in the graph are presented as the mean + sem. Sample size calculation estimated that 5 samples were required to accept the outcome of a statistical test to see an effect of $2x10^{-3}$ mm^2.

The percentage of MDCs that attached to Fn was also calculated to be 42 % ± 4.2 % of the unsorted parental population. The attachment experiment was performed according to Chapter 2.4.2.1.2. The attachment experiments were performed on three patients (n=3) in triplicate and presented as mean± sem.

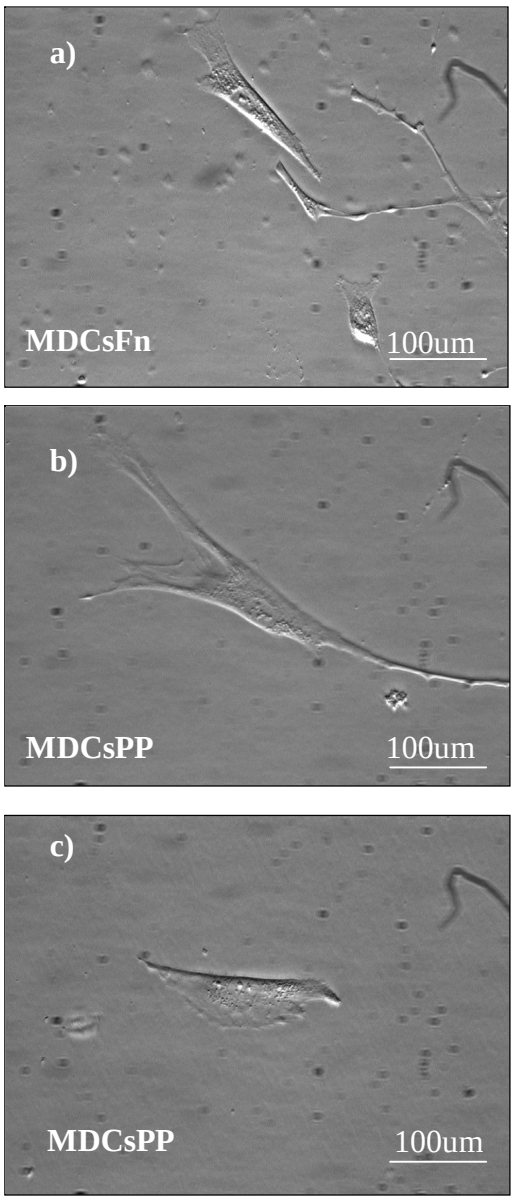

Figure 4.5. MDCsFn contained the smaller cells of MDCsPP. a) MDCsFn, b)+c) MDCsPP. MDCsPP consisted of cells of various sizes. MDCsFn appeared to contain a relative homogeneous population of smaller, rounded cells. Thirty cells were measured per well. All experiments (n=3) were performed in triplicates of wells. Magnification x40.

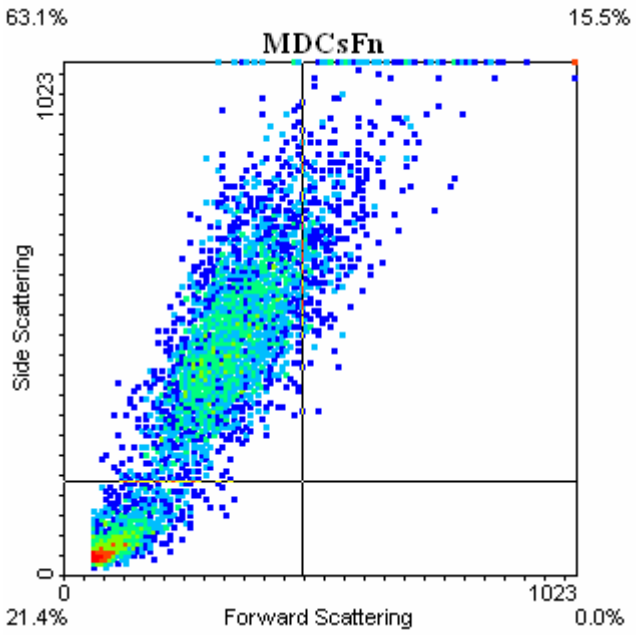

(a)

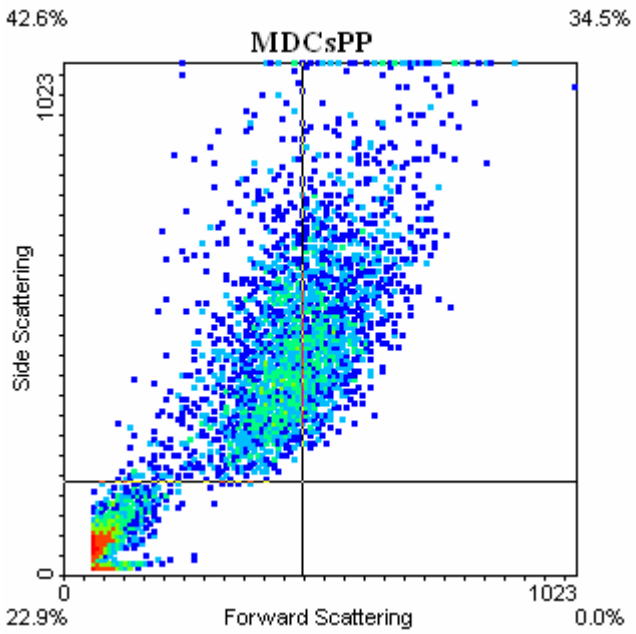

(b)

Figure 4.6. Density plots of a) MDCsFn and b) MDCsPP. MDCsFn are smaller in size compared to MDCsPP assessed by Forward Scattering. All experiments were performed on three patients (n=3) in triplicate. MDCsPP contained 16.6 ± 8 % cells that were larger than MDCsFn. Result presented as mean±sem.

Both the differences in cell size and range of cell size could be shown by flow cytometry (Figure 4.6). The size was measured by Forward Scattering and granularity was measured by Side Scattering of the two populations. This result confirmed the

previous findings that MDCsFn consisted of a smaller cell population than MDCsPP (Figure 4.4 - 4.5). MDCsPP contained 16.6 ± 8 % cells that were larger than MDCsFn.

4.3.2.2 MYOGENICITY

Muscle tissue contains a variety of cells (see Chapter 1.3.1), including satellite cells and MPCs that can fuse and form myotubes *in vitro*. As muscle tissue MDCsPP consist of a variety of cells and the percentage of myogenic cells to human MDCsPP have previously been determined to be between 5-45 % (Lewis *et al*, 2000), the potential of the two subpopulations, MDCsFn and MDCsPP, to form myotubes after 4 days in myogenic media was investigated in this section. After 4 days, the MDCsFn clearly expressed fewer desmin expressing cells *i.e.* MPCs (Figure 4.7a), compared to MDCsPP cultures (Figure 4.7b). The MDCsPP could easily fuse to multi-nuclei, desmin and α-sarcomeric actin myotubes (Figure 4.7 b). This can have several explanations, either the MDCsFn consist of a less myogenic cell population or they consist of a more immature cell population, as indicated by previous results (Chapter 4.3.2.1), which need more time to differentiate into MPCs and myotubes. Deasy *et al* (2001) have suggested that pluripotent cells derived from mice muscle tissue are in fact precursors to satellite cells. It is hard to perform a robust experiment to investigate if either of these hypotheses is correct. Myogenic MDCs cultures are known to be very hard to keep in monolayer culture for more than 6 days (experience from EDI), so it is impossible to quantify the myotube formation over a longer period of time.

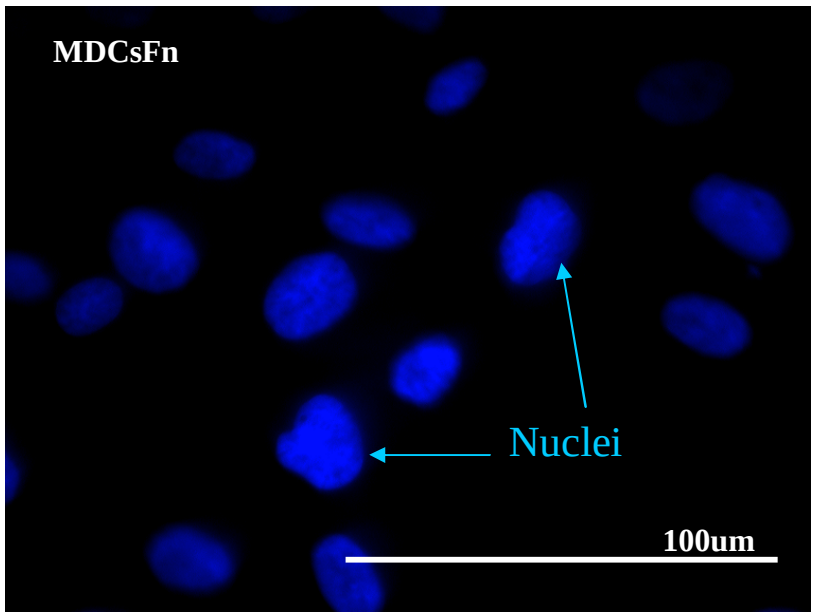

(a)

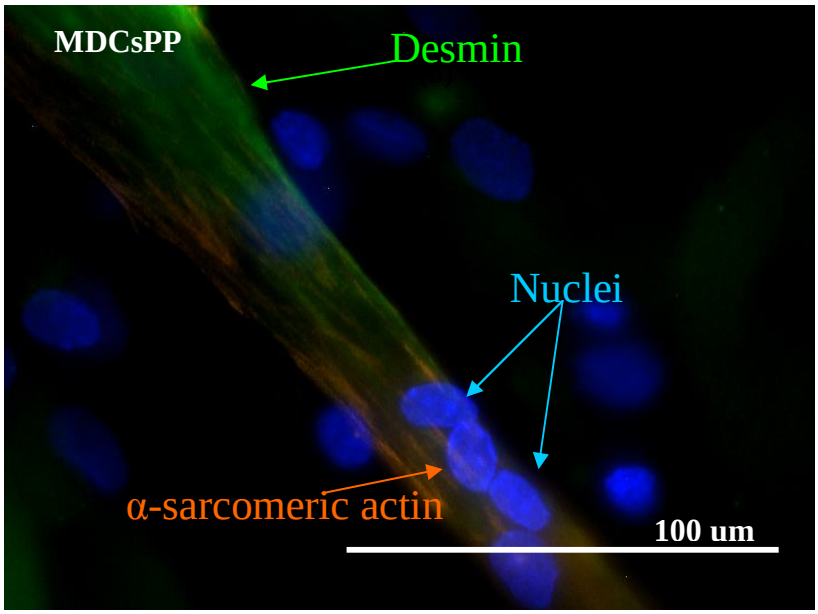

Figure 4.7 a) MDCsFn and b) MDCsPP after 4 days in myogenic media. The cells in the MDCsFn cultures appeared to not be able to form myotubes after 4 days in myogenic media. In the MDCsPP cultures there were desmin (green), and α-sarcomeric actin (red) expressing multinuclei (blue) myotubes. Figure shows a typical image of stained MDCsFn and MDCsPP. The experiments were performed on three patients (n=3) in triplicates. Magnification x60.

4.3.2.3 CD56 AND STRO-1 EXPRESSION

The importance of CD56 in myogenesis has previously been studied and it has been identified as a satellite stem cell marker (Mackey *et al*, 2009). As shown in chapter 1, pure $MDCs^{CD56-}$ cultures are not able to express myogenin or α-sarcomeric actin and can therefore not undergo terminal myogenic differentiation. On the other hand it was shown that when pure $MDCs^{CD56+}$ cultures were placed in myogenic media the incorporation of nuclei in the myotubes was higher than compared to MDCsPP (Sinanan *et al*, 2004). Sinanan *et al* (2004) also suggested that MDCs with low expression of CD56 could be cells that are not restricted to the myogenic lineage. In this part the CD56 expression of MDCsFn and MDCsPP was studied. It was found for all tested patients that MDCsFn expressed less CD56 than MDCsPP (trend 3/3). However, both the CD56 expression and the magnitude of reduction varied between the investigated patients (Figure 4.8).

Stro-1 antibody identifies bone marrow stromal cell population in adult bone marrow (Simmons & Torok-Storb, 1991). It has been shown that bone marrow derived Stro-1+ cells are able to differentiate into cell types with phenotypic characteristics of osteoblast, adipocytes and smooth muscle (Gronthos *et al*, 1994). Stro-1+ has also been used as an isolation marker, alone (Gronthos *et al*, 1994) or together with ALP for osteogenic precursor cells (van den Dolder & Jansen, 2007). Hence, the expression of Stro-1 on MDCsFn and the MDCsPP was analysed by flow cytometry. The results between the patients were not consistent; only one tested patient out of three expressed Stro-1. For this patient, the MDCsFn expressed higher levels, 10.0 ± 4.7 %, of Stro-1 than MDCsPP, 4.6± 0.8. The result was presented as mean of triplicates ± 1sd.

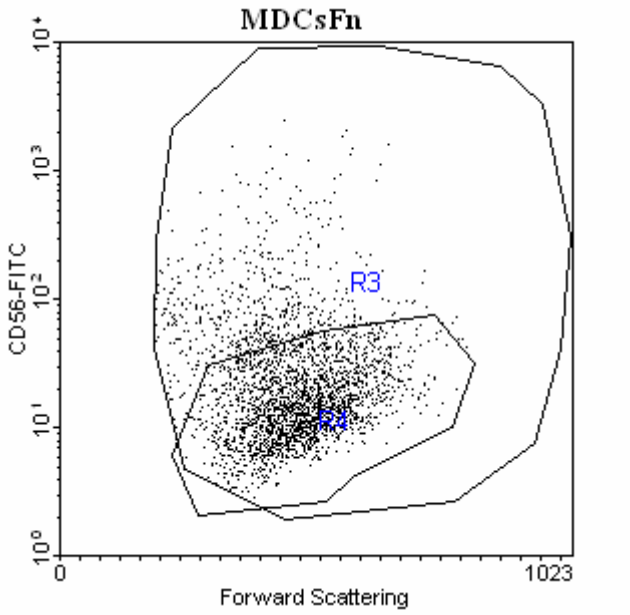

a)

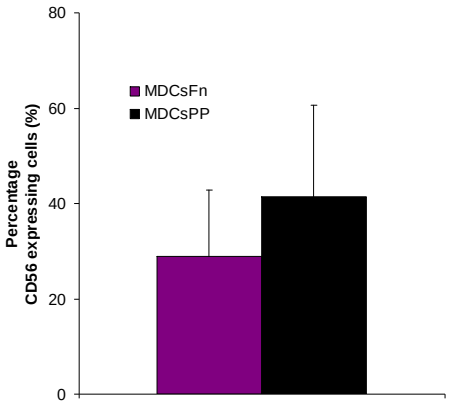

b)

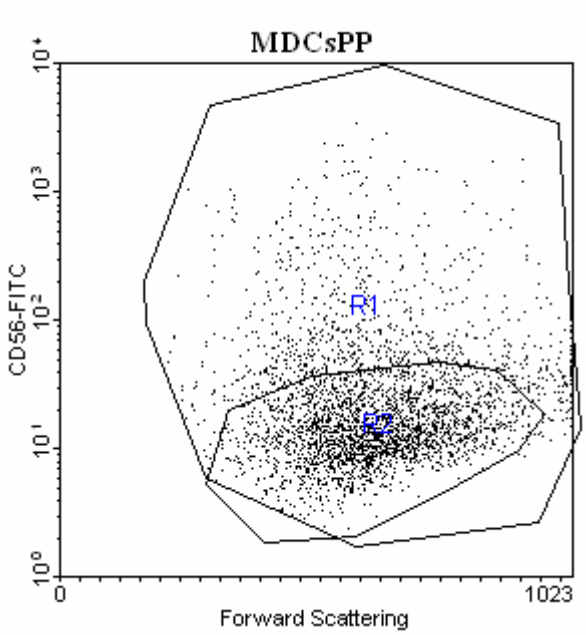

c)

Figure 4.8. CD56 expression of MDCsFn and MDCsPP. Dotplot over the expression of CD56 in a) MDCsFn and b) MDCsPP.

c) The difference between the two populations was consistent (trend 3/3). The experiments were performed on three patients (n=3) in triplicates. The results are presented as mean + sem. Sample size calculation estimated that 3 samples were required to accept the outcome of a statistical test to see an effect of 10 %.

4.3.2.4 OSTEOGENIC GENE EXPRESSION OF MDCsFN AND MDCsPP

To further compare the osteogenic potential of the two populations their gene expression was compared by qPCR (Table 4.1). The expression of Runx2, Col1A1 and OP was assessed after 2 weeks in culture media i.e. DMEM with 20% FBS and antibiotics (Table 2.2). Runx2 is an essential transcription factor for osteogenic differentiation (Jonason *et al,* 2009) and Col1A1 is the major component in the organic part of the osteogenic ECM (Pace *et al*, 2001). OP has a function as an attachment protein linking cells to the bone mineral and is also considered to be late osteogenic marker (Kazanecki *et al*, 2007). The MDCsFn expressed higher mean levels of Runx2 and Col1A1 compared to MDCsPP. However, the upreglation was only consistent for Col1A1 (trend 3/3).

Table 4.1. The gene expression of Runx2, Col1A1 and OP in MDCsFn compared to MDCsPP. Experiments performed in culture media *i.e.* DMEM with 20% FBS and antibiotics (see Table 2.2 for media definition) and measured by qPCR**.** The experiments were performed on three patients (n=3) in triplicates. The samples were normalized to MDCsPP and experiment was performed accordingly Chapter 2.9. Results presented as mean ± sem**.** Sample size calculation estimated that 4 samples were required to accept the outcome of a statistical test to see an effect of a 3-fold regulation.

GENE ASSAY	FOLD CHANGE IN GENE EXPRESSION (MDCsFN / MDCsPP)	TREND (UPREGULATION)
Runx2	3.1± 1.0	2/3
Col1A1	3.6± 2.0	3/3
OP	0.73± 0.08	1/3

It should be noted that OP was not upregulated when MDCsFn was compared to MDCsPP. This might be due to the versatile function of OP. It is known that OP has a functional role in the osteogenic ECM (Kazanecki *et al*, 2007), but it also has a function in myogenic and inflammatory processes in the early stages of muscle regeneration (Uaesoontrachoon *et al*, 2008). Hence, is it difficult to draw any conclusion from the gene expression of OP.

4.3.2.5 MINERALIZATION

Mineralization of the cells ECM has been of a measure for terminal differentiation of osteogenic cultures and it is, in general, measured by Alizarin Red S (De Oliva *et al*, 2009). In this study the mineralization process of the two populations have been investigated. Both MDCsFn and MDCsPP in osteogenic media started to express consistent higher mineral levels, measured by Alizarin Red S, compared to MDCsFn and MDCsPP in control media after 3 week (trend 3/3 for both comparisons). At week 3, there was no difference between the mineralization of MDCsFn and MDCsPP in osteogenic media. MDCsFn in osteogenic media started to have consistent higher levels of mineralization, compared with MDCsPP, after 4 weeks (trend 3/3). The MDCsFn and MDCsPP in control media did not show any consistent mineralization differences. The trend with more mineralization with time and that MDCsFn expressing higher levels than MDCsPP was consistent for all mineralization experiments; however, the exact amount of mineralization was experiment dependent. Experiments of MDCsFn and MDCsPP were performed in parallel.

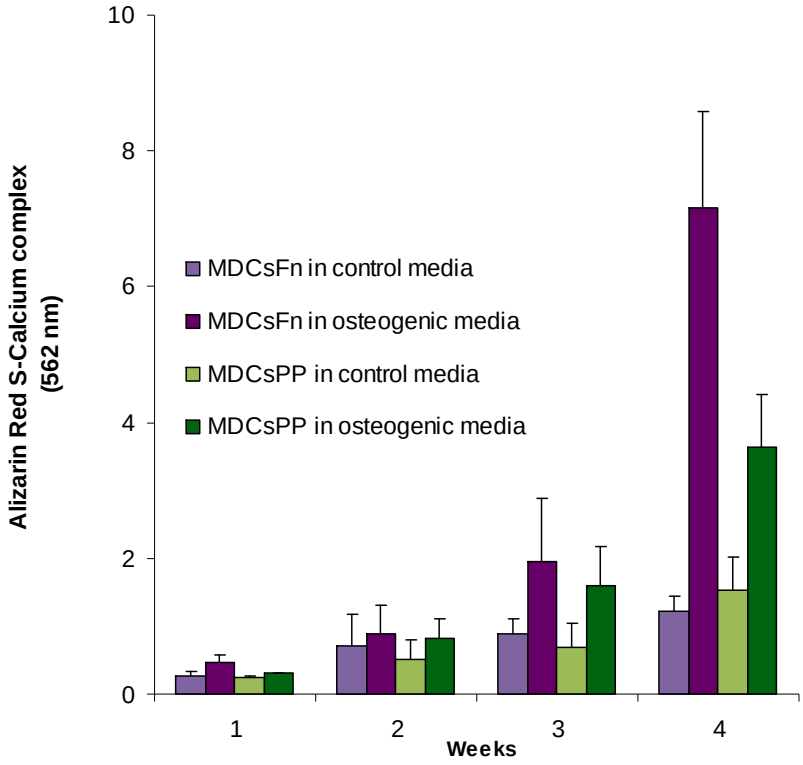

Figure 4.9. Comparison of the mineralisation process by MDCsFn and MDCsPP over 4 weeks. Mineralisation detected by Alizarin Red S increased with time for both MDCsFn and MDCsPP in osteogenic media. At week 4, mineralisation by MDCsFn was consistently (trend 3/3) higher than MDCsPP in osteogenic media. The experiments were performed on three patients (n=3) in triplicate and results presented as mean + sem. Sample size calculation estimated that 4 samples were required to accept the outcome of a statistical test to see an effect of 3 units at week 4.

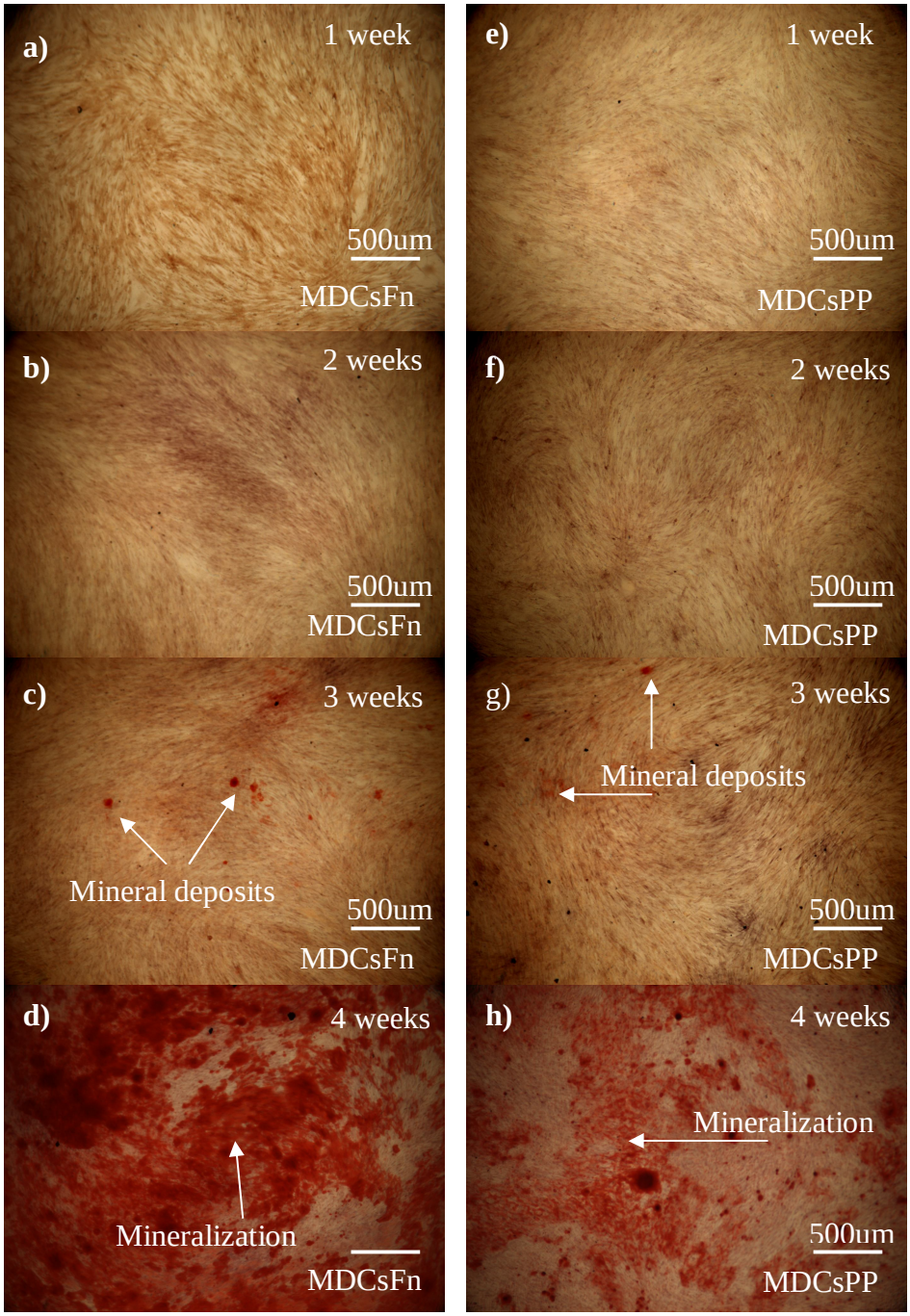

Figure 4.10. Alizarin Red S staining of MDCsFn and MDCsPP in osteogenic media over 4 weeks. a)-d) MDCsFn and e)-h) MDCsPP after a) + e) 1 week, b)+ f) 2 weeks, c)+g) 3 weeks, d) + h) 4 weeks. For both MDCsFn and MDCsPP, there is an accumulation of mineral over time. MDCsFn expressed higher levels of mineralization compared to MDCsPP after 4 weeks. The experiments were performed on three patients (n=3) in triplicates. Magnification x4.

4.4 SUMMARY

In this chapter, various subpopulations of MDCs were isolated in order to identify the subpopulation with the highest osteogenic potential. The method used for this isolation relied on the differential adhesion of the subpopulations to adhere to different substrates (Fn, Gel, TCP). It was found that the cells that adhered to Fn within 20 min expressed highest levels of ALP activity, compared to the other subpopulations, after the cells had been in osteogenic media for 1 week (Figure 4.2). Since ALP activity has been described as an early osteogenic marker (Weiss *et al*, 1986), this subpopulation, MDCsFn, was selected for further analyses and comparisons with the unsorted parental population, MDCsPP. The MDCsFn population appeared to have a more homogeneous size distribution than MDCsPP and consisted of approximately 42% of the original MDCs (Chapter 4.3.2.1; Table 4.2). The cells in the MDCsFn population were smaller and more rounded cells compared to MDCsPP (Figure 4.4-4.6), this population also expressed higher levels Col1A1, measured by qPCR, compared to MDCsPP in control media (Table 4.1).

Not surprisingly, the MDCsFn showed higher levels of mineralization compared to MDCsPP after the cells had been in osteogenic media for 4 weeks (4.9-4.10). This data together suggests that the MDCsFn represent the more osteogenic population of MDCsPP.

Table 4.2 Summary of results from Chapter 4. Comparison of MDCsFn and MDCsPP**.** All results presented as mean ±sem apart from *Stro-1 result, which is from the only patient that expressed Stro-1 and is presented as mean ± 1 std.*

CHARACTERISTICS	MDCsFN	MDCsPP
Size (mm^2)	$4.4x10^{-3}$	$5.7\ x10^{-3}$
Attachment (%)	42 ± 4.2	100
CD56 expression (%)	18.2 ±9.8	33.9± 21.8
Stro-1 expression (%)	*10.0 ± 4.7*	*4.6± 0.8*
Runx2 gene expression	3.1± 1.0	1
Col1A1 gene expression	3.6± 2.0	1
OP gene expression	0.73± 0.08	1
Mineralization **- after 4 weeks in osteogenic media**	7.2±1.4	3.6± 0.8

CHAPTER 5:

RESULT SECTION 3

-COMPARISON OF OSTEOGENESIS OF MDCsFn AND MSCs

5.1 INTRODUCTION SPECIFIC FOR RESULT SECTION 3

In the previous chapter, Result section 2, the MDCsFn were identified as the more osteogenic fraction of the parental population, MDCsPP. In this chapter, the osteogenic differentiation of MDCsFn was compared with bone marrow-derived MSCs. The ALP activity, ALP expression and mineralization were studied over a time period of 4 weeks. Furthermore, at week 2, samples of MDCsFn and MSCs in osteogenic and control media were collected and analysed by qPCR Array for 46 osteogenic genes (Table 5.1; Table A9.2-A9.3).

5.2 METHODS SPECIFIC FOR RESULT SECTION 3

5.2.1 Q-PCR ARRAY

A qPCR array was designed in the format of 2x48 genes in a 96-well plate (Figure 5.1; Table 5.1), where two genes were used as housekeeping genes: GapdH and 18S, ribosomal RNA. The gene assays were designed and supplied by Applied Biosystems (Table A9.2). To increase the accuracy both GapdH and S18 were used as control genes in the analyses. The gene expression levels were analysed for MDCsFn from 3 patients and MSCs from 3 patients; however, the samples were not patient matched and only one sample and replicate per patient was performed.

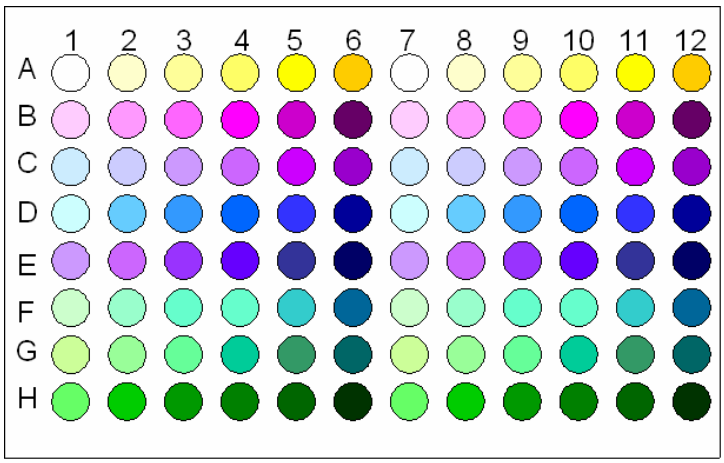

Figure 5.1. Layout of the qPCR Array with 2x48 gene assays.

Table 5.1. Location for gene assays in the 2x48 qPCR array.

Well location	Gene assay	Well location	Gene assay	Well location	Gene assay	Well location	Gene assay
A01/A07	18S	C01/C07	COL1A1	E01/E07	DSPP	G01/G07	TGF-β3
A02/A08	GAPDH	C02/C08	COMP	E02/E08	RUNX2	G02/G08	TGFBR1
A03/A09	ALP	C03/C09	DMP1	E03/E09	SMAD1	G03/G09	TGFBR2
A04/A10	AMBN	C04/C10	FGFR1	E04/E10	SMAD2	G04/G10	TUFT1
A05/A11	AMELY	C05/C11	FGFR2	E05/E11	SMAD3	G05/G11	TWIST1
A06/A12	ARSE	C06/C12	FGFR3	E06/E12	SMAD4	G06/G12	TWIST2
B01/B07	BMP2	D01/D07	FLT1	F01/F07	SMAD7	H01/H07	VDR
B02/B08	BMP4	D02/D08	GDF10	F02/F08	SMAD9	H02/H08	VEGFA
B03/B09	BMP7	D03/D09	BSP	F03/F09	SOX9	H03/H09	VEGFB
B04/B10	CALCR	D04/D10	MMP13	F04/F10	SPARC	H04/H10	OSTERIX
B05/B11	CASR	D05/D11	MMP2	F05/F11	OP	H05/H11	WNT5A
B06/B12	CDH11	D06/D12	MSX1	F06/F12	TGF-β1	H06/H12	PTHR1

5.3 RESULTS FOR RESULTS SECTION 3

In this section, MDCsFn and MSCs were seeded at a density of 5000 cells/cm^2 and cultured until confluency *i.e.* 10000 cells/cm^2 (as described in Chapter 2.3) before osteogenic differentiation medium was added to the cells.

5.3.1 ALP ACTIVITY AND EXPRESSION

The ALP activities of the two cell types *i.e.* MDCsFn (Figure 5.2) and MSCs (Figure 5.3) were compared over a period of 4 weeks in osteogenic media where culture media was used as control.

The highest mean level of ALP activity of MDCsFn was found after 2 weeks; thereafter, it decreased (Figure 5.2). However, the peak of ALP activity appeared to be patient dependent for one patient it occurred at week 2 and for two patients at week 3. MDCsFn in osteogenic media showed a trend of higher levels of ALP activity, in all tested patients, throughout the tested time period than in control media apart from week 4 (trend 3/3 for time points 1, 2 and 3). At week 4 the ALP activity of MDCsFn in osteogenic media was higher in two patients and lower in one patient compared to control media. The ALP activity of MDCsFn in control media also varied between time points; the ALP activity was lower for the later time points *i.e.* week 4 than the earlier *i.e.* week 1 (Figure 5.2; trend 3/3). The patient variations in ALP activity were very large for MDCsFn; at week 2, when the ALP activity had its peak, the patient that showed the highest ALP activity had 150 times higher ALP activity than the patient with the lowest.

In MSCs the ALP activity appeared to also have reached its peak at week 2 and decreased rapidly thereafter (Figure 5.3). However, the peak of ALP activity appeared to be patient dependent for one patient it occurred at week 1 and for two patients at week 2. MSCs in osteogenic media showed throughout the tested time period higher

ALP activity than in control media at each time point tested apart from week 2 (trend 3/3 for time points 1, 3 and 4). At week 2 the ALP activity of MSCs in osteogenic media was higher in two patients and lower than control in one patient. There was a difference in ALP activity for MSCs over time for both MSCs in osteogenic as well as control media; the ALP activity was lower at later time points *i.e.* week 3 and 4 than the earlier *i.e.* week 1 and 2 (Figure 5.3; trend 3/3 for all comparisons). The pattern of ALP activity in MSCs in control media was the same as for cells in osteogenic media *i.e.* the highest mean ALP activity was measured at 2 weeks (Figure 5.3; trend 3/3). This result could suggest that MSCs in control media underwent a certain level of osteogenic differentiation that most likely was initiated by cell contact (Tang *et al*, 2010). The patient variations of ALP activity were moderate for MSCs; at week 2, when the ALP activity had its peak, the patient that had the highest ALP activity had only 1.7 times higher ALP activity than the patient with the lowest.

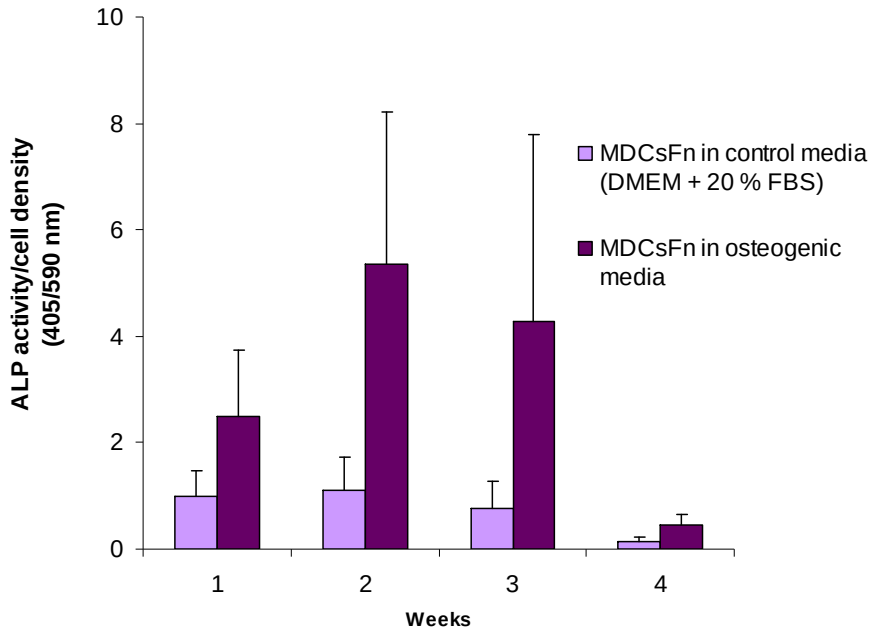

Figure 5.2. ALP activity in MDCsFn. ALP activity in MDCsFn appeared to increase until week 2 or 3; thereafter, it decreased. The peak of ALP activity was patient dependent, for one patient it occurred at week 2 and for two patients it occurred at week 3. The experiments were performed in three patients (n=3) in triplicates. Results presented as mean+sem. Sample size calculation estimated that 10 samples were required to accept the outcome of a statistical test to see an effect of 1 unit.

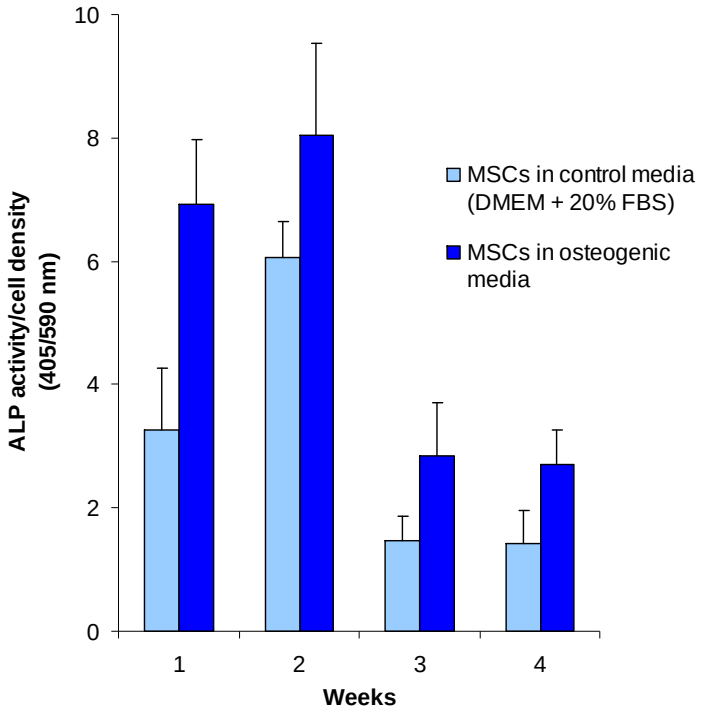

Figure 5.3. ALP activity in MSCs over time. ALP activity in MSCs appeared to peak of ALP at 2 weeks; thereafter the ALP activity rapidly decreased. The peak of ALP activity was patient dependent for one patient it occurred at 1 week and for two patients it occurred at 2 weeks. The experiments were performed on three patients (n=3) triplicates. Results presented as mean+sem. Sample size calculation estimated that 10 samples were required to accept the outcome of a statistical test to see an effect of 1 unit.

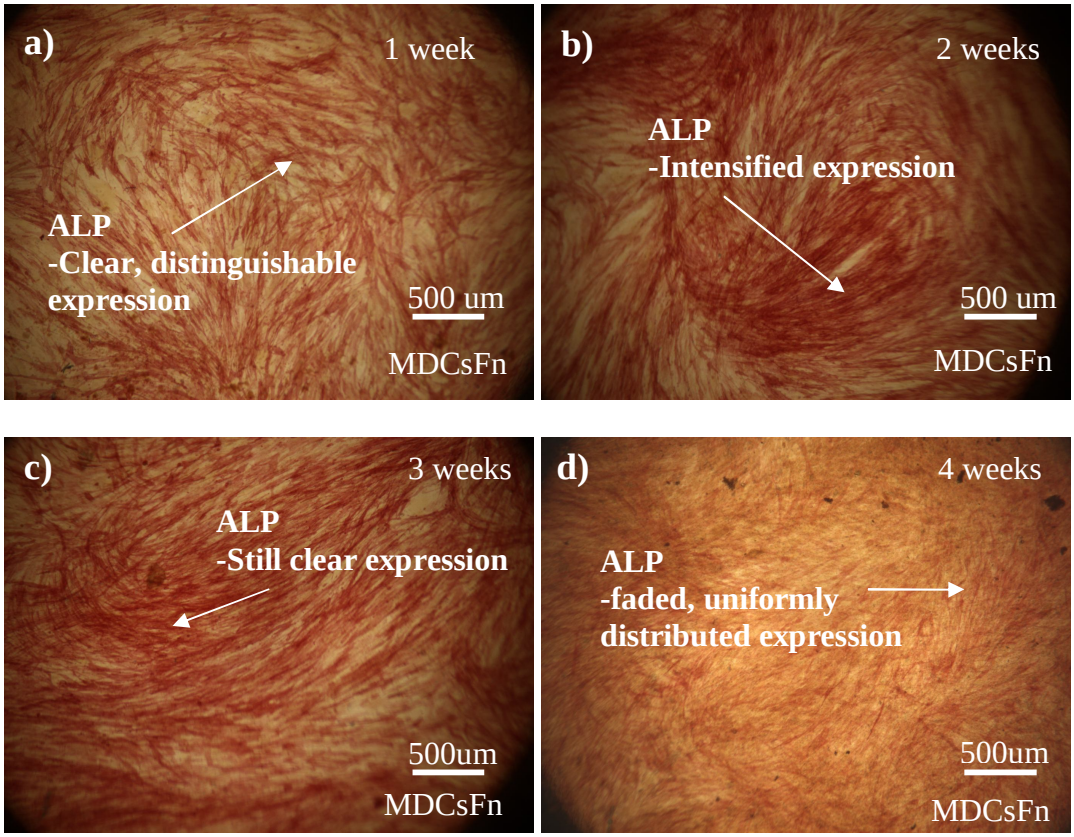

Figure 5.4. ALP staining of MDCsFn over 4 weeks. The MDCsFn showed a time-dependent pattern of ALP expression (pink). The ALP expression was strongest after 2 weeks. MDCsFn in osteogenic media after a) 1 week, b) 2 weeks, c) 3 weeks and d) 4 weeks. The experiments were performed in three patients (n=3) in triplicates. Magnification x4.

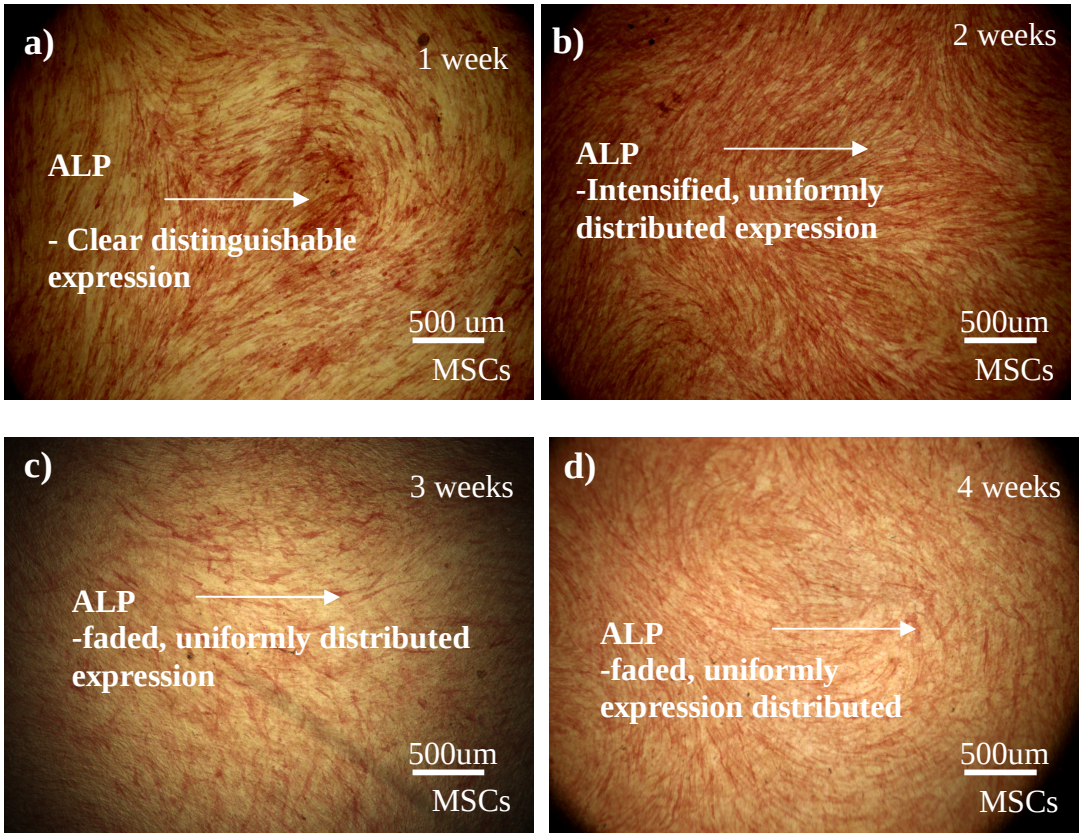

Figure 5.5. ALP staining of MSCs during 4 weeks. The MSCs showed a time-dependent pattern of ALP expression (pink). The ALP expression was strongest after 2 weeks. MSCs in osteogenic media after a) 1 week, b) 2 weeks, c) 3 weeks and d) 4 weeks. The experiments were performed on three patients (n=3) in triplicates. Magnification x4.

5.3.2 MINERALIZATION

Mineralization was assessed by Alizarin Red S staining and quantification by extracting the stain and measuring using a spectrophotometer. The results showed that the mineralization increased over the time period studied *i.e.* 4 weeks by both MDCsFn and MSCs.

Mineralization by MDCsFn increased over time, the largest change induced by osteogenic media occurred between week 3 and 4 (Figure 5.6 -5.7). At every time point,

there were higher levels of mineral on MDCsFn in osteogenic compared to MDCsFn in control media (trend 3/3 for all time points). For MDCsFn in control media there was a slight increase of mineralization over time (trend 3/3 between week 1 and 4). The mineralization of MDCsFn appeared to be less patient dependent than its ALP activity; there was only a 1.7-fold difference between the tested MDCsFn that expressed most mineralization and the MDCsFn that expressed least mineralization at 4 weeks.

Mineralization by MSCs increased over time, the largest increase in osteogenic media occurred between week 3 and 4 (Figure 5.8- 5.9; trend 3/3). At every time point there were higher levels of mineral on MSCs in osteogenic compared to MSCs in control media (trend 3/3 between all time points). For MSCs in control media, there was also a slight increase over time (trend 3/3 between week 1 and 4). Mineralization of MSCs appeared to be relatively consistent between patients, with only a 2-fold difference between the highest and lowest levels detected at week 4.

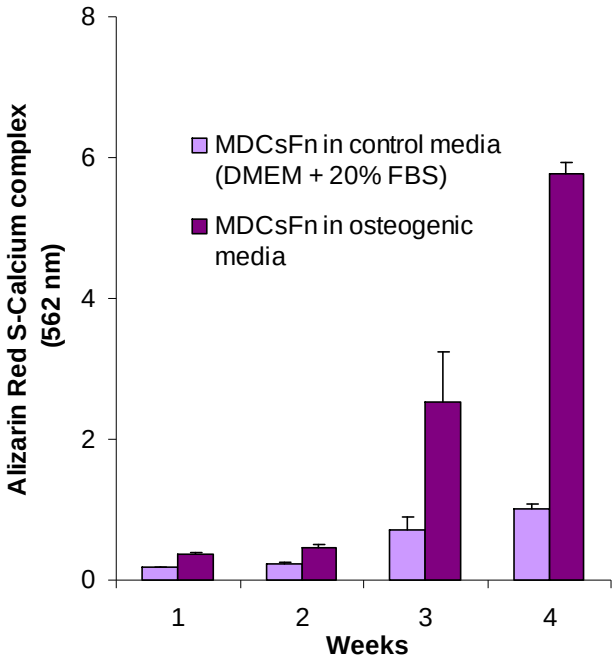

Figure 5.6 Alizarin Red S-Calcium quantification of MDCsFn. The mineralisation increased rapidly from week 3 to 4 (trend 3/3). The experiments were performed on three patients (n=3) in triplicates. Result presented as mean+sem. Sample size calculation estimated that 5 samples were required to accept the outcome of a statistical test to see an effect of 2 units.

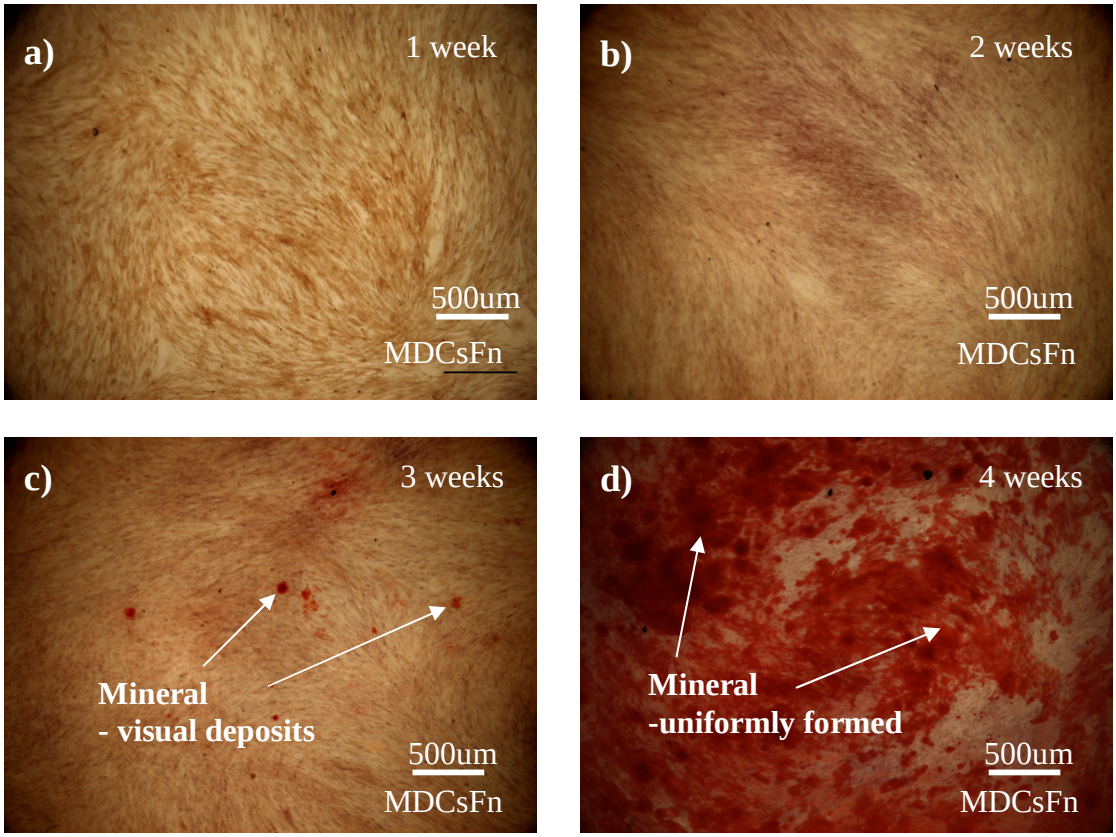

Figure 5.7. Alizarin Red S staining of MDCsFn over 4 weeks. After 3 weeks the first deposits could be seen on MDCsFn. There was a large increase in mineralization of MDCsFn between week 3 and 4. MDCsFn in osteogenic media at a) 1 week, b) 2 weeks, c) 3 weeks and d) 4 weeks. All experiments were performed on three patients (n=3) in triplicates. Magnification x4. Note: Same images as in 4.10.

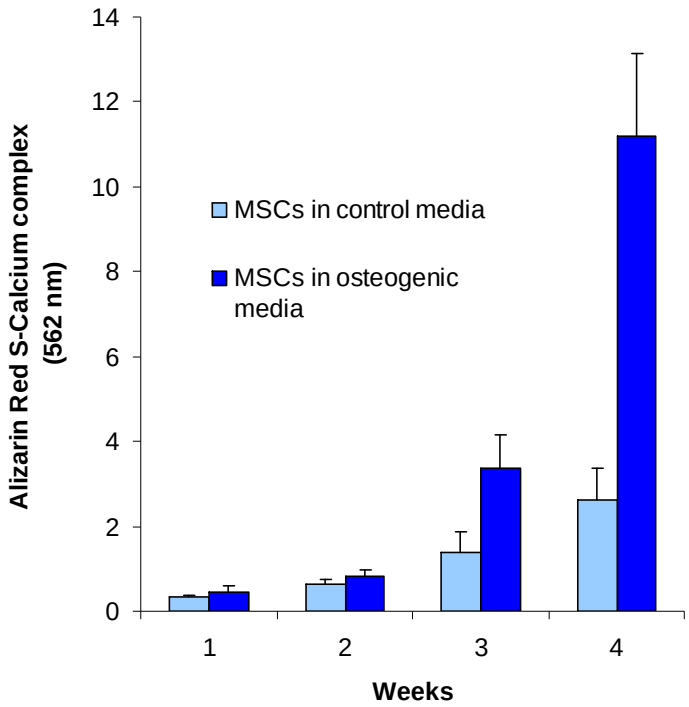

Figure 5.8. Alizarin Red S-Calcium quantification of MSCs. The mineralization of MSCs in osteogenic media increased slowly from week 1 to 2 and thereafter more rapidly, with the largest difference between week 3 and week 4 (trend 3/3). The experiments were performed in three patients (n=3) in triplicates. Result presented as mean+sem. Sample size calculation estimated that 5 samples are required to accept the outcome of a statistical test to see an effect of 2 units.

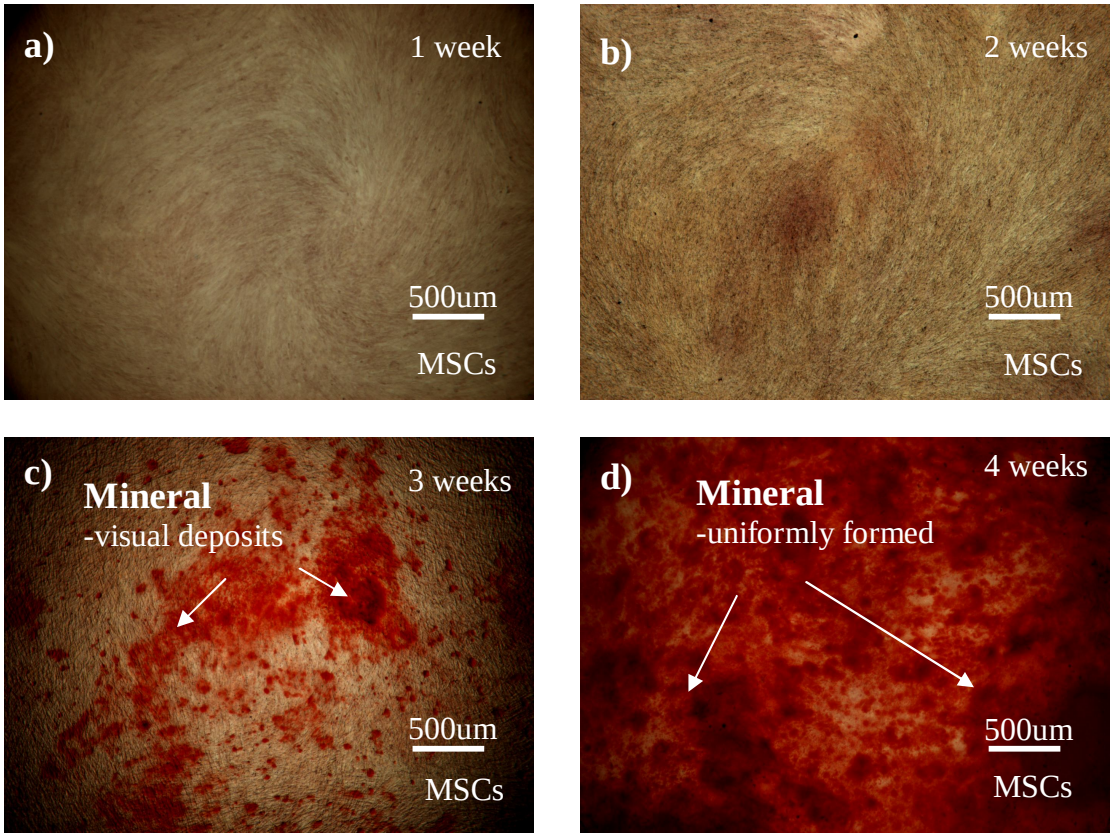

Figure 5.9 Alizarin Red S-Calcium staining of MSCs over 4 weeks. After 3 weeks the first deposits could be seen on MSCs. There was a large mineralisation increase between week 3 and 4. MSCs in osteogenic media at a) 1 week, b) 2 weeks, c) 3 weeks and d) 4 weeks. The experiments were performed on three patients (n=3) in triplicates. Magnification x4.

5.3.3 Q-PCR ARRAY OF OSTEOGENIC GENES

Gene expression of MDCsFn and MSCs was analysed at 2 weeks in either osteogenic or control media by qPCR Array (for experimental details, see Chapter 2.9 and Chapter 5.2.1).

5.3.3.1 UNDETECTED GENES

There were several genes that were undetected in both MDCsFn and MSCs (Table 5.2). Most of these genes are expressed by non-osteblastic lineages; both Ameloblastin enamel matrix protein (AMBN) and Amelogenin Y-chromosomal (AMELY) are expressed by ameloblasts (Hatakeyama *et al*, 2009), Calcitonin receptor (CALCR) is known to be only detected in osteoclasts (Dacquin *et al*, 2004), CASR in the parathyroid glands (Theman & Collins, 2009), Dentin sialophosphoprotein (DSPP) is odontoblast specific (Thyagarajan *et al*, 2001) and DMP1 is a dentin protein and its expression might be restricted to odontoblats in humans (Martinez *et al*, 2009). Osterix, which often has been described as a master regulator for osteogenic differentiation in mice, was also negative. There have been indications that Osterix might only be expressed in human embryonic tissue, not in adult tissue (Gao *et al*, 2004). BMP-7 was not detected in any of the MSCs samples, but was detected in one of the MDCsFn samples. Several BMPs, including BMP-7, are known to induce osteogenic differentiation in osteoblastic precursor cells, but BMP-7 is in general considered to be less osteogenic potent than other BMPs, such as BMP-2 and -4 (Cheng *et al*, 2003). Very little research has studied the expression of BMPs during osteogenic differentiation in stem cells; in general, BMPs, including BMP-2-4 and -7, are added *in vitro* to induce osteogenesis, and no data was found in the literature to explain the absence of BMP-7 in MSCs.

Table 5.2. Summary of undetected genes in MDCsFn and MSCs and suggested explanation why the genes were not expressed. *Not expressed in MSCs, detected in one sample of MDCsFn

GENE	SUGGESTED EXPLANATION
AMBN	Secreted by ameloblasts (Hatakeyama *et al*, 2009)
AMELY	Secreted by ameloblasts (Hatakeyama *et al*, 2009)
BMP-7*	- Unknown reason
CALCR	-Expressed on osteoclasts not osteoblasts (Dacquin *et al*, 2004)
CASR	-Expressed on the parathyroid glands (Theman & Collins, 2009)
DMP1	- Dentin protein (Martinez *et al*, 2009).
DSPP	-odontoblast specific expression (Thyagarajan *et al*, 2001)
OSTERIX	-Only detected in embryonic human tissue not in adult human tissue (Gao *et al*, 2004)

There were also some genes in MDCsFn, Fibroblast growth factor receptor 1 (FGFR-1), FGFR-2, Growth differentiation factor 10 (GDF10), BSP and Matrix metalloproteinase 13 (MMP13), that were irregularly expressed in the patients *i.e.* were detected in some patient samples but not in others. FGFR-1 and FGFR-2 are involved in the formation of long bones as a negative regulator (Deng *et al*, 1996; White *et al*, 2005), GDF10 is a member of the TGF-β super family but its *in vivo* function is not clear (Hino *et al*, 1996), BSP is expressed in fully differentiated osteoblasts (Kim *et al*, 1994), and MMP13 plays a part in bone remodelling by degrading the ECM (Laush *et al*, 2009). The impact of these genes not being consistently activated, for future bone engineering applications, is hard to evaluate without a valid *in vivo* model.

5.3.3.2 UP AND DOWNREGULATION

5.3.3.2.1 MDCsFN

The expression of most up-or-down regulated genes in MDCsFn showed patient-dependent inconsistency in their expression. This could be due to patient-dependent variation in time the cells need to differentiate *i.e.* how easy the cells commit to the osteogenic lineage. There can also be variations in the stage of maturity of the cells within and between the patient samples. It was previously established (Figure 5.2) that the ALP activity of MDCsFn in osteogenic media was higher than in control media at 2 weeks (trend 3/3); however, on mRNA level ALP expression was not consistent increased (trend 2/3; Figure 5.10). This finding could be explained by the lag period there is between gene expression and protein production.

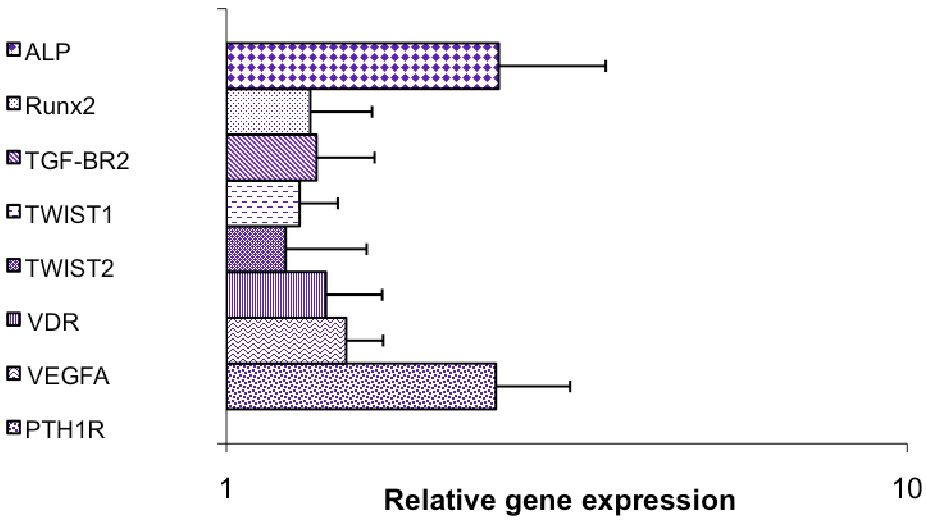

Figure 5.10. Upregulation of genes in MDCsFn after 2 weeks in osteogenic media compared to control media. None of the genes were significantly upregulated. Definition of upregulation was that there was a ≥ 0.2 unit positive difference between the mean gene expression in osteogenic media compared to MDCsFn in control media**.** The experiment was performed on three patients (n=3). Results presented as mean+sem. The gene expression of cells in osteogenic media was normalized to cells in control media (for more experimental details see Chapter 2.9). Sample size calculation estimated that 199 samples are required to accept the outcome of a statistical test to see an effect of 0.2 unit.

The gene that was most upregulated in 2 patients was PTH1R; however, it was not consistent upregulated (trend 2/3) in MDCsFn. PTH1R is considered to be an osteoblastic marker since it is expressed on osteoblasts (Ahlstrom *et al*, 2009). PTH1R is the receptor for PTH and together they are considered to be the most important regulators of calcium ion homeostasis *in vivo* (Mannstadt *et al*, 1999; Huang *et al*, 2001; Pioszak & Xu, 2008).

Despite the upregulation of PTH1R, in 2 patients, it appeared as at 2 weeks in osteogenic media the MDCsFn were still in an early stage in their osteogenic differentiation, since Runx2 was not upregulated (Figure 5.10).

The two TWIST factors, 1 (trend 2/3) and 2 (trend 1/3), might be slightly upregulated, at least in some patients (Figure 5.10). It has been hypothesized that the expression of TWIST 1 and TWIST 2 must be decreased to allow Runx2 expression to increase (Bialek *et al*, 2004; Chapter 1.2.2). It is believed that the expression of TWIST1 and TWIST2 maintains cells in an osteoprogenitor or preosteoblast-like state to prevent premature osteoblast differentiation (Lee *et al*, 2000; Bialek *et al*, 2004).

These results suggest that the cells were at a crossroad at 2 weeks, where they could be ready to commit to an osteoblastic phenotype. The upregulation of VDR (trend 2/3) and VEGFA (trend 3/3; Figure 5.10) in some patients is hard to interpret since VDR is known to have dual effects; in early osteogenic cultures it can inhibit osteogenic differentiation and in later cultures it can promote osteogenic differentiation (St-Arnaud, 2008). The impact of VEGFA on osteogenic differentiation is controversial; studies have claimed that VEGFA can enhance osteogenesis (Mayer *et al*, 2005) as well as it can have a suppressive effect (Shonmeyr *et al*, 2010). In experiments performed by Shonmeyr *et al* (2010), VEGFA suppressed the mRNA expression of BMP-2. This is in accordance with results in this study; VEGFA is upregulated in MDCsFn while (Figure 5.10) BMP-2 (trend 3/3) is downregulated (Figure 5.11).

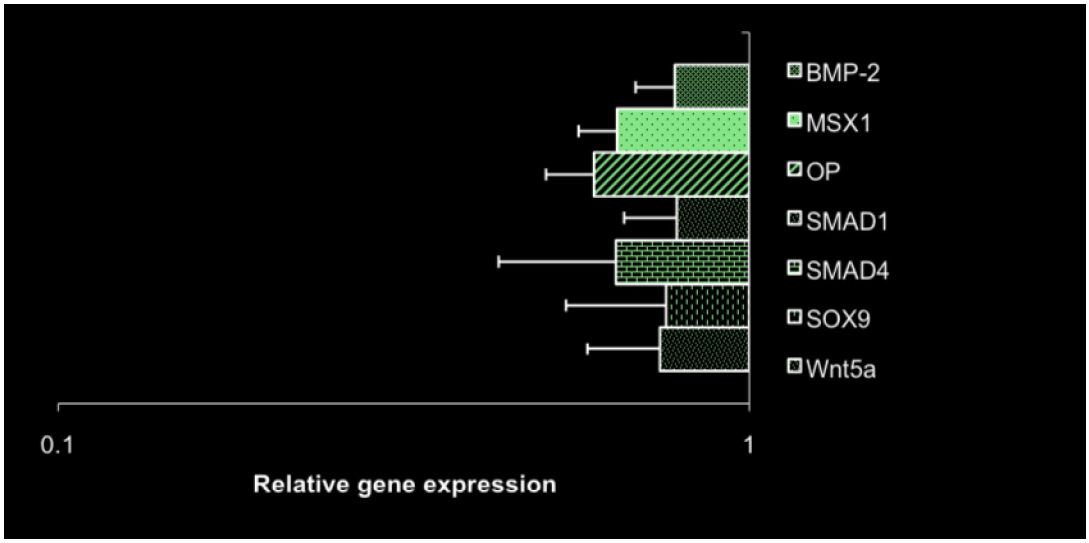

Figure 5.11. Downregulation of genes in MDCsFn after 2 weeks in osteogenic media compared to control media. Muscle segment homeobox 1 (MSX1; trend 3/3) and OP (trend 3/3) were consistently downregulated in MDCsFn after 2 weeks in osteogenic media compared to cells control media. Definition of downregulation was that there was a ≥ 0.2 unit negative difference between the mean gene expression in osteogenic media compared to MDCsFn in control media**.** The experiments were performed on three patients (n=3). Results presented as mean-sem. The gene expression of cells in osteogenic media was normalized to cells in control media (for more experimental details see Chapter 2.9). Sample size calculation estimated that 199 samples were required to accept the outcome of a statistical test to see an effect of 0.2 units.

As mentioned above, BMP-2 (trend 3/3) was downregulated after 2 weeks in osteogenic media. BMPs, *e.g.* BMP-2, induce osteogenesis by binding to BMPs receptors, which then phosphorylate transcription factors, such as Smad1 that forms a complex with Smad4 in the nucleus. Hence, it is logical that when BMP-2 is downregulated Smad1 (trend 2/3) and Smad4 (trend 2/3) are also downregulated (Figure 5.11).

Indication that osteogenesis was undergoing was that Sox9 (trend 2/3) was found to be downregulated in MDCsFn in two patients. Sox9 is mostly known as a marker for chondrogenesis, and researchers have found it can suppress bone formation (Hattori *et al*, 2010).

Two genes to encode mineralization proteins, OP and MSX1 were downregulated (Kazanecki *et al*, 2007). These two proteins are considered markers for terminal differentiation (Blin-Wakkach, 2001) is not surprisingly since at 2 weeks, MDCsFn had not started to mineralize (Figure 5.6 and 5.8). These results suggested that MDCsFn could differentiate along the osteogenic lineage despite their muscle origin.

5.3.3.2.2 MSCs

The gene expression of MSCs was more consistent than for MDCsFn. Both the ALP activity of MSCs in osteogenic media (Figure 5.3) and the mRNA levels of ALP expression were not consistently increased (trend 2/3; Figure 5.12). One patient sample had its ALP activity peak at week 1, this could explain the inconsistency in the mRNA expression of the MSCs.

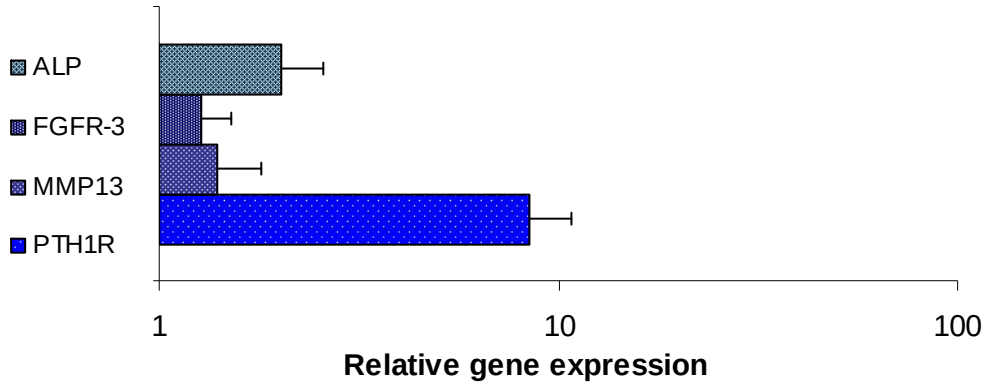

Figure 5.12. Upregulation of genes in MSCs after 2 weeks in osteogenic media compared to control media. PTH1R was consistently increased in MSCs in osteogenic media compared with control media (trend 3/3). Definition of upregulation was that there was a ≥ 0.2 unit positive difference between the mean gene expression in osteogenic media compared to MDCsFn in control media**.** The experiments were performed on three patients (n=3). Results presented as mean+sem. The gene expression of cells in osteogenic media was normalized to cells in control media (for more experimental details see Chapter 2.9). Sample size calculation estimated that 199 samples are required to accept the outcome of a statistical test to see an effect of 0.2 units.

PTH1R was upregulated in MSCs (Figure 5.12; trend 3/3); it is known that dex can induce upregulation of PTH1R (Ahlstrom *et al*, 2009). This has been described as a combined event with upregulation of ALP and Runx2 (Ahlstrom *et al*, 2009). Whilst this is in accordance with this study in terms of ALP, the MSCs expressed decreased levels of Runx2 (Figure 5.13; trend 3/3).

Many genes were downregulated in MSCs that had been in osteogenic media compared with MSCs in control media (Figure 5.13). Both BMPs that were expressed, BMP-2 (trend 3/3) and-4 (trend 3/3), and the BMP related protein GDF10 (trend 3/3) were downregulated at 2 weeks in osteogenic media. Consequently, as explained in Chapter

5.3.3.2.1, the following cascade of Smad proteins was also downregulated (Figure 5.13; trend 3/3 for both Smad 1 and 4).

In contrast to MDCsFn, the VEGFA in MSCs was downregulated (Figure 5.13; trend 3/3) in all patients. Genes that encode protein that characterize late or terminal differentiation *i.e.* MSX1 (trend 3/3), OP (trend 3/3) and Secreted protein, acidic, cysteine-rich (SPARC; trend 3/3) were also downregulated (Figure 5.13) in all tested patients.

The expression of the TWIST factors in MSCs in osteogenic media were in level with the gene expression in control media and the lack of downregulation of these factors could mean that the cells still have to decrease for Runx2 to get upregulated.

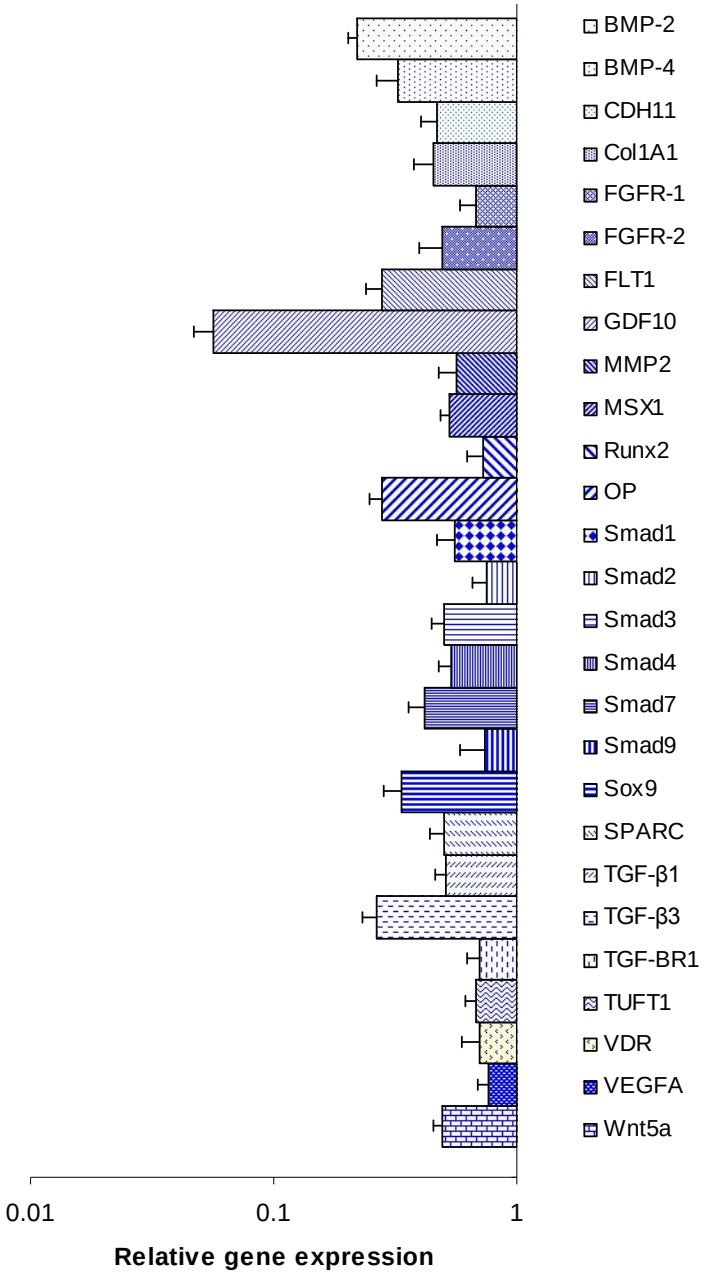

Figure 5.13. Downregulation of genes in MSCs after 2 weeks in osteogenic media compared to control media. Definition of downregulation was that the mean gene expression of the three patients is ≥ 0.2 units negative difference in MSCs in osteogenic media compared to MSCs in control media**.** The experiments performed on three patients (n=3). Results presented as mean-sem. The gene expression of cells in osteogenic media was normalized to cells in control media (for more experimental details see Chapter 2.9). Sample size calculation estimated that 199 samples were required to accept the outcome of a statistical test to see an effect of 0.2 units.

5.4 SUMMARY

In this chapter, MDCsFn and MSCs were compared in terms of mineralization and ALP activity and expression over 4 weeks. Thereafter, the gene expression of 46 genes involved in the osteogenic differentiation were analysed by qPCR when the cells had been 2 weeks in osteogenic media alternative control media.

For both cell types, MDCsFn and MSCs, the ALP activity first increased until week 1-3, thereafter it decreased. The decrease was more rapid for MSCs (Figure 5.3) than for MDCsFn (Figure 5.2). This agrees with the results of Jackson *et al* (2009), who compared the ALP activity of MDCs from traumatized muscle from unspecific anatomical location with MSCs. They found that the ALP activity of both MDCs and MSCs first increased and then later decreased.

As showed previously in this study, both MDCsFn and MSCs were able to mineralise (Chapter 3-5) and the mineralization process for the two cell types appeared to require approximately 4 weeks (Figure 5.6-5.9). In general, researchers incubate MSCs 1 to 2 weeks in osteogenic media before ALP analysis (Gronthos *et al*, 1994; Romanov *et al*, 2005; Aslan *et al*, 2006) and 3 to 4 weeks before mineralisation assay (Gronthos *et al*, 1994; Aslan *et al*, 2006).

In order to analyse the gene expression during osteogenic differentiation, the cells were analysed at 2 weeks in either osteogenic or control media. Many genes were downregulated in osteogenic media compared to cells in control media, especially for MSCs (Figure 5.13). At 2 weeks, it was not expected that late markers such as BSP or OP to be upregulated; however, also early markers such as Runx2 and Cadherin-11 (CDH11) were downregulated for MSCs. One explanation could be that the TWIST factors 1 and 2 regulate Runx2 by preventing premature differentiation (Chapter 1.2.2). Liu *et al* (2008) also found that Runx2 and Col1A1 was not upregulated by 2 weeks in osteogenic media in MSCs. The role of CDH11 in human osteogenesis is not clear; in mice it has been proven to promote cancer metastasis to bone (Chu *et al*, 2009). It is

also important to remember that throughout osteogenic differentiation there is a constant crosstalk between signals (Katoh, 2008), so the results might due to the time point. It is likely that many of the genes that were downregulated at 2 weeks either already have been upregulated or would be upregulated if different time point had been chosen.

Whilst there was a reasonably consistent gene regulation for the MSCs, the regulation of MDCsFn was more inconsistent (Chapter 5.3.3.1 and Chapter 5.3.3.2.1). This could be due to the higher patient variations within the MDCsFn or that the MDCsFn are more heterogeneous in terms of their differential potential capacity than the MSCs. This is expected since bone marrow-derived MSCs have their niche in the bone and MDCsFn have their's in the muscle. It appeared as MSCs had a higher osteogenic capacity compared to MDCsFn in terms of PTH1R upregulation, ALP expression and mineralization (Figure 5.10; Figure 5.12). However, in this chapter it was proven that MDCsFn were remarkable similar to MSCs, despite their different anatomical origin, in terms of gene expression, ALP activity and expression and mineralisation capacity (Figure 5.2-5.9).

Table 5.3. Summary of results from Chapter 5. Comparison of the osteogenic potential of MDCsFn and MSCs. ALP activity and mineralisation presented as mean±sem. *Not expressed in MSCs, detected in one sample of MDCsFn

	MDCsFn	**MSCs**
ALP activity **- at 2 weeks**	5.4±2.9	8.0±1.5
Mineralisation **-at 4 weeks**	11.2±1.9	5.8±0.16
Undetected gene expression	AMBN, AMELY, BMP-7*, CALCR, CASR, DMP1, DSPP, OSTERIX	AMBN, AMELY, BMP-7, CALCR, CASR, DMP1, DSPP, OSTERIX

CHAPTER 6:

RESULT SECTION 4

- IMPACT OF TI ON MDCsFN AND MSCs

6.1 INTRODUCTION SPECIFIC FOR RESULT SECTION 4

The results from the previous chapter, Chapter 5, demonstrated that MDCsFn and MSCs exhibit several similarities in osteogenic differentiation behaviour. Both populations had similar ALP and mineralization pattern and they also expressed a similar subset of osteogenic genes (see Chapter 5). In this chapter, the interaction of MDCsFn and MSCs on three different Ti surfaces that are or have been commercially available as dental implants have been studied. The surfaces were 1) SMO, a polished, smooth surface, 2) SLA, a rough sandblasted, acid-etched hydrophobic surface and 3) SLActive, a hydrophilic SLA surface. The impact of Ti surfaces on MDCsFn and MSCs was assessed in terms of metabolic activity and cell death.

6.2 METHODS SPECIFIC FOR RESULT SECTION 4

6.2.1 PRE-TREATMENT OF SMO AND SLA DISCS*

***Performed by Straumann AG**

In order to form pre-treated Ti discs, grade 2 Ti sheets, *i.e.* commercially pure Ti, were used and degreased by acetone and thereafter treated by a mixture of 2% ammonium fluoride/ 2 % hydrofluoric acid/10 % nitric acid solution (Figure 6.1).

The SMO was polished to a mirror finish with a 10 um diamond paste in oil and finally with a 0.06 um SiO_2 suspension (as described in Rupp *et al*, 2006). The SLA were made of pre-treated surfaces that had been coarse grit-blasted with corundum grit, 0.25-0.50 mm, at 5 bar until the surface became uniform grey before they were acid-etched with hydrochloric acid and sulphuric acid solution (as described in Martin *et al*, 1995; Rupp *et al*, 2006). The preparation of the discs, both SMO and SLA, were finalised by the discs being rinsed in deionised water before steam autoclaving.

The SLActive discs were produced with same sandblasting and acid-etchning procedure as SLA surfaces, but to increase their wettability or hydrophilicity the SLActive discs were rinsed under nitrogen to prevent exposure to air and stored in degassed isotonic sodium chloride solution in a sealed glass tube (Figure 6.2). This was done in order to protect the surface from hydrocarbon and carbide contamination of Ti surface *i.e.* contamination that increases the hydrophobicity of the oxidelayer on the Ti surface (Rupp *et al*, 2006). The sterilization of SLActive was performed by γ-irradiation overnight (as described in Zhao *et al*, 2005).

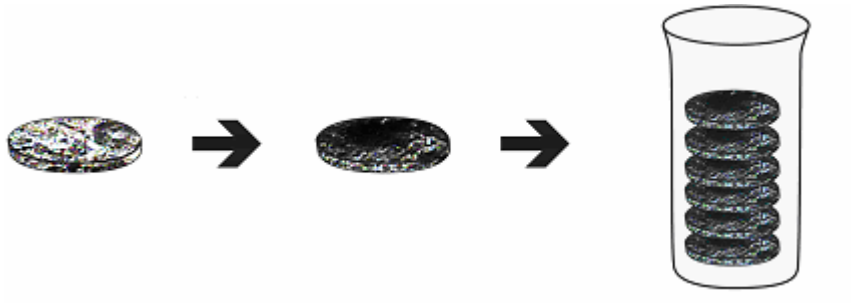

Figure 6.1. Scheme over production of SMO and SLA discs. Ti discs, 15 mm in diameter, were cut out from a sheet of 1.1 mm thick grade 2 Ti *i.e.* commercially pure Ti. Ti discs were degreased by acetone before pre-treated by a mixture of 2% ammonium fluoride/ 2 % hydrofluoric acid/10 % nitric acid solution at 55 °C for 30 s. Thereafter, SMO was polished to a mirror finish with a 10 um diamond paste in oil and finally with a 0.06 um SiO_2 suspension, whereas SLA were treated by coarse grit-blasted with 0.25-0.50 mm corundum grit at 5 bar until the surface became uniform grey, followed by acid-etching. Both surface types were rinsed in deionised water before steam autoclaving in 121 °C for 15 min.

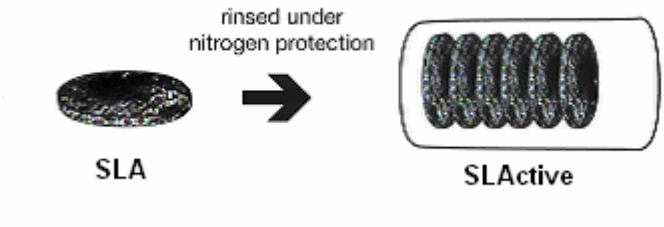

Figure 6.2. Hydrophobic SLA is transformed to hydrophilic SLActive. SLActive are SLA discs that have increased hydrophilicity. SLActive surfaces have been protected from air by nitrogen before they were stored in glass tubes containing isotonic NaCl solution. The discs were finally sterilized by γ-irradiation at 25 kGreys overnight.

The protection from air gives the SLActive surface a water contact angle of 0° (Table 6.1). A water contact angel of 0° means that that the surface's has an extremely hydrophilic character (Table 1.4; Rupp *et al*, 2006; Zhao *et al*, 2005).

6.2.2 FURTHER TREATMENT OF TI SURFACES

Before use in the cell culture experiments SMO and SLA surfaces were cleaned in 10% nitric acid for 10 min on each side before they were washed thoroughly with sterile deionised water to remove all nitric acid residues. The discs were left to dry in a sterile environment before treated by UV in a Coast-air Steristrom 2537å for an hour on each side. Using nitric acid in combination with UV to sterilise the discs means the use of alcohol or autoclaving can be avoided; alcohol and autoclaving can increase hydrophobicity (Zhao *et al*, 2005). The SLActive discs were delivered sterilised in a sealed glass vial (Figure 6.2) and were used straight after the package was broken.

Table 6.1. Physical data of the three tested Ti discs SMO, SLA and SLActive. Data taken from Brett *et al*, 2004; Zhao *et al*, 2005; Rupp *et al*, 2006; Straumann communication)

DISC	**SMO**	**SLA**	**SLActive**
Treatment	Polished	Sandblasted, acid-etched	SLA protected from air
Attachment area (mm^2)	25	33.9	33.9
Roughness levels (Ra/um)	0.06	4.0	4.0
Hydrophilic/ hydrophobic	Hydrophobic	Hydrophobic	Hydrophilic
Thickness (mm)	1.1	1.1	1.1
Diameter (mm)	15	15	15
Water contact angle (°)	95.76±4.0	138.3±4.2	0

6.3 RESULTS FOR RESULT SECTION 4

6.3.1 THE IMPACT OF TI ON METABOLIC ACTIVITY

6.3.1.1 MDCsFN ON TI

MDCsFn were seeded, at a density of 1000 cells/cm^2 in culture media, onto the three Ti surfaces *i.e.* SMO, SLA and SLActive, and TCP to study if the roughness and hydrophilicity of the surfaces had any impact on the metabolic activity of MDCsFn over 5 weeks in culture media. The metabolic activity measured by Alamar Blue is used as a measurement for the cell number.

MDCsFn cultured on SLA and SLActive showed throughout the test period a lower metabolic activity than on SMO and TCP (trend 3/3 for both conditions for all time points). There was no consistent difference between TCP and SMO or between SLA and SLActive throughout the test period (Figure 6.3).

The metabolic activity of MDCsFn increased over time on all the surfaces. After 4 weeks the metabolic activity on TCP and SMO appeared to have reached a plateau, probably due to confluency (Figure 6.3). There was a lag period, week 0-2, on both SLA and SLActive before the cell number *i.e.* metabolic activity started to increase (Figure 6.3). After 5 weeks, it appeared that the cell number on SLA and SLActive still had not reached its plateau (Figure 6.3).

The initial metabolic activity, at time point 0, was lower on SLA and SLActive compared to SMO and TCP (trend 3/3 for both conditions). This indicates that the rough surface is causing cell death of MDCsFn and it is very likely that this cell death is responsible for the lag phase on SLA and SLActive (Figure 6.3).

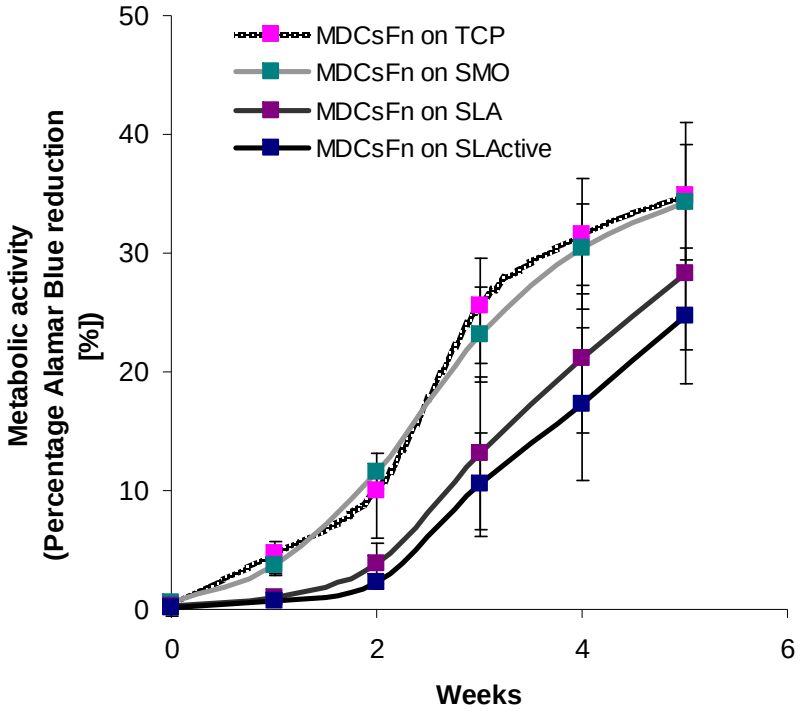

Figure 6.3. Metabolic activity of MDCsFn on the Ti surfaces over 5 weeks. There was a lag period for the MDCsFn on SLA and SLActive of approximately 2 weeks. Seeding cell density was 1000 cells/cm^2. There was a consistent difference between SMO/TCP and SLA/SLActive during the whole tested period (trend 3/3 for both conditions for all time points). Experiments were performed in three patients (n=3) and in triplicates. Results presented as mean ± sem. Sample size calculation estimated that 4 samples were required to accept the outcome of a statistical test to see an effect or variation of 10% of the metabolic activity compared to TCP at 5 weeks.

6.3.1.2 MSCs ON TI

MSCs were seeded, at a density of 1000 cells/cm^2 in culture media, onto the three Ti surfaces *i.e.* SMO, SLA and SLActive, and TCP to study if the roughness and hydrophilicity of the surfaces had any impact on the metabolic activity of MSCs over 4 weeks. The metabolic activity measured by Alamar Blue is used as a measurement for the cell number.

Initially, MSCs on SLA and SLActive showed lower metabolic activity than on SMO and TCP; there was also a decrease in metabolic activity on SMO compared to TCP at time point 0. The difference between SLA or SLActive and SMO or TCP was consistent (trend 3/3 at week 0 and 1) until week 2 (Figure 6.4). After 3 weeks, there were no consistent trends in metabolic activity on TCP, SMO, SLA and SLActive (Figure 6.4).

A likely explanation is that the cells had reached confluency on all the surfaces after 3 weeks. Interestingly, there was lower metabolic activity, on SLActive (trend 3/3) at 4 weeks compared to TCP, SMO and SLA (Figure 6.4). The explanation for this behaviour might lay in the hydrophilicity of SLActive and that the cells on the hydrophilic surfaces are not able to use the surface area as efficiently as on the comparable SLA surface.

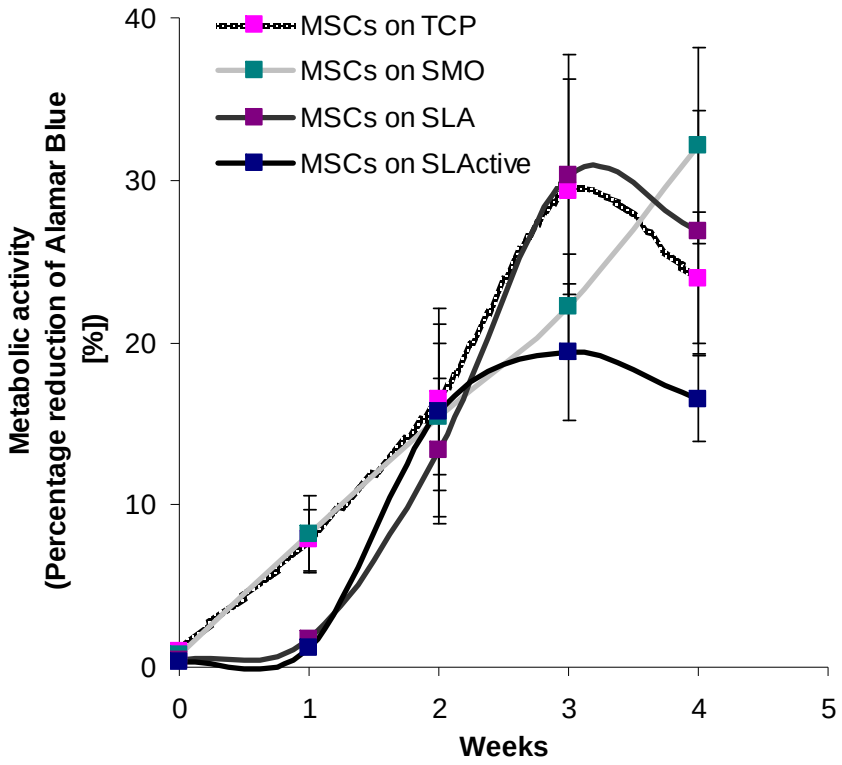

Figure 6.4. Metabolic activity of MSCs on the Ti surfaces over 4 weeks in culture media. There was a lag period during the first week for the MSCs proliferating on the SLA and SLActive (trend 3/3). Seeding cell density was 1000 cells/cm^2. Experiments were performed with three sets of patients (n=3) and in triplicates for each set. Results presented as mean ± sem. Sample size calculation estimated that 4 samples are required to accept the outcome of a statistical test to see an effect or variation of 10% of the metabolic activity compared to TCP at 5 weeks.

6.3.1.2.1 MSCs ON TI OVER 10 DAYS MEASURED BY MTT

The metabolic activity of MSCs for day 1, 5 and 10 was studied by MTT in order to confirm and investigate the lag period detected in Chapter 6.3.1.2. The cells were seeded at the same density, 1000 cells/cm^2, as in Chapter 6.3.1.2. The metabolic activity measured by Alamar Blue is used as a measurement for the cell number.

At day 1, there were no consistent differences between the metabolic activity by MSCs on TCP, SMO or SLA but there was a consistent difference between TCP and SLActive (tren 2/2; Figure 6.5). At day 5, there was a consistent difference of the metabolic activity between TCP or SMO and SLA or SLActive (trend 2/2 for all comparisons), but not between TCP and SMO or between SLA and SLActive. At day 10, there was a consistent difference between the metabolic activity on TCP and the other surfaces *i.e.* SMO, SLA and SLActive (trend 2/2 for all three comparisons); however, there was no consistent difference between SLA and SLActive. On all surfaces the metabolic activity increased between day 1 and day 10; this increase was only consistent between day 5 and 10 (Figure 6.5; 2/2 for all conditions). Since metabolic activity could be used as a measurement for cell number, this is in accordance with Wall *et al* (2009) findings that MSCs cultured on the rough surfaces underwent a decrease in cell number early in culture.

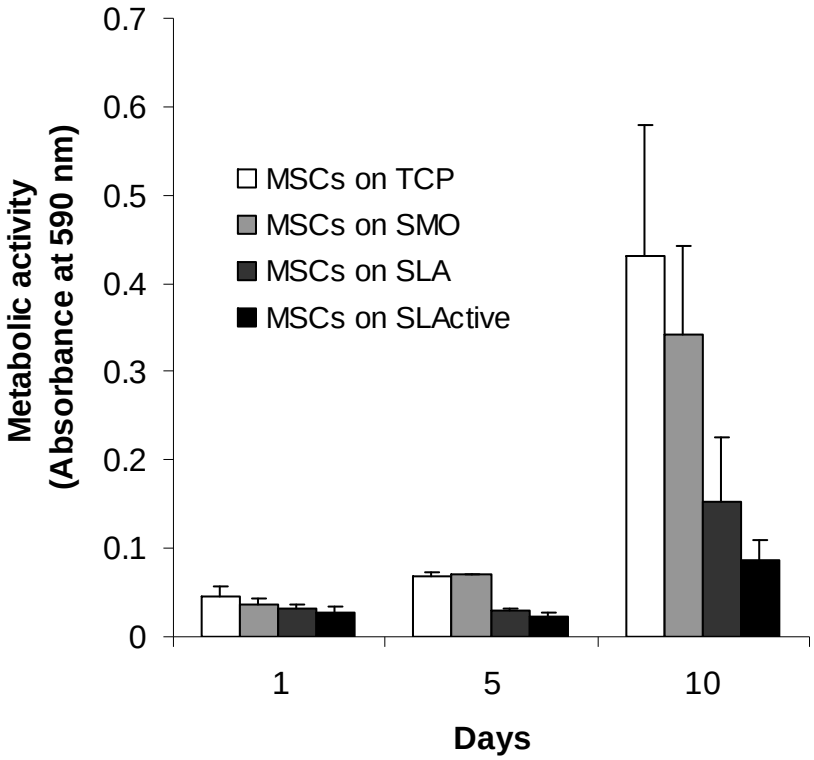

Figure 6.5. Metabolic activity of MSCs on Ti surfaces over 10 days. The cell number, measured by MTT, was increased over 10 days for cells on all the surfaces. The increase was consistently higher on SMO and TCP surfaces compared to SLA and SLActive at day 10 (trend 2/2). Seeding density was 1000 cells/cm^2. Experiments were performed on two patients (n=2) and in triplicates for each set. Results presented as mean + sem. Sample size calculation estimated that 52 samples were required to accept the outcome of a statistical test to see an effect of 0.4 units.

6.3.2 THE IMPACT OF TI ON CELL DEATH

6.3.2.1 MDCsFN

It was hypothesized that the initial lag period (Figure 6.3) detected on SLA and SLActive was caused by cell death. In order to investigate this hypothesis, cells were seeded, 10 000 cells/cm^2, on Ti discs and analyzed for apoptosis and necrosis by flow cytometry after 24 h.

Cells on SLActive underwent both more apoptosis and necrosis compared with the other surfaces; however, there was a clear pattern of the impact of the surfaces on both apoptosis and necrosis, where SLA had less apoptosis and necrosis than SLActive, but more than on SMO and TCP (trend 3/3 for both comparisons); there were no consistent difference between apoptosis and necrosis on TCP and SMO.

Table 6.2. Percentage apoptosis, necrosis and metabolic activity of MDCsFn detected on the four surfaces *i.e.* TCP, SMO, SLA and SLActive. Experiments were performed on three patients (n=3) and in triplicates for each set. Results presented as mean ± sem.

	TCP	**SMO**	**SLA**	**SLActive**
APOPTOSIS (%)	1.5±0.4	2.0±0.6	4.7±0.3	10.2±1.5
NECROSIS (%)	3.4±0.2	3.4±0.5	6.6±1.1	8.4±0.7
METABOLIC ACTIVITY(%)	95±0.5	94.7±1.0	88.7±1.4	77.4±0.6

MDCsFn on SLActive underwent approximately 2.2-fold more apoptosis (Table 6.2; Figure 6.7a) compared to cells on SLA. This increment in apoptosis could be due to the

higher hydrophilicity of the SLActive compared to SLA; cells on SLActive also underwent consistently more necrosis than cells on SLA (trend 3/3). Cells on SLA underwent both more apoptosis and necrosis than cells on SMO or TCP (trend 3/3). There was no consistent difference in the amount of apoptosis or necrosis of the cells on TCP and SMO. There was a reverse relationship between live cells and dying or dead cells (Figure 6.7 c). The increased cell death on SLA and especially SLActive, explains the earlier detected lag period of MDCsFn (Figure 6.3).

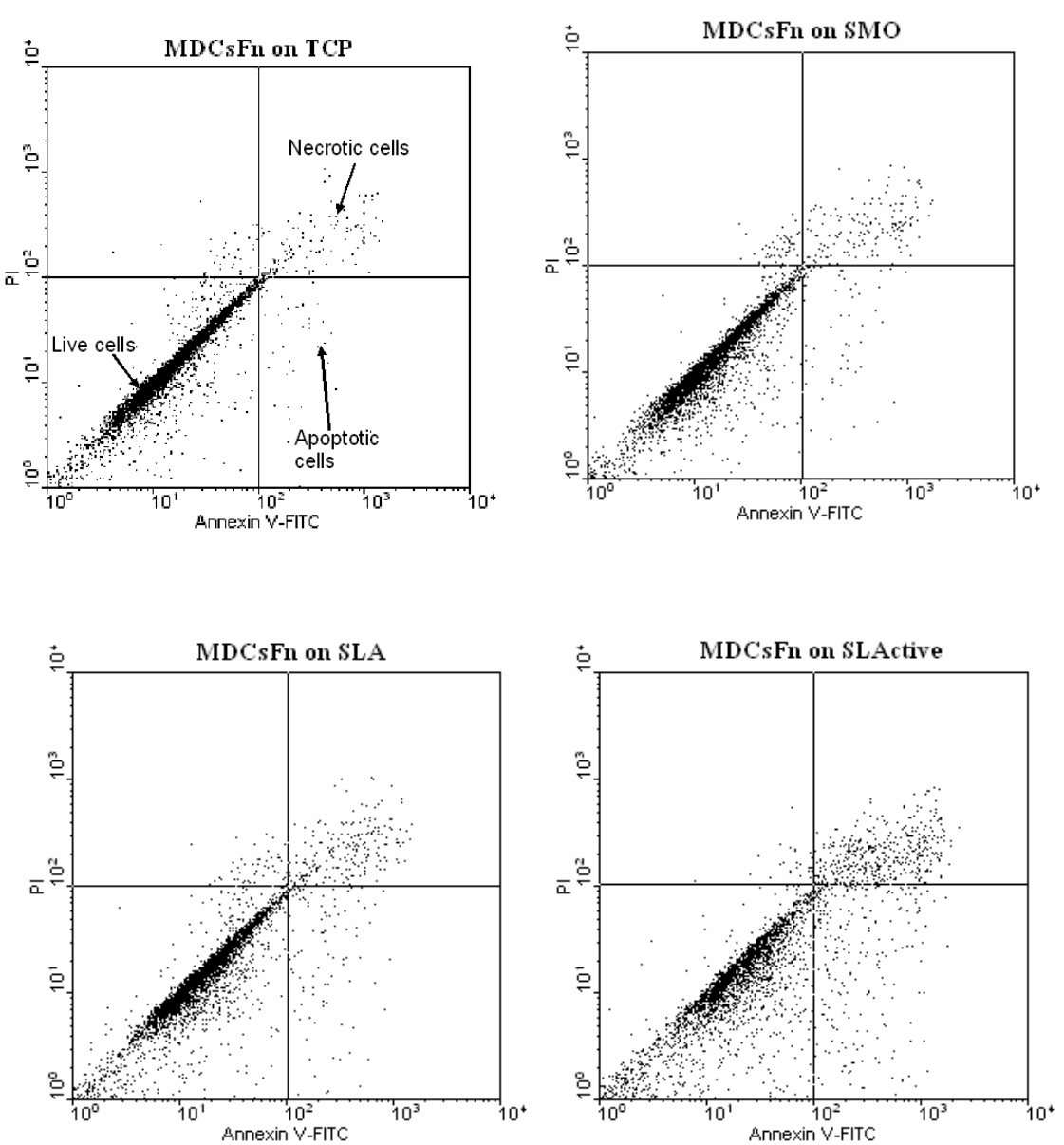

Figure 6.6. Dot plots of early apoptosis and necrosis of MDCsFn on TCP, SMO, SLA and SLActive assessed by flow cytometry. Cells on SLActive underwent more apoptosis and necrosis compared with the other surfaces; however, there was a clear pattern for both apoptosis and necrosis where: TCP=SMO<SLA<SLActive. Early apoptotic cells stained only positive for Annexin-V, necrotic cells stained positive for both Annexin-V and PI and live cells were negative for both Annexin-V and PI.

a)

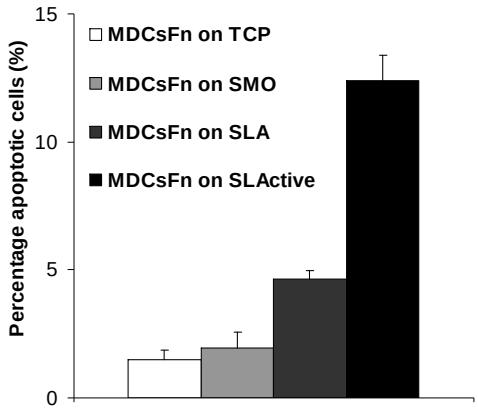

b)

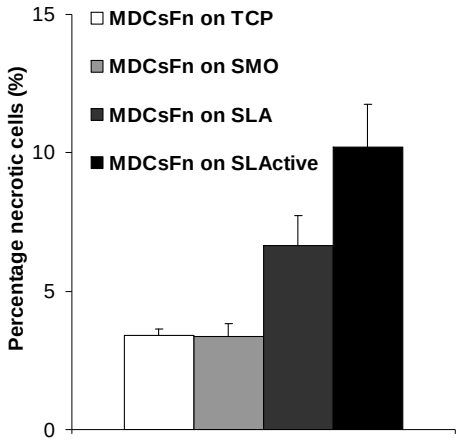

c)

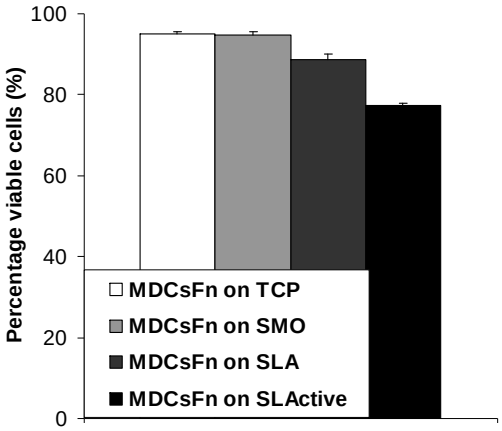

Figure 6.7. Percentage of MDCsFn on TCP, SMO, SLA and SLActive that underwent a) apoptosis, b) necrosis, or c) were alive after 24 h. Cells on SLActive underwent more a) apoptosis and b) necrosis compared with the other surfaces (trend 3/3); however, there was a clear pattern for both apoptosis and necrosis where: TCP=SMO<SLA< SLActive. There were more viable cells on TCP and SMO compared to SLA and SLActive (trend 3/3 for all comparisons). Experiments were performed with three patients (n=3) in triplicates. Results presented as mean + sem. Sample size calculation estimated that 5 samples are required to accept the outcome of a statistical test to see an effect of 2%.

6.3.2.2 MSCs

It was hypothesized that the initial lag period (Figure 6.4) detected on SLA and SLActive was caused by cell death. In order to investigate this hypothesis cells were seeded, 10000 cells/cm^2, on Ti discs and analyzed for apoptosis and necrosis by flow cytometry after 24 h.

In terms of necrosis there was no detected difference between SLActive and SLA but MSCs on SLActive underwent approximately 1.7-fold more apoptosis compared to cells on SLA (Table 6.3). This is likely caused by the increment in hydrophilicity of the SLActive compared to SLA. There was more apoptosis and necrosis on SLActive or SLA than on SMO or TCP (trend 3/3 for all comparisons). There was consistently more necrosis on SMO than on TCP surfaces after 24 hours (trend 3/3). As a consequence of the increased apoptosis and necrosis on SLActive, there was a decrease in its number of viable cells compared to the other surfaces (Figure 6.8 and 6.9c; trend 3/3). The detected increment in cell death on SLA and especially SLActive could explain the earlier detected lag period of MSCs (Figure 6.4).

Table 6.3. Percentage apoptosis, necrosis and metabolic activity of MSCs detected on the four surfaces *i.e.* TCP, SMO, SLA and SLActive. Experiments were performed on three patients (n=3) and in triplicates for each set. Results presented as mean ± sem.

	TCP	**SMO**	**SLA**	**SLActive**
APOPTOSIS (%)	10.0± 1.8	12.0± 1.0	14.9 ± 2.2	26.0± 0.4
NECROSIS (%)	6.4±1.8	12.0±0.6	16.9 ±1.6	18.3 ± 0.4
METABOLIC ACTIVITY(%)	83.6± 1.8	76.0± 1.3	68.2±2.4	55.7±0.3

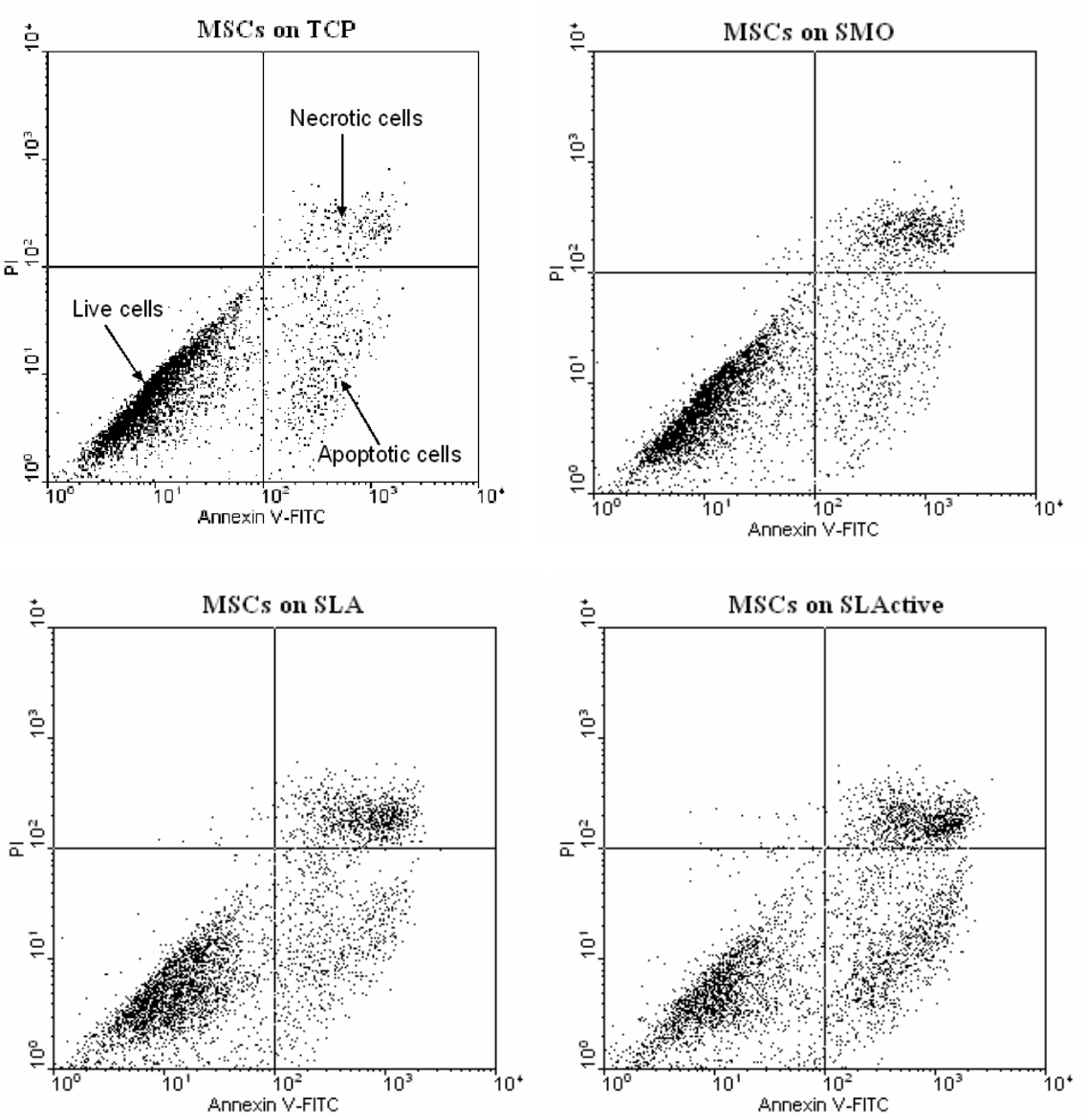

Figure 6.8. Dot plots of early apoptosis and necrosis of MSCs on TCP, SMO, SLA and SLActive assessed by flow cytometry. Cells on SLActive underwent more apoptosis compared with the other surfaces; MSCs on SLA and SLActive underwent more apoptosis and necrosis than SMO or TCP. Early apoptotic cells stained positive for only Annexin-V, necrotic cells stained positive for both Annexin-V and PI and live cells were negative for both Annexin-V and PI. All experiments were performed on three patients (n=3) in triplicates.

a)

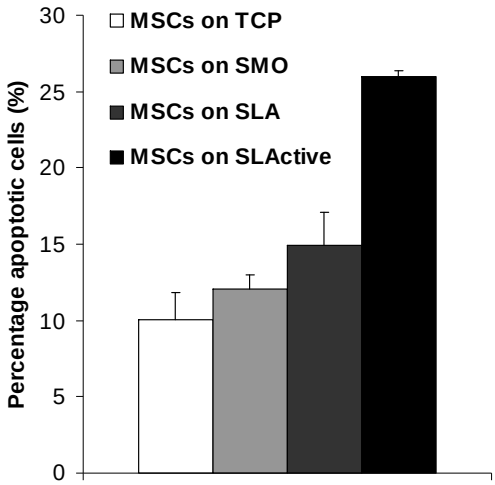

b)

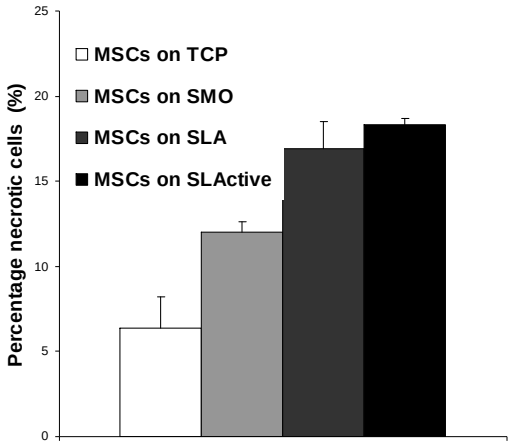

c)

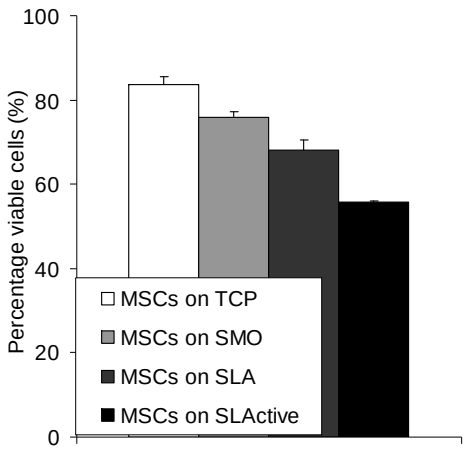

Figure 6.9. Percentage of MSCs on TCP, SMO, SLA or SLActive that underwent a) apoptosis, b) necrosis, or c) were alive after 24 h. MSCs on SLActive underwent more apoptosis and necrosis compared to the other surfaces (trend 3/3). There were more viable cells on TCP compared to SMO, SLA and SLActive (trend 3/3). All experiments (n=3) were performed in triplicates. Results presented as mean + sem. Results presented as mean + sem. Sample size calculation estimated that 5 samples are required to accept the outcome of a statistical test to see an effect of 2%.

6.3.3 ANALYSIS OF BONE FORMATION ON TI

There are several issues associated with analyzing osteogenic differentiation and mineralization on Ti. Ti is opaque, which makes it difficult to study the differentiation pathway, using microscopy. Using the quantitative method of Alizarin Red S that previously been used in this thesis also has limitations when used on Ti.

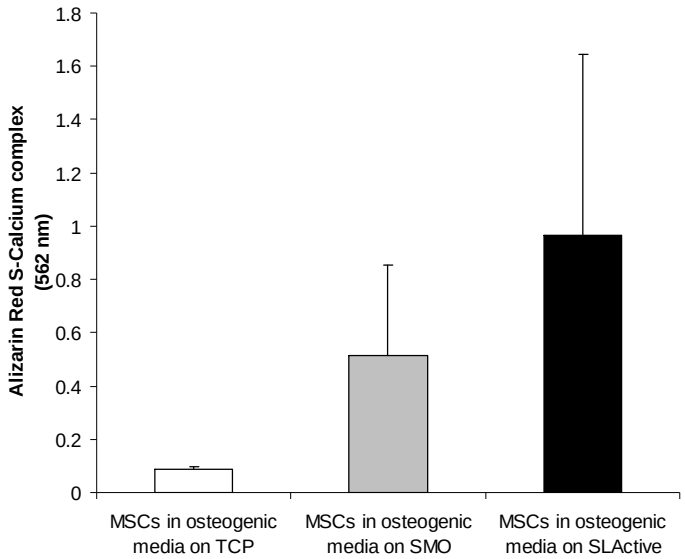

Figure 6.10. Alizarin Red S quantification of MSCs on various Ti surfaces at 1 week. More calcium was detected on SLActive than on TCP after 1 week in osteogenic media. Experiment was performed in triplicates and results presented as mean + 1std.

Alizarin Red S forms complex with calcium in the hydroxyapatite; however, calcium is also secreted when cells undergo cell death. As shown in this chapter, cells on SLActive undergo more cell death than on SMO (Figure 6.7; Figure 6.9) and can cause a bias interpretation of the results.

In order to analyse the cells' ALP activity MDCsFn were first seeded on Ti for 24 h before harvesting and then reseeded on TCP in osteogenic media. In this experiment

higher levels were detected in cells that had been seeded onto TCP or SMO than SLActive (trend 3/3). This is the opposite result to the expected since SLActive has been superior in terms of bone formation *in vivo* (Schwartz *et al*, 2008; Zöller *et al*, 2008; Morton *et al*, 2010).

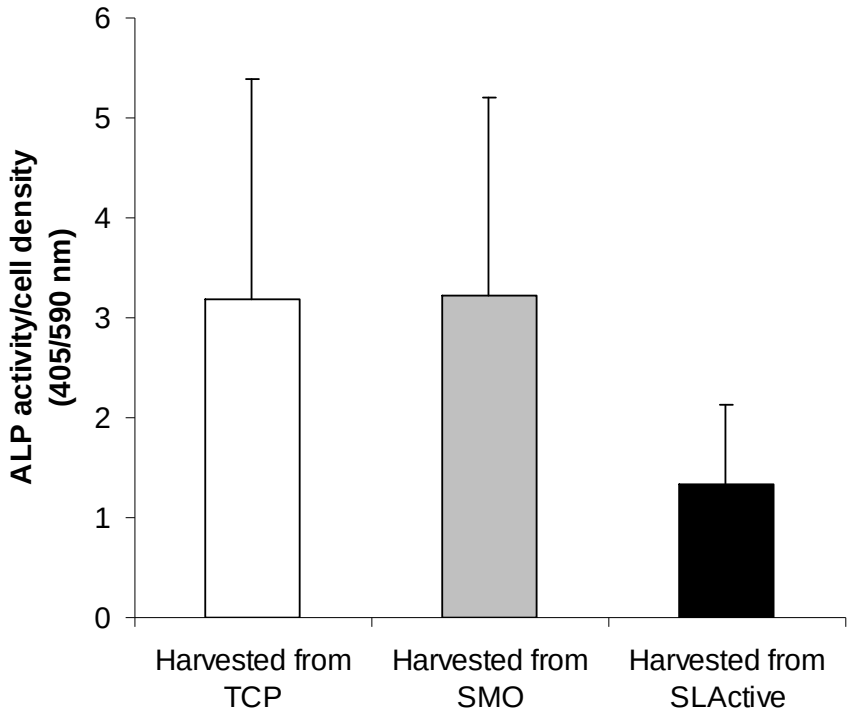

Figure 6.11. Measured ALP activity on MDCsFn at 1 week in osteogenic media. First, the cells had been harvested from various Ti discs and then reseeded on TCP. Higher ALP activity was detected in MDCsFn that had been harvested from TCP or SMO (trend 3/3) than from SLActive. Experiments were performed on three patients (n=3) in triplicates and results presented as mean+sem. Results presented as mean + sem. Sample size calculation estimated that 10 samples are required to accept the outcome of a statistical test to see an effect of 1 unit.

Partly due to the limitations of *in vitro* techniques in terms of studying cells interaction with scaffolds, a lot of researchers have used *in vivo* models to analyse the bone formed on scaffolds (Schwartz *et al*, 2008). Another reason is that bone is a complex tissue

(Chapter 1.2) and consists of several types of cells *i.e.* osteoblast, osteocytes and osteoclasts. *In vitro* assays, such as Alizarin Red S, can give a good indication of the cells capacity to mineralize, but cannot predict the bone remodeling process and the impact of the various cell types.

6.4 SUMMARY

In this chapter the biocompatibility of different Ti surfaces with MSCs and MDCsFn was studied. The two cell types exhibit many similarities, but also differences.

When cells were seeded on SLA and SLActive, there was a lag period for both MDCsFn (Figure 6.3) and MSCs (Figure 6.4) before the metabolic activity, which was interpreted as cell number, started to increase; this lag period could not be detected on SMO or TCP. The lag period appeared to last 1 week for MSCs and 2 weeks for MDCsFn. Throughout the test period, MDCsFn showed consistent lower cell number on SLA or SLActive compared to SMO or TCP. Initially for MSCs, there was the same pattern but this only lasted until week 2 between the tested surfaces thereafter there was no difference.

It is previously known that MSCs (Wall *et al*, 2009), MG63, an immature osteoblastic cell line, (Zhao *et al*, 2005; Kim *et al*, 2006) and osteoblasts (Brett *et al*, 2004) initially have lower viability on rough Ti surfaces compared to smooth. In this chapter, it has been shown that this is also true for MDCsFn (Figure 6.3; Figure 6.6-6.7).

It should be noted that MDCsFn expressed a higher percentage (Figure 6.7) of viable cells on all surfaces, compared to MSCs (Figure 6.9). For example, on SLActive approximately 80% of MDCsFn were viable after 24 hours (Table 6.2) compared to 55% of MSCs (Table 6.3).

Interestingly, the surface that induced highest levels of cell death, SLActive, is the surface that has shown superior osseointegration in bone implants *in vivo* (Rupp *et al*, 2006; Schwartz *et al*, 2008; Zöllner *et al*, 2008; Morton *et al*, 2010). This leads to the question if the cell death plays a role in osseointegration. If no, this could imply that the increased metabolic activity of MDCsFn on SLActive could mean that MDCsFn would be better to osseointegrate than MSCs.

Table 6.4. Summary of results from Chapter 6. Comparison of the impact various Ti discs, with different roughness and hydrophilicity, have on MDCsFn and MSCs.

	MDCsFn	**MSCs**
Lag period on SMO compared to TCP	No	No
Lag period on SLA compared to TCP	Yes – 2 weeks	Yes – 1 weeks
Lag period on SLActive compared to TCP	Yes – 2 weeks	Yes – 1 weeks
Trend for apoptosis	TCP=SMO<SLA< SLActive	TCP<SMO<SLA< SLActive
Trend for necrosis	TCP=SMO<SLA< SLActive	TCP<SMO<SLA< SLActive.
Trend for viability	SLActive<SLA<SMO=TCP	SLActive<SLA<SMO<TCP

CHAPTER 7:

DISCUSSION

7.1 DISCUSSION

The main aim for this thesis was to investigate the potential to use MDCs or the osteogenic subpopulation of MDCs, which were isolated by adherence within 20 min to Fn and named MDCsFn (Chapter 4), in bone engineering applications. It is probable that a scaffold of some sort will be needed to form engineered bone. Ti has been suggested as a suitable scaffold material due to its osseointegrative capacity (Granström, 2007).

The use of osteogenic cells seeded onto a Ti scaffold could have at least two applications in clinical bone regeneration. First, osteogenic cells could be used to regenerate new bone to replace bone tissue that had to be removed due to trauma or cancer. In order to regenerate new bone an anatomical mesh will most likely will be needed to form the new tissue. Second, osteogenic cells could be seeded onto Ti implants, *e.g.* dental hip or knee implants, to enhance osseointegration.

Bone marrow-derived MSCs have already shown promising results in bone regeneration applications in human (Warnke *et al*, 2004) and in sheep (Frosch *et al*, 2006); the advantage of using progenitor cells, and not mature cells, such as osteoblasts in tissue regeneration, is the progenitor cells possibility to expand (Alhadlaq & Mao, 2005). However, in order to obtain bone marrow-derived MSCs whole bone marrow is aspirated. This can cause morbidity and have a negative impact on the patient's immune system. Thus, in order to regenerate new bone tissue without lowering the patient's immune system an alternative source of osteogenic cells must be used. One potential source is adult adipogenic stem cells (ASCs); ASCs are more abundant than bone marrow-derived MSCs and can differentiate along the osteogenic, chondrogenic, adipogenic and neurogenic lineage. Due to these properties ASCs are used in clinical trials (Lindroos *et al*, 2010). However, in this study we have evaluated the potential to use osteogenic MDCs as an alternative source for MSCs in bone regeneration applications.

7.1.1 THE DIFFERENTIAL POTENTIAL OF THE CELLS

The cells' "stem cellness" in terms of their differentiation potential was studied. There is a consensus among many researchers that to qualify as stem cells, the cell should be clonogenic, self-renewing and multipotent, giving rise to at least three different lineages (Torella *et al*, 2007). In this study, differentiation along the osteogenic, myogenic and adipogenic lineages were tested. There were cells within the MDCs population that could mineralize in osteogenic media (Figure 4.10), fuse to myotubes in myogenic media (Figure 3.6) and form lipid droplets in adipogenic media (Figure 3.10). This might indicate that there are cells within MDCs that are truly multipotent or MDCs consist of various cell types that can differentiate along one lineage or a combination of both.

Differentiation experiments of isolated subpopulations of MDCs conducted for this thesis suggested that the myogenic MDCs are different from the osteogenic MDCs (Figure 4.7). This indicates that MDCs consist of various cell types that can differentiate along various lineages. This claim would contradict the hypothesis of a communal precursor or stem cell for osteogenic cells and myogenic MDCs that various researchers have suggested (Bosch *et al*, 2000; Deasy *et al*, 2001). One theory that would explain the findings of this thesis that osteogenic MDCs differ from myogenic MDCs is that the osteogenic cells residing within muscle tissue not are precursor cells to myoblasts but belong to another cell type *e.g.* pericytes. Craniofacial muscle is derived from the mesoderm lineage, but bone and pericytes are neural crest derived. Neural crest cells are known for their affinity for Fn (Hall, 2009) and it has also been discovered that there are neural crest cells with progenitor and stem cell capacity in adults (Dupin *et al*, 2007).

Furthermore, there are several important differences between this study and the study by Bosch *et al* (2000) that led up to the communal precursor hypothesis. Firstly, the two studies were performed in different species, human *versus* mouse, secondly, the muscle

was derived from different anatomical parts and thirdly, Bosch *et al* (2000) used a different isolation method than the one used in this study.

There is a possibility that the decreased level of myogenicity of MDCsFn (Figure 4.7) is simply due to the technical difficulties of keeping myotubes in long-term culture (Chapter 4.3.2.2). If the more 'stem cell'-like MDCs with osteogenic potential are precursor cells to satellite cells they might need longer than 4 days in myogenic media to express myogenic markers, such as desmin or fuse to myotubes; therefore, MDCsFn might appear less myogenic than the parent population which consist of a mixture of cell types, such as myogenic precursor cells and the more immature 'stem cell'-like population.

When Ozeki *et al* (2006) studied myogenic differentiation of MDCs, they found that there was high degree of heterogeneity within their isolated α_7-fraction; MDCsFn population might also be heterogeneous. It is possible that there is a smaller subset of 'stem cell-like' cells within the MDCs that can differentiate along all of the lineages in this study and that other cells are immature lineage-specific progenitor cells.

As mentioned previously in this chapter, it was established in this thesis that the cells early adherent, with the first 20 min, to Fn *i.e.* MDCsFn belonged to the more osteogenic subpopulation compared to the cells in the parental population, MDCsPP (Chapter 4). Also previously, Fn has been used for the isolation of progenitor cells with multipotentiality from various tissues, such as neonatal foreskin (Jones & Watt, 1993) and cartilage (Dowthwaite *et al*, 2004). Fn is an important ECM protein during tissue repair where Fn-rich ECM has multiple biological functions acting as a chemo-attractant and adhesive substrate for mesenchymal and epithelial cells that migrate into damaged tissues (Limper & Roman, 1992). This could explain why a more stem cell-like population has a high affinity to Fn. It has been suggested by some researchers (Jones & Watts, 1993) that this selection is due to the high expression of β_1 integrin on Fn adherent cells. However, it is known that β_1-integrin is expressed on various cell types in the human body, such as mesenchymal cells, inflammatory cells (Limper &

Roman, 1992), smooth muscle cells (Deb *et al*, 2004) and skeletal muscle cells (Lewis *et al*, 2001). Thus, using β_1-integrin to identify and isolate the multipotent cells is not sufficient. Unfortunately, today there is no reliable single marker to use for isolation of "stem cell-like" cells. This makes it more difficult in the quest of identifying cells for tissue engineering applications. Nevertheless, it might be vital to establish if MDCs consists of a multipotent stem cell population or a population of multipotent cells or maybe both before the cells are used in clinical applications to avoid trans-differentiation.

MSCs mineralized in osteogenic media and formed lipid droplets in adipogenic media; however, MSCs alone did not fuse to myotubes *in vitro* at least not with the myogenic media used in this study. It is mentioned in the literature that MSCs are able to differentiate along the myogenic lineages; however, very little research has actually been published, especially regarding human cells, in this area. Thus, in this study MSCs have not been proven to be able to differentiate along three different lineages but there is a consensus that MSCs are capable to differentiate along, apart from the mentioned osteogenic and adipogenic, the chondrogenic lineage (Pittenger *et al*, 1999). It should be noted that not all MSCs are multipotent. When cloned MSCs were placed in osteogenic, adipogenic or chondrogenic differentiation media, it was found that only a small proportion of cells were able to differentiate along all three lineages. Fukiage *et al* (2008) found that within a group of 100 MSC clones only five of them showed tri-directional differentiation, 78 clones showed the potential to differentiate into either one-or two lineages, and 17 clones did not show any differentiation potential. For clinical bone regeneration applications it is important to identify the MSCs with the osteogenic potential.

7.1.2 OSTEOGENIC CAPACITY

The osteogenesis of MDCsFn and MSCs showed remarkable similarities in terms of mineralization, gene expression, ALP activity and expression. The results of the qPCR

Array in chapter 5 showed that PTH1R was upregulated under osteogenic conditions by MSCs, consistently, (Figure 5.12) and by MDCsFn, inconsistently (Figure 5.10). It has previously been established that PTH1R and PTH are the most important regulators of calcium ion homeostasis *in vivo* (Mannstadt *et al*, 1999; Huang *et al*, 2001; Pioszak & Xu, 2008). PTH is used in the clinic to treat osteoporosis (Borba & Mañas, 2010). *In vivo* the synthesis and secretion of PTH and PTH1R are known to be largely regulated by the extracellular concentration of calcium and phosphate, which is monitored by the CASR of the parathyroid glands (Mannstadt *et al*, 1999; Pioszak & Xu, 2008). This cannot be the case in this *in vitro* study since CASR is only expressed in the parathyroid glands (Theman & Collins, 2009) and was not detected in either MDCsFn or MSCs cultures (Table 5.3). The upregulation of PTH1R can therefore be seen as an indication that PTH1R can have several functions in osteogenesis.

It should be noted that the gene expression of the qPCR Array were analysed at 2 weeks. If another time point had been chosen, most likely the expression pattern would have been different. For early genes such as ALP and Runx2 an earlier time point *e.g.* 1 week would have been suitable and for late genes such as SPARC and OP a later time point *e.g.* 3 weeks would have been suitable. Hence, it would have been optimal to do a time course; however, this was not possible due to financial restrictions.

There appeared to be more consistency of the gene regulations for MSCs compared to MDCsFn (Figure 5.10; 5.11) between patients. This is probably due to natural higher patient variations within the MDCsFn in terms of osteogenesis or that the MDCsFn consist of a more heterogeneous population compared to MSCs. This might have an impact for clinical applications; MDCsFn might be an excellent alternative to MSCs in future clinical applications for some patients, but not in others.

7.1.3 THE USE OF SCAFFOLDS

In general it is considered that a scaffold is needed to direct the proliferated cells into the desired 3-D structure of the formed bone tissue. For successful osseointegration between the material and the cells, several factors have been suggested, such as implant material and design, bone status and surgical techniques (Ellingsen *et al*, 2000).

Various types of material have been used as scaffolds in bone applications, such as ceramics, polymers and metals. Calcium-sulphate-hemihydrate ($2CaSO_4H_2O$) and hydroxyapatite are included in the group of ceramics and have been used as bone graft substitute in bone cancer treatment (Schindler *et al*, 2008). Polymers, such as polylactic acid and polyglycolic acid, are resorbable biomaterials that are characterized by degradation that is mainly caused by hydrolysis and enzymatic disintegration (Pneumaticos *et al*, 2009). Polymers have been used in the healing bone fractures (Pneumaticos *et al*, 2009). However, for the majority of long-term implanted materials in bone, it is preferred to use an inert material, such as Ti (Ellingsen *et al*, 2000).

The similarities between the two cell types, MDCsFn and MSCs, were also seen when they were placed on the various Ti surfaces *i.e.* SMO, SLA and SLActive. Both MDCsFn (Figure 6.3) and MSCs (Figure 6.4) showed initially low levels of increased metabolic activity *i.e.* a lag period on SLA and SLActive compared to SMO and TCP. This phenomenon with initial decrease of metabolic activity on rough compared to smooth Ti surfaces has been reported earlier for MSCs (Wall *et al*, 2009), MG63 an immature osteoblastic cell line (Zhao *et al*, 2005; Kim *et al*, 2006) and osteoblasts (Brett *et al*, 2004). In this thesis, it has been shown that this is also the case for MDCsFn (Figure 6.3, 6.6-6.7). The unsolved question is if initial decreased metabolic activity on rough compared to smooth Ti surfaces is a general cell response or a specific response for mesenchymal cells. It is known that OP has an anti-apoptotic effect (Denhart *et al*, 2001), so by having a surface that induces apoptosis, the cells with higher level of OP, *i.e.* the more osteogenic cells, would survive preferentially.

The surface that expresses highest levels of cell death, SLActive, is the surface that has shown superior osseointegration in bone implants *in vivo* (Schwartz *et al*, 2008). The effect of Ti surfaces on the metabolic activity and cell death appeared to be cell type dependent; there was a higher percentage MDCsFn approximately 80% that survived on SLActive compared to MSCs, where approximately only 55% were viable. It would be interesting to investigate if this is correlated with the cells' levels of OP. This raises the question if the SLActive surface is selecting the more osteogenic population, *i.e.* the population that expresses more OP, or if the cell death initiates the body's regenerative system. MSCs are believed to migrate to the regenerative site *i.e.* the implant site; however, it cannot be excluded that osteogenic precursor cells are also recruited from muscle tissue near to the implant site *i.e.* osteogenic MDCs.

7.1.4 COMPARISON OF MDCs RESULTS COMPARED WITH LITERATURE

In this thesis an osteogenic subpopulation was isolated from the parental population of MDCs. The cells were isolated by differential adhesion to Fn; other researchers have previously used the cells' adhesion properties to Fn to isolate stem cell-like populations (Chapter 1.4.3). However, the previously isolated cells, by Fn adhesion, have all been isolated from non-myogenic tissue, such as neonatal foreskin (Jones & Watt, 1993), cartilage (Dowthwaite *et al*, 2004) and oral mucosa (Davies *et al*, 2010).

In order to isolate stem cell-like MDCs, researchers have in general used the cells adhesion properties to collagen where the more stem cell-like population is considered to adhere to collagen after several hours. Qu-Petersen *et al* (2002) developed an isolation method for MDCs derived from mice where the muscle was first enzymatically digested before the cells were isolated by differential adhesion to collagen. This method was developed for mouse-derived MDCs. In mice, cells isolated according to Qu-Petersen *et al* (2002) protocol have shown differentiation capacity along myogenic, neural, endothelial (Qu-Petersen *et al*, 2002) and osteogenic lineages

(Bosch *et al*, 2000). They have also been characterized and demonstrated the expression of marker Bcl-2, all MRFs and Sca-1 (Deasy *et al*, 2001), which is not expressed on human cells. Differential adhesion to collagen has also been used to isolate human cells from orbicular oris muscle (Bueno *et al*, 2009). It is not possible to apply this method to massetter muscle since it is too hard to enzymatically digest (previous experience in the lab at EDI). It is considered that the MDCs that migrate out of the tissue by using the explant method is a more homogeneous population than you get by enzymatically digesting whole tissue.

The main advantages of isolating osteogenic MDCs by Fn adhesion compared to collagen adhesion are that it is quicker and less labour intensive. In addition, it is developed to isolate the more osteogenic population in humans.

7.1.5 ORIGIN OF OSTEOGENIC MDCs

The origin of osteogenic MDCs has been discussed in the literature; some researchers have suggested that MDCs that are not restricted to the myogenic lineage actually are MSCs (Jankowski *et al*, 2002). Another suggestion is that osteogenic MDCs are related to pericytes (Peng & Huard, 2004; Crisan *et al*, 2008) *i.e.* pericytes and non-myogenic linage restricted MDCs and MSCs have a common origin. Pericytes, which are located along the vasculature, were originally described as a population of osteoprogenitor cells because pericytes participate in bone regeneration after injury (Diaz-Flores *et al* 1992), they can undergo osteogenic differentiation *in vitro* (Brighton *et al*, 1992; Doherty *et al*, 1998) and *in vivo* (Doherty *et al*, 1998). Other researchers consider that some bone marrow stem cells can circulate through different tissues and possibly contribute to the stem cell pool of local tissues; much evidence indicates that resident stem cells are the cells primarily responsible for the regeneration or repair of local tissues (Sethe *et al*, 2006). In addition, the niche, *i.e.* muscle or bone, of these cells might have affected the cells even though they have a common origin.

7.1.6 OSTEOGENIC MDCs IN VIVO

It should be remembered that this study has been performed in monolayer. It is not clear how well a monolayer of MSCs represent the *in vivo* surrounding in the bone where the MSCs represent only a small fraction of the cells present. Bone tissue with bone marrow consists of a 3-D network of ECM and various cell types, such as haematopoietic cells, stromal cells, adipocytes, endothelial cells and pericytes. Therefore, it is hard to predict how suitable MDCsFn would be *in vivo* in bone regeneration applications. This question is especially important since even though osteoblasts and myoblasts have very different phenotypes, they have an over lap in proteins *e.g.* IGF-1 and OP. The question is if the niche and pre-differentiation will keep the MDCsFn in the osteogenic lineage *in vivo* or if, they are truly multipotent, there will be transdifferentiation along the myogenic lineage.

The osteogenic cocktail of dex, L-ascorbic acid and β-GP has been proven to be effective *in vitro*; however, BMPs might be a more representative method to activate bone formation *in vivo*. Shen *et al* (2004) demonstrated that genetically engineered MDCs expressing BMP-4 could heal a skull bone defect. However, to translate this method in to clinical practice, the vectors have to be safe, which today appears to be a major obstacle (Wu & Ertl, 2008). Therefore, to take this research into a clinical setting other methods to deliver the osteogenic cues must be used.

Finally, it can be concluded that the osteogenic fraction *i.e.* MDCsFn could be used as an alternative to MSCs in bone regeneration applications due the similar osteogenic behavior of the two cell types established in this thesis. The MDCsFn might, however, consist of cells with lower osteogenic potential compared to MSCs. It should be remembered that obtaining MDCsFn does have the advantage over MSCs of reducing morbidity and not lowering the immune system. Thus, the future decision to whether use MSCs or osteogenic MDCs in clinical bone regeneration applications might be taken on a patient-to-patient basis.

7.2 FUTURE PERSPECTIVES

As discussed in Chapter 7.1, it might be important for transferring this work to the clinic to establish if the MDCs consist of a multipotent population or a population of multipotent cells or both. In order to establish this, clonal experiments on MDCs or MDCsFn should be performed in a similar manner as Fukiage *et al* (2008) perfomed on MSCs. It would also be useful to screen the MDCsFn for surface markers (Table 7.1); a full screen was not performed in this thesis due to time restraints.

Table 7.1. Suggested markers to study the MDCsFn phenotype.

MARKER	DESCRIPTION
CD34	- Transmembrane protein (D'Alessandro *et al*, 2009) - Expressed on HSCs (D'Alessandro *et al*, 2009) and mouse MSDCs (Deasy *et al*, 2001)
CD44	- Glycoprotein involved in cell-cell interactions, cell adhesion and migration (Jothy, 2003) - Expressed on various cell types, including human MSCs (Lin *et al*, 2008)
CD45	- Transmembrane protein (Saunders & Johnson, 2010) - Leukocyte specific (Saunders & Johnson, 2010)
CD56	- Adhesion molecule (Sinanan *et al*, 2004) - Used as a satellite cell marker (Mackey *et al*, 2009)
CD90	- Used as a marker for MSCs (Abdallah & Kassem, 2008)
CD105	- Used to isolate osteogenic cells (Aslan *et al*, 2006) - Expressed on MSCs (Abdallah & Kassem, 2008)
CD106	- Vascular cell adhesion molecule - Expressed on various cell types, including MSCs and endothelial cells (Liu *et al*, 2008)
C-kit	- Expressed on cardiac muscle stem cells (Miyamoto *et al*, 2010)
M-cadherin	- Cell surface protein involved in promyogenic signaling initiated by cell-cell contact (Krauss, 2010) - Used as a satellite cell marker (Krauss, 2010)
Stro-1	- Uncharacterized cell surface epitope (Gronthos *et al*, 1994) - Expressed by human MSCs and erythrocytic cells (Gronthos *et al*, 1994) - Has been used as a marker for osteogenic progenitor cells (Marie & Fromigue, 2006)

In order to fully evaluate the potential to use osteogenic MDCs in clinical bone regeneration applications *in vivo* experiments will ultimately need to be performed. As mentioned earlier, the 2-D *in vitro* model might not be a very representative model for the mechanisms *in vivo*. There have been attempts to mimic the *in vivo* structure by the use of 3-D collagen gels (Buxton *et al*, 2008); however, these gels have not been evaluated as to how representative they are in comparison to *in vivo* environment. It is important to remember, when research is transferred from *in vitro* human cell work to *in vivo* animal work, that there will always be species differences.

In order to analyze the *in vivo* bone regeneration potential of MDCsFn and decide which Ti surface, *i.e.* out of SMO, SLA and SLActive, is the more suitable. It has been well established that SLActive is better for osseointegration *in vivo* (Schwartz *et al*, 2008), but it is important to establish if it is the optimal surface for bone regeneration as well. By testing Ti scaffolds of various roughness and hydrophilicity it might be able to decide which one would be more suitable for bone regeneration. One could adapt Warnke *et al* (2004) protocol (read reference for more details). In this case Ti scaffolds, full with bone mineral and osteogenic cells, of the three different Ti surfaces would be constructed. Hydroxyapatite coating has shown to increase the amount of ingrowth and attachment of bone over the implant surface (Coathup *et al*, 2001). The MDCsFn could be marked *e.g.* with quantum dots to decide if the MDCsFn are responsible for the bone formation or if the cells only function as recruiter of other regenerative cells.

CHAPTER 8:

REFERENCES

CHAPTER 8: REFERENCE

Abdallah BM, Kassem M, 2008, Human mesenchymal stem cells: from basic biology to clinical applications, Gene Ther. 15(2):109-16

Ahdjoudi S, Lasmoles F, Oyajobi, Lomri A, Delannoy Ph, Marie PJ, 2001, Reciprocal control of osteoblast/chondroblast and osteoblast/adipocytes differentiation of multipotent clonal human marrow stromal F/STRO-1+ cells, J Cell. Biochem. 81(1):23-38

Ahlström M, Pekkinen M, Lamberg-Allard C, 2009, Dexamethasone downregulates the expression of parathyroid hormone-related protein (PTHrP) in mesenchymal stem cells, Steroids 74(2):277-82

Alberts B, Johnson A, Lewis J, Raff M, Roberts K, Walter P, 2002, Molecular biology of the cell, 4th edition, Garland Science

Alhadlaq A, Mao JJ, 2004, Mesenchymal Stem Cells: Isolation and Therapeutics, Stem Cells Dev. 13(4):436-48

Alhadlaq A, Mao JJ, 2005, Tissue-Engineered osteochondral constructs in the shape of an articular condyle, J. Bone Joint Surg. Am. 87(5):936-44

Allen RE, Boxhorn LK, 1989, Regulation of Skeletal Muscle Satellite Cell Proliferation and Differentiation by Transforming Growth Factor-Beta, Insulin-like Growth Factor I, and Fibroblast Growth Factor, J. Cell. Phys. 138:311-15

Alliston T, Choy L, Ducy P, Karsenty G, Derynck R, 2001, TGF-beta-induced repression of CBFA-1 by Smad3 decreases CBFA-1 and osteocalcin expression inhibits osteoblast differentiation, Embo. J., 20(9):2254-72

Ambrosio F, Kadi F, Lexell J, Fitzgerald GK, Boninger ML, Huard J, 2009, The effect of muscle loading on the skeletal muscle regenerative potential: an update of current research findings relating to aging and neuromuscular pathology. Am. J. Phys. Med. Rehabil. 88:145-55

Andriamanalijaona R, Duval E, Raoudi M, Lecourt S, Vilquin JT, Marolleau JP, Pujol JP, Galera P, Boumediene K, 2008, Differentiation potential of human muscle-derived cells towards chondrogenic phenotype in alginate bead culture, Osteoarthitis Cartilage, 16(12):1509-18

CHAPTER 8: REFERENCE

Aslan H, Zilberman Y, Kandel L, Liebergall M, Oskouian RJ, Gazit D, Cazit Z, 2006, Osteogenic differentiation of noncultured immunoisolated bone-marrow derived CD105+ Cells, Stem Cells 24:1728-37

Beauchamp JR, Heslop L, Yu DS, Tajbakhsh S, Kelly RG, Werning A, Buckingham ME, Partridge TA, Zammit PS, 2000, Expression of CD34 and Myf5 defines the majority of quiescent adult skeletal muscle satellite cells, J. Cell Biol.151:1221-34

Bialek P, Kern B, Yang X, Schrock M, Sosic D, Hong N, Wu H, Yu K, Ornitz DM, Olson EN, Justice MJ, Karsenty G, 2004, A twist code determines the onset of osteoblast differentiation, Dev. Cell 6:423-35

Blanco-Bose WE, Yao CC, Kramer RH, Blau HM, 2001, Purification of mouse primary myoblasts bases on alpha 7 integrin expression, Exp. Cell. Res. 265:212-20

Blin-Wakkach C, Lezot F, Ghoul-Mazgar S, Hotton D, Monteiro S, Teillaud C, Pibouin L, Orestes-Cardosos S, Papagerakis P, Macdougall M, Robert B, Berdal A, 2001, Endogeneous Msx1 antisense transcript: in vivo and in vitro evidences, structure, and potential involvement in skeleton development in mammals, PNAS 98(13)7336-41

Borba VZC, Mañas NCP, 2010, The use of PTH in the treatment of osteoporosis, Arq. Bras. Endocrinol. Metab. 54(2):213-19

Bosch P, Musgrave DS, Lee JY, Cummins J, Shuler F, Ghivizzani SC, Evans C, Robbins PD, Huard J, 2000, Osteoprogenitor cells within skeletal muscle, J. Orthop. Res. 18:933-44

Bourne S, Polak JM, Hughes SPF, Buttery LDK, 2004, Osteogenic differentiation of Mouse Embryonic Stem cells: Differential gene expression analysis by cDNA microarray and purification of osteoblasts by cadherin-11 magnetically activated cell sorting, Tissue Eng. A 10(5/6):796-806

Brandao-Bunch A, Utting JC, Orriss IR, Arnett TR, 2005, Acidosis inhibits bone formation by osteoblasts in vitro by preventing mineralization, Calcified Tissue Int. 77:167-74

Brett PM, Harle J, Salih V, Mihoc R, Olsen I, Jones FH, Tonetti M, 2004, Roughness response genes in osteoblasts, Bone 35:124-33

Brighton CT, Lorich DG, Kupcha R, Reilly TM, Jones AR, Woodbury RA II, 1992,The pericyte as a possible osteoblast progenitor cell. Clinical Orthop. 1992 (275):287-99

Bueno DF, Kerkis I, Costa AM, Martins MT, Kobayashi GS, Zucconi E, Fanganiello RD, Salles FT, Almeida AB, do Amaral CE, Alonso N, Passos-Bueno MR, 2009, New source of muscle-derived stem cells with potential for alveolar bone reconstrction in cleft lip and/or palate patients, Tissue Eng. A 15(2):427-35

Buxton PG, Bitar M, Gellynck K, Parkar M, Brown RA, Young AM, Knowles JC, Nazhat SN, 2008, Dense collagen matrix accelerates osteogenic differentiation and rescues the apoptotic response to MMP inhibition, Bone 43(2):377-85

Canalis E, Economides AN, Gazzerro E, 2003, Bone morphogenetic proteins, their antagonists, and the skeleton, Endocr. Rev. 24:218-35

Carlqvist K.H, Lewis M.P, Hunt N.P, Shah R., 2010, Regeneration of jaw muscle-potential cellular mechanisms, Sem. Orthod., 16(2):147-52

Charge SB, Rudnicki MA., 2004, Cellular and molecular regulation of muscle regeneration, Physiol. Rev. 84:209-38

Chen D, Zhao M, Mundy GR, 2004, Bone morphogenic proteins, Growth factors 22(4):233-41

Cheng BH, Jiang W, Phillips FM, Haydon RC, Peng Y, Zhou L, Luu HH, An N, Breyer B, Vanichakarn P, Szatkowski JP, Park JY, He C-T, 2003, Osteogenic activity of the fourteen types of human bone morphogenetic proteins (BMPs), J. Bone Joint Surg. 85(8):1544-52

Chinen J, Buckley RH, 2010, Transplantation immunology: Solid organ and bone marrow, J. Allergy Clin. Immunol. 125(2): 324-35

Chu K, Cheng C-J, Ye X, Lee Y-C, Zurita AJ, Chen D-T, Yu-Lee L-Y, Zhang S, Yeh ET, Hu MC-T, Logothetis CJ, Lin S-H, 2009, Cadherin-11 promotes the metastasis of prostate cancer cells to bone, Mol. Cancer Res. 6(8):1259-1267

Clemmons DR, 2009, Role of IGF-1 in skeletal muscle mass maintenance, Trends Endo. Metab. 20(7):349-356

Coathup MJ, Blunn GW, Flynn N, Williams C, Thomas NP, 2001, A comparison of bone remodeling around hydroxyapatite-coated, porous-coated and grit-blasted hip replacement retrieved at post-mortem, J. Bone Joint Surg. Br. 83 (1):118-123

Collins CA, Olsen I, Zammit PS, Heslop L, Petrie A, Partridge TA, Morgan JE, 2005, Stem cell function, self-renewal and behavioural heterogeneity of cells from the adult muscle satellite cell niche, Cell 122:289-301

Cornelison DD, Wold BJ, 1997, Single Cell Analysis of regulatory gene expression in quiescent and activated mouse skeletal muscle. Dev. Biol.191, 270-283

Corsi KA, Schwartz EM, Mooney DJ, Huard J, 2007, Regenerative medicine in orthopaedic surgery, J. Orthop. Res. 25:1261-1268

Crisan M, Yap S, Casteilla L, Chen C-W, Corselli M, Parl TS, Andriolo G, Sun B, Zheng B, Zhang L, Norotte C, Teng P-N, Traas J, Schugar R, Deasy BM, Badylak S, Buhring H-J, Giacobino J-P, Lazzari L, Huard J, Peault B, 2008, A perivascular origin for mesenchymal stem cells in multiple human organs, Cell Stem Cell 3:301-313

Dacquin R, Davey RA, Laplace C, Levasseur R, Morris HA, Goldring SR, Gebre-Medhin S, Galson DL, Zajac JD, Karsenty G, 2004, Amylin inhibits bone resorption while the calcitonin receptors control bone formation in vivo, JCR, 164(4):509-514

Davies LC, Locke M, Webb RD, Robert JT, Langley M, Thomas DW, Archer CW, Stephens P, 2010, A multipotent neural crest-derived progenitor cell population is resident within the oral mucosa lamina propria, Stem Cells Dev. 19 (6):819-30

Davis LA, zur Nieden NI, 2008, Mesodermal fate decisions of a stem cell: the Wnt switch, Cell Mol. Life Sci. 65(17):2658-74

De Oliva MA, Maximiano WMA, de Castro LMS, da SilvaPE, Fernandes RR Jr, Ciancaglini P, Beloti MM, Nanci A, Rosa AL, De Oliveira PT, 2009, Treatment with a growth factor-protein mixture inhibits formation of mineralized nodules in osteogenic cell cultures grown on titanium, J. Histochem. Cytochem. 57(3):265-276

Deasy BM, Jankowski RJ, Huard J, 2001, Muscle-derived stem cells: characterization and potential for cell mediated therapy, Blood cells Mol.Dis. 27(5):924-933

Deb A, Skelding KA, Wang S, Reeder M, Simper D, Caplice NM, 2004, Integrin profile and in vivo homing of human smooth muscle progenitor cells, Circulation 110(17):2673-2677

Dempster DW, 2006, Anatomy and functions of the adult skeleton, Primer on The Metabolic Bone Diseases and Disorders of Mineral Metabolism, 6th Ed, The American Society for Bone and Mineral Research

Deng C, Wynshaw A, Zhou F, Kuo A, Leder P, 1996, Fibroblast growth factor receptor 3 is a negative regulator of bone growth, Cell 84:911-921

Denhart DT, Noda M, O'Regan AW, Pavlin D, Berman JS, 2001, Osteopontin as a mean to cope with environmental insults: regulation of inflammation, tissue remodeling and cell survival, J. Clin. Invest. 107(9):1055-1061

Deutsch D, Palmon A, Fisher LW, Kolodny N, Termine JD, Young MF, 1991, Sequencing of bovine enamelin (Tuftelin) a novell acidic enamel protein, J. Biol. Chem. 266(24):16021-16028

Diaz-Flores L, Guiterrez R, Lopez-Alonso A, Gonzalez R, Varela H, 1992, Pericytes as a supplementary source of osteoblasts in periosteal osteogenesis, Clin. Orthop. (275):280-286

Doherthy MJ, Ashton BA, Walsh S, Beresford JN, Grant ME, Canfield AE, 1998, Vascular pericytes express osteogenic potential in vitro and in vivo. J. Bone. Miner. Res. 13(5):828-838

Dowthwaite GP, Bishop JA, Redman SN, Khan IM, Roonet P, Evans DJR, Haughton L, Bayram Z, Boyer S, Thomson B, Wolfe MS, Archer CW, 2004, The surface of articular cartilage contains a progenitor cell population, J. Cell Sci. 117:889-897

Duff SE, Li C, Garland JM, Kumar S, 2003, CD105 is important for angiogenesis; evidence and potential application, The FASEB Journal 17:984-992.

Dupin E, Calloni G, Real C, Goncalves-Trentin A, Le Douarin NM, 2007, Neural crest progenitors and stem cells, C.R. Biol. 330:521-529

Ellingsen JE, Thomsen P, Lyngstadaas SP, 2000, Advances in dental implant materials and tissue regeneration, Periodontology 41:136-156

Farhadieh RD, Gianoutsos MP, Yu Y, Walsh WR, 2004, The role of bone morphogenetic proteins BMP-2 and BMP-4 and their related postreceptor signalling system (Smads) in distracted osteogenesis of the mandible, J. Craniof. Surg. 15(5):714-718

Fischer C, Mazzone M, Jonckx B, Carmeliet P, 2008, FLT1 and its ligands VEGFB and PIGF; drug targets for anti-angiogenic therapy, Nature Rev. Cancer 8:942-956

Fox JM, Chamberlain G, Ashton BA, Middleton J, 2007, Recent advances into understanding of mesenchymal stem cell trafficking, Br. J. Haematol., 137(6):491-502

Frosch KH, Dreng A, Krause P, Viereck V, Miosge N, Werner C, Schild D, Sturmer EK, 2006, Stem cell-coated titanium implants for the partial joint resurfacing of the knee, Biomaterials 27:2542-2549

Fukiage K, Aoyama T, Shibata KR, Otsuka S, Furu M, Kohno Y, Ito K, Jin Y, Fujita S, Fujibayashi S, Neo M, Nakayama T, Nakamura T, Toquchida J, 2008 Expression of vascular cell adhesion molecule-1 indicates the differentiation potential of human bone marrow stromal cells, Biochem Biophys Res Commun.365(3):406-412

Gao J, Dennis JE, Muzic RF, Lundberg M, Caplan AI, 2001, The dynamic in vivo distribution of bone marrow-derived mesenchymal stem cells after infusion, Cells Tissue Org 169:12-20.

Gao Y, Jheon A, Nourkeyhani H, Kobayashi H, Ganss B, 2004, Molecular cloning, structure, expression, and chromosomal localization of the human Osterix (SP7) gene, Gene 341:101-110

Goldspink DE, Burniston JG, Ellison GM, Clark WA, Tan L-B, 2004, Catecholamine-induced apoptosis and necrosis in cardiac and skeletal myocytes of the rat in vivo: the same or separate death pathway, Exp. Physiol. 407-416

Goseki-Sone M, Orimo H, Iimura T, Miyazaki H, Oda K, Shibata H, Yanagishita M, Takagi Y, Watanabe H, Shimada T, Oida S, 1998, Expression of the mutant (1735T-DEL) tissue-nonspecific alkaline phophatase gene from hypophosphatasia patients, J. Bone Mineral Res. 13(12): 1827-1834

Granstrom G, 2007, Craniofacial osseointegration, Oral Diseases, 13:261-269

Grenier J, Teiller M-A, Grifone R, Kelly RG, Duprez D, 2009, Relationship between neural crest cells and cranial mesoderm during head muscle development, PLoS One 4(2):e4381

Gronthos S, Graves SE, Ohta S, Simmons PJ, 1994, The STRO-1+ fraction of adult human bone marrow contains the osteogenic precursors, Blood 84:4164-4173

Hall BK, 2009, The neural crest and neural crest cells in vertebrate development and evolution, Springer Science

Hao J, Varshney RR, Wang D-A, 2008, TGF-β3: a promising growth factor in engineered organogenesis, Expert Opinion Biol. Ther. 8 (10):1485-1492

Hatakeyama J, Fukumoto S, Nakamura T, Haruyama N, Suzuki S, Hatakeyama Y, Shum L, Gibson CW, Yamada Y, Kulkarni AB, 2009, Synergistic roles of amelogenin and ameloblastin, J. Dent. Res. 88(4):318-322

Hattori, Muller C, Gebhard S, Bauer E, Pausch F, Schlund B, Bosl MR, Hess A, Surmann-Schmitt C, von der Mark H, de Crombrugghe B, von der Mark K, 2010, SOX9 is a major negative regulator of cartilage vascularisation, bone marrow formation and endochondral ossification, Development 137:901-911

Hill CS, Duran S, Lin Z, Weber K, Holtzer H, 1986, Titin and myosin, but not desmin are linked during myofibrillogenesis in postmitotic mononucleated myoblasts, J. Cell Biol. 103 (6): 2185-2196

Hino J, Takao M, Takeshita N, Konno Y, Nishizawa T, Matsuo H, Kangawa K, 1996, cDNA cloning and genomic structure of human bone morphogenic protein -3b (BMP-3b), Biochem. Biophys. Res. Commun. 223:304-310

Hotchkiss RS, Strasser A, McDunn JE, Swanson PE, 2009, Cell death, New Eng. J. Med. 361:1570-83

Huang W, Chung U-I, Kronenburg HM, de Crombrugge B, 2001, The chondrogenic transcription factor Sox-9 is a target of signalling by the parathyroid hormone-related peptide in the growth plate of endochondral bones, PNAS 98(1):160-165

Huss FRM, Kratz G, 2001, Mammary epithelial cell and adipocytes co-cultured in a 3-D matrix; The first step towards tissue-engineered human breast tissue, Cells Tissues Organ 169:361-367

Inman GJ, Nicholas FJ, Hill CS, 2002, Nucleocytoplasmic shuttling of smads 2,3, and 4 permits sensing of TGF-β receptor activity, Mol. Cell 10:83-294

Isenmann S, Arthur A, Zannettino ACW, Turner JL, Shi S, Glackin CA, Gronthos S, 2009, Twist family of basic helix-loop-helix transcription factors mediate human mesenchymal stem cell growth and commitment, Stem Cells 27:2457-2468

Ito Y, Miyazono K, 2003, Runx transcription factors as key targets of TGF-β superfamily signalling, Current Opin. Gen. Dev. 13:43-47

Iwai T, Murai J, Yoshikawa H, Tsumaki N, 2008, Smad7 inhibits chondrocyte differentiation at multiple steps during endochondral bone formation and down-regulates p38 MAPK pathway, J. Biol. Chem.. 283(40):27154-27164

Jackson WM, Aragon AB, Bulken-Hoover JA, Nesti LJ, Tuan RS, 2009, Putative heterotopic ossification progenitor cells derived from traumatized muscle, J. Orthop. Res. 27(12):1645-51.

Jager M, Fischer J, Dohrn W, Li X, Ayers DC, Czibere A, Prall WC, Lensing-Hohn S, Krauspe R, 2008, Dexamethasone modulates BMP-2 effects on mesenchymal stem cells in vitro, J. Orthop. Res. 26(11):1440-1448

Jankowski RJ, Deasy BM, Huard J, 2002, Muscle-derived stem cells, Gene Ther. 9:642-647

Jonason JH, Xiao G, Zhang M, Xing L, Chen D, 2009, Post-translational regulation of Runx2 in bone and cartilage, J. Dent. Res. 88(8):693-703

Jones PH, Watt, 1993, Separation of human epidermal stem cells from transit amplifying cells on the basis of differences in integrin function and expression, Cell 73: 713-724

Kang SJ, Shin KS, Song WK, Ha DB, Chung CH, Kang M-S, 1995, Involvement of Transglutaminase in Myofibril Assembly of Chick Embryonic Myoblasts in Culture, J. Cell Biol., 130 (5) 1995 1127-1136

Katoh M, 2008, Cancer genomics and genetics of FGFR2, Int. J. Oncol. 33:233-237

Kazanecki CC, Uzwiak DJ, Denhardt DT, 2007, Control of osteopontin signalling and function by post-translational phosphorylation and protein folding, J. Cell. Biochem. 102:912-924

Khan SN, Cammisa FP, Sandhu SS, Diwan AD, Girardi FP, Lane JM, 2005, The biology of bone grafting, J. Am. Acad. Orthop. Surg. 2005:13:77-86

Khosla S, Westendorf JJ, Oursler MJ, 2008, Building bone to reverse osteoporosis and repair fractures, J. Clin. Inv. 118(2):421-428

Khouja HI, Bevington A, Kemp GJ, Russell RGG, 1990, Calcium and Orthophosphate deposits in vitro do not imply osteoblast-mediated mineralization by betaglycerophosphae in the absence of osteoblasts, Bone 11:385-391

Kim M-J, Kim W-C, Lim Y-J, Heo S-J, 2006, Microrough surface affects biologic response in MG63 osteoblast-like cells, J. Biomed. Mat. Res. A, 79(4):1023-32

Kim RH, Shapiro HS, Li JJ, Wrana JL, Sodek J, 1994, Characterization of the human bone sialoprotein (BSP) gene and its promoter sequence, Matrix Biol. 14:31-40

Kolf CM, Cho E, Tuan RS, 2007, Biology of adult mesenchymal stem cells: regulation of niche, self-renewal and differentiation, Arth. Res. Ther. 9:204

Korda M, Hua J, Little NJ, Heidari N, Blunn GW, 2009, The effect of mesenchymal stromal cells on the osseoinduction of impaction grafts, Tissue Eng. Part A, 2:675-83

Lancioni HL, Lucentini L, Palomba A, Fulle S, Micheli MR, Panara F, 2007, Muscle actin isoforms are differentially expressed in human satellite cells isolated from donors of different ages, Cell Biol. Int. 31:180-185

Laush E, Keppler R, Hilbert K, Cormier-Daire V, Nikkel S, Nishimura G, Unger S, Spranger J, Superti-Furga A, Zabel B, 2009, Mutations in MMP9 and MMP13 determine the mode of inheritance and clinical spectrum of metaphyseal anaplasia, Am. J. Hum. Gen. 85:168-178

Lee J-H, Kosinski PA, Kemp DM, 2005, Contribution of human bone marrow stem cells to individual skeletal myotubes followed by myogenic gene activation, Exp. Cell Res. 307:174-182

Lee JY, Qu-Petersen Z, Cao B, Kimura S, Jankowski R, Cummins J, Usas A, Gates C, Robbins P, Wernig A, Huard J, 2000, Clonal isolation of muscle-derived cells capable of enhancing muscle regeneration and bone healing, J. Cell Biol., 150(5):1085-1099

Lee MS, Lowe G, Flanagan S, Kuchler K, Glackin CA, 2000, Human dermo-1 has attributes similar to twist in early bone development, Bone 27(5):591-602

Lee OK, Kuo TK, Chen WM, Lee KD, 2004, Isolation of mulipotent mesenchymal stem cells from umbilical cord blood, Blood 103:1669-1675

Lewis MP, Machell JRA, Hunt NP, Sinanan ACM, Tippett HL, 2001, The extracellular matrix of muscle-implications for manipulation of craniofacial musculature, Eur. J. Oral Sci. 109:209-221

Lewis MP, Tippett HL, Sinanan AC, Morgan MJ, Hunt NP, 2000, Gelatinase-B (Matrix Metalloproteinase-9; MMP-9) secretion is involved in the migratory phase of human and murine muscle cell cultures, J. Muscle Res. Cell Motil. 21:223-233

Limper & Roman, 1992, Fibronectin a versatile matrix protein with roles in thoracic development repair and infection, Chest 101 (4):1663-1673

Lindroos B, Suroonen R, Miettinen S, 2010, The potential of adipose stem cells in regenerative medicine, Stem Cells Rev, DOI: 10.1007/s1205-010-9193-7

Ling Y, Rios HF, Myers ER, Lu Y, Feng JQ, Boskey AL, 2005, DMP1 depletion decreases bone mineralization in vivo: an FTIR imaging analysis, J. Bone Miner. Res. 20(12):2169-2177

Liu F, Akiyama Y, Tai S, Maruyama K, Kawaguchi Y, Muramatsu K, Yamaguchi K, 2008, Changes in the expression of CD106, osteogenic genes, and transcription factors involved in the osteogenic differentiation of human bone marrow mesenchymal stem cells, J. Bone Miner. Metab. 26:312-320

Liu Y, Hunzinker EB, Layrolle P, De Brujin JD, de Groot K, 2004, Bone morphogenic protein 2 incorporated into biomimetic coating retains its biological activity, Tissue Eng. 10:101-108

Mackey AL, Kjaer M, Charifi N, Henriksson J, Bojsen-Moller J, Holm L, Kadi F, 2009, Assessment of satellite cell number and activity status in human skeletal muscle biopsies, Muscle & Nerve 40:455-465

Mackie EJ, 2003, Osteoblasts: novel roles in orchestration of skeletal architecture, Int. J. Biochem. Cell Biol. 35:1301–1305

Mannstadt M, Juppner H, Gardella TJ, 1999, Receptors for PTH and PTHrP: their biological importance and functional properties, Am. J. Physiol. 277(2):F665-75

Marie PJ, Fromigue O, 2006, Osteogenic differentiation of human-derived mesenchymal stem cells, Reg. Med. 1(4):539-548

Marom R, Shur I, Solomon R, Benayahu D, 2005, Characterization of adhesion and differentiation markers of osteogenic marrow stromal cells. J. Cell. Physiol. 202(1):41-48

Marsell R, Einhorn TA, 2009, The role of endogenous bone morphogenetic proteins in normal skeletal repair, Injury 40(53):54-57

Martin JY, Schwartz Z, Hummert TW, Schraub DM, Simpson J, Lankford J, Dean DD, Cochran DL, Boyan BD, 1995, Effect of titanium surface roughness on proliferation, differentiation, and protein-synthesis of human osteoblast like cells, J. Biomed. Mater. Res. 29(3):389-401

Martinez EF, da Silva LAH, Furuse C, de Araujo NS, de Araujo VC, 2009, Dentin matrix protein 1 (DMP1) expression in developing human teeth, Br. Dent. J. 20(5):365-69

Mayer H, Bertram H, Lindenmaier W, Korff T, Weber H, Weich H, 2005, Vascular endothelial growth factor (VEGF-A) expression in human mesenchymal stem cells; autocrine and paracrine role on osteoblastic and endothelial differentiation, J. Cell Biochem. 95(4):827-39

Meleti Z, Shapiro IM, Adams CS, 2000, Inorganic phosphate induces apoptosis of osteoblast-like cells in culture, Bone 27(3):359-66

Miyake T, Cameron AM, Hall BK, 1997, Stage-specific expression pattern of alkaline phosphatise during the development of the first arch skeleton in inbred C57BL/6 mouse embryos, J. Ant. 190:239-60

Mitchell KJ, Pannerec A, Cadot B, Parlakian A, Besson V, Gomes ER, Marazzi G, Sassoon DA, 2010, Identification and characterization of a non-satellite cell muscle resident progenitor during postnatal development, Nature Cell Biology 3 (12):257-66

Morton D, Bornstein MM, Wittneben J-G, Martin WC, Ruskin JD, Hart CN, Buser D, 2010, Early loading after 21 days of healing of a nonsubmerged titanium implants with chemically modified sandblasted and acid-etched surface; two-year results of a prospective two-center study, Clin. Impl. Dent.Rel. Res. 12(1):9-17

Muraglia A, Cancedda R, Quarto R, 2000, Clonal mesenchymal progenitors from human bone marrow differentiate in vitro according to a hierarchical model, J. Cell Sci. 113(7)1161-6

Newton G, Weremowicz S, Morton CC, Copeland NG, Gilbert DJ, Jenkins NA, Lawler J, 1994, Characterization of human and mouse cartilage oligomeric matrix protein, Genomics 24: 435-439

Niida S, Kondo T, Hiratsuka S, Hayashi S-I, Amizuka N, Noda T, Ikeda K, Shibuya M, 2005, VEGF receptor 1 signaling is essential for osteoclast development and bone marrow formation in colony-stimulating factor 1-deficient mice, PNAS 102(39):14016-21

Oldberg A, Jirskog-Hed B, Axelsson S, Heinegard D, Pierschbacher M, Ruoslathi E, 1990, Regulation of bone sialoprotein mRNA by steroid hormones, J Cell Biol. 109:3138-86

Ono N, Nakashima K, Schipani E, Hayata T, Ezura Y, Soma K, Kronenberg Hm, Noda M, 2007, Constitutively active parathyroid hormone receptor signalling in cells in osteoblastic lineage suppresses mechanical unloading-induced bone resorption, J. Biol. Chem. 282(35):25509-16

Ozeki N, Lim M, Yao C-C, Tolar M, Kramer RH, 2006, α7 integrin expressing human fetal myogenic progenitors have stem cell-like properties and are capable of osteogenic differentiation, Exp. Cell Res. 312:4162-80

Pace JM, Athinson M, Willing MC, Wallis G, Byers PH, 2001, Deletion and duplication of Gly-Xaa-Xaa triplet repeats in the triple helical domains of type 1 collagen chains disrupt helix formation and results in several types of osteogenesis imperfects, Hum. Mut. 18:319-26

Parenti G, Meroni G, Ballabio A, 1997, The sulfatase gene family, Current Opin. Gen. Dev.7:386-91

Peng H, Huard J, 2004, Muscle-derived stem cells for musculoskeletal tissue regeneration and repair, Transplant Immunol. 12: 311-19

Phipps SMO, Berletch JB, Andrews LG, Tollefsborg TO, 2007, Aging cell culture, Methods Mol Biol, 371:9-19

Pioszak AA, Xu EH, 2008, Molecular recognition of parathyroid hormone by its G protein-coupled receptor, PNAS 105(13):5034-39

Pittenger MF, Mackay AM, Beck SC, Jaiswal RK, Douglas R, Mosca JD, Moorman MA, Simonetti DW, Craig S, Marshak DR, 1999, Multilineage potential of adult human mesenchymal stem cells, Science 284:143-47

Pneumaticos SG, Triantafyllopoulos GK, Basdra EK, Papavassiliou AG, 2009, Segmental bone defects; from cellular and molecular pathways to the development of novel biological treatments, JCMM -ePub ahead of print.

Qu-Petersen Z, Deasy B, Jankowski R, Ikezawa M, Cummins J, Pruchnic R, Mytinger J, Cao, B, Gates C, Wernig A, Huard J, 2002, Identification of a novel population of muscle stem cells in mice: potential for muscle regeneration, JCR 157(5):851-64

Rauccio A, Bellosta P, Grassi R, Basilico C, Mansukhani A, 2007, Osteoblast proliferation or differentiation is regulated by relative strengths of opposing signalling pathways, J. Cell. Physiol. 215:442-51

Romanov YA, Darevskaya AN, Merzlikina NV, Buravkova LB, 2005, Mesenchymal stem cells from human bone marrow and adipose tissue: Isolation, Characterization, and differentiation potentialities, Cell Techn. Biol. Med. 3:138-43

Rubin H, 1997, Cell aging in vivo and in vitro, Mech. Aging Dev. 98:1-35

Rupp F, Scheideler L, Olshanska N, de Wild M, Wieland M, Geis-Gerstorfer J, 2006, Enhancing surface free energy and hydrophilicicty through chemical modification of microsctructure titanium implant surfaces, J Biomed. Mater. Res. A 76(2):323-34

Schiltz C, Marty C, de Vernejoul M-C, Geoffrey V, 2008, Inhbition ofosteoblastic metalloproteinases in mice prevents bone loss induced by oestrogen defiency, J. Cell. Biochem. 104:1803-1817

Schindler OS, Cannon SE, Briggs TWR, 2008, Composite ceramic bone graft substitute in the treatment of locally aggressive benign bone tumours, J. Orthop. Surg. 16(1):66-74

Schonmeyr BH, Soares M, Avraham T, Clavin NW, Gewalli F, Mehrara BJ, 2010, Vascular endothelial growthfactor inhibits bone morphogenetic protein 2 expression in rat mesenchymal stem cells, Tissue Eng. Part A 16(2):653-62

Schwartz Z, Lohmann CH, Oefinger J, Bonewald LF, Dean DD, Boyan BD, 1999, Implant surface characteristics modulate differentiation behaviou of cells in the osteoblastic lineage, Adv. Dent. Res. 13:38-48

Schwarz F, Sager M, Ferrari D, Herten M, Wieland M, Becker J, 2008, Bone regeneration in dehiscence-type defects at non-submerged and submerged chemically modified (SLActive) and conventional SLA titanium implants; an immunohistochemical study in dogs, J. Clin. Period., 35:64-75

Seale P, Rudnicki MA, 2000, A new look at the origin, function, and 'stem-cell' status of muscle satellite cells. Dev. Biol., 218:115-24.

Sethe S, Scutt A, Stolzing A, 2006, Aging of mesenchymal stem cells, Aging Res. Rev. 5:91-116

Shen H-C, Peng H, Usas A, Gearthart B, Fu FH, Huard J, 2004, Structural and functional healing of a critical size segmental bone defect by transduced muscle-derived cells expressing BMP4, J. Gene Med., 6(9):984-91

Sikavitsas VI, Temenoff JS, Mikos AG, 2001, Biomaterials and bone mechanotransduction, Biomaterials 22:2581-93

Simmons PJ, Torok-Storb B, 1991, Identification of stromal cell-precursors in human bone marrow by a novel monoclonal antibody, Stro-1, Blood 78(1):55-62

Sinanan ACM, Hunt NP, Lewis MP, 2004, Human adult craniofacial muscle-derived cells: neural-cell adhesion-molecule (NCAM; CD56)-expressing cells appear to contain multipotential stem cells, Biotechnol. Appl. Biochem. 1:25-34

Sinanan ACM, Buxton PG, Lewis, 2006, Muscling in on stem cells. Biol. Cell 98:203-14

Sommerfeldt DW, Rubin CT, 2001, Biology of bone and how it orchestrates the form and the function of the skeleton, Eur. Spine J. 10:S86-95

Sotiropoulou PA, Perez SA, Salagianni M, Baxevanis CN, Papamichail M, 2005, Characterization of the optimal culture conditions for clinical scale production of human mesenchymal stem cells, Stem Cells, 24:462-71

St-Arnaud, 2008, The direct role of vitamin D on bone homeostasis, Arch. Biochem. Biophys. 15;473(2):225-30

Stanford CM, Jacobson PA, Eanes ED, Lembke LA, Midura RJ, 1995, Rapidly forming apatitic mineral in an osteoblastic cell line (UMR 106-01 BSP), J Biol Chem 270(16):9420-8

Stenderup K, Justensen J, Clausen C, Kassem, 2003, Aging associated with decreased maximal life span and accelerated senescence of bone marrow stromal cells, Bone 33(6):919-26

Stewart CEH, Rittweger J, 2006, Adaptive processes in skeletal muscle: molecular regulators and genetic influences, J Musculoskelet. Neuronal Interact. 6(1):73-86

Tait JF, 2008, Imaging of apoptosis, J. Nucl. Med. 49(10):1573-6

Tang J, Peng R, Ding J, 2010, The regulation of stem cell differentiation by cell-cell contact on micropatterned material surface, Biomaterials 31:2470-76

Tang Y, Wu X, Lei W, Pang L, Wan C, Shi Z, Zhao L, Nagy TR, Peng X, Hu J, Feng X, Hui WV, Wan M, Cao X, 2009, TGF-β1-induced migration of bone mesenchymal stem cells couples bone resorption and formation, Nat. Med. 15(7):757-65

Termine JD, Kleinman HK, Whitson SW, Conn KM, McGarvey ML, Martin GR, 1981, Osteonectin, a bone specific protein linking mineral to collagen, Cell 26:99-105

Theman TA, Collins MT, 2009, The role of the calcium-sensing receptors in bone biology and pathophysiology, Curr. Pharm. Biotechnol. 10 (3):289-301

Thibodeau GA, Patton KT, 2007, Anatomy and Physiology, 6th Edition, Mosby Elsevier

Thyagarajan T, Sreenah T, Cho A, Wright JT, Kulkarni AB, 2001, Reduced expression of dentin sialophosphoprotein is associated with dysplastic dentin in mice overexpressing transforming growth factor-β1 in teeth, J. Biol. Chem. 276(14):11016-20

Tokoyoda K, Hauser AE, Nakayama T, Radbruch A, 2010, Organization of immunological memory by bone marrow stroma, Nat. Rev. Immunol. 10:193-200

Torella D, Ellison GM, Karakikes I, Nadal-Ginard B, 2007, Resident cardiac stem cells, Cell Mol. Life Sci. 64(6):661-73

Tseng Y-H, Kokkotuo E, Schulz TJ, Huang TL, Winnay JN, Taniguchi CM, Tran TT, Suzuki R, Espinoza DO, Yamamoto Y, Ahrens MJ, Dudley AT, Norris AW, Kulkarni RN, Kahn CR, 2008, New role of bone morphogenetic protein 7 in brown adipogenesis and energy expendiature, Nature 454(7207):1000-4

Tullbert-Reinert H, Jundt G, 1999, In situ measurement of collagen synthesis by human bone cells with a Sirius Red based colorimetric microassay: effects of transforming growth factor β2 and ascorbic acid 2-phopshate, Histochem. Cell Biol. 112:271-276

Uaesoontrachoon K, Yoo H-J, Tudor EM, Pike RN, Mackie EJ, Pagel CN, Osteopontin and skeletal muscle myoblasts: Association with muscle regeneration and regulation of myoblast function in vitro, Int. J. Biochem. Cell Biol. 40:2303-14

Usas A, Huard J, 2007, Muscle-derived stem cells for tissue engineering and regenerative therapy, Biomaterials 28:5401-6

Utting JC, Robins SP, Brandao-Burch A, Orriss IR, Behar J, Arnett TR, 2006, Hypoxia inhibits the growth, differentiation and bone forming capacity of rat osteoblasts, Exp. Cell Res. 312: 1693-702

Vacanti V, Kong E, Suzuki G, Sato K, Canty JM, Lee T, 2005, Phenotypic changes of adult porcine mesenchymal stem cells induced by prolonged passaging in culture, J. Cell. Physiol. 205:194-201

Van der Dolder J, Jansen JJ, 2007, Enrichment of osteogenic cell populations from rat bone marrow stroma, Biomaterials 28:249-55

Wall I, Donos N, Carlqvist K, Jones F, Brett PM, 2009, Modified titanium surfaces promote accelerated osteogenic differentiation of mesenchymal stromal cells in vitro, Bone 45(1):17-26

Wang EA, Rosen V, D'Alessandro J.S, Bauduy M, Cordes P, Harada T, Israel DI, Hewick KM, Kerns KM, LaPan P, 1990, Recombinant human bone morphogenic protein induces bone formation, Proc. Natl. Acad. Sci. U.S.A 87:2220-4

Warnke PH, Springer ING, Wiltfang J, Acil Y, Eufinger H, Wehmoller M, Russo PAJ, Bolte H, Sherry E, Behrens E, Terheyden H, 2004, Growth and transplantation of a custom vascularised bone graft in man, Lancet 364:766-70

Weiss MJ, Henthorn PS, Laferty MA, Slaughter C, Raducha M, Harris H, 1986, Isolation and characterization of a cDNA encoding a human liver/bone/kidney-type alkaline phospahatse, Proc. Natl. Acad. Sci. 83:7182-6

White KE, Cabral JM, Davis SI, Fishburn T, Evans WE, Ichikawa S, Fields J, Yu X, Shaw NJ, McLellan NJ, McKeown C, FitzPatrick D, Yu K, Ornitz DM, Econs MJ, 2005, Mutations that cause osteoglophonic dysplasia define novel roles for FGFR1 in bone elongation, Am. J. Hum. Genet. 76:363-7

Wu T-L, Ertl HCJ, 2008, Immune barriers to successful gene delivery, Trends Mol. Med. 15(1):32-39

Young HE, Mancini ML, Wright RP, Smith JC, Black Jr AC, Reagan CR, Lucas PA, 1995, Mesenchymal stem cells reside within the connective tissues of many organ, Dev. Dyn., 202: 137-144

Zhao G, Schwartz Z, Wieland M, RuppF, Geis-Gerstorfer J, Cochran DI, Boyan BD, 2005, High surface energy enhances cell response to titanium substrate microstructure, J. Biomed. Mat. Res. A 1;74(1):49-58

Zöller A, Ganeles J, Korostoff J, Guerra F, Krafft T, Brägger U, 2008, Immediate and early non-occlusal loading of Straumann implants with a chemically modified surface (SLActive) in the posterior mandible and maxilla; interim results from a prospectiove multicentre randomized-control study, Clin.. Oral. Impl.. Res. 19; 442-50

Zuba-Surma EK, Kucia M, Ratajczak J, Ratajczak MZ, 2009, “Small stem cells” in adult tissue: very small embryonic-like stem cells (VSELs) stand up!, Cytometry A 75(1):4-13

CHAPTER 9:

APPENDIX

A9.1.1 PROTOCOLS

A9.1.2 PFA

The 4% PFA was prepared by dissolving 20 g PFA in 250 ml deionised water. To the solution, 5 drops of 10 M NaOH was added. The solution was stirred and heated to 60 °C in a water bath until the solution was clear. Finally, 2xPBS was added to the solution and the pH was adjusted to 7.3.

A9.1.3 PBS+

PBS was made up from tablets and 1 mM of CaCl2 and 1mM MgCl2 was added to the PBS solution. The pH was adjusted to 7.4.

A9.1.4 FN

The Fn was diluted in PBS+ to a concentration of 10 ug/ml. The Fn/PBS+ solution was aliquoted a 40 ml and stored at -20 °C.

A9.1.5 GEL

The purchase Gel solution was diluted from 2% to 0.2 % by sterile PBS. The solution was stored at 4 °C.

A9.1.6 MATERIAL

Table A9.1. List of purchased cells.

PRODUCT	COMPANY	CAT# NO
MSCs	Tulane Centre for Gene Therapy	N/A

Table A9.2. List of gene assays.

PRODUCT	COMPANY	CAT# NO
ALPL	Applied Biosystems	Hs00758162_m1
AMBN	Applied Biosystems	Hs00212970_m1
AMELY	Applied Biosystems	Hs00795181_m1
ARSE	Applied Biosystems	Hs00163677_m1
BMP2	Applied Biosystems	Hs00154192_m1
BMP4	Applied Biosystems	Hs00370078_m1
BMP7	Applied Biosystems	Hs00233477_m1
BSP	Applied Biosystems	Hs00173720_m1
CALCR	Applied Biosystems	Hs00156229_m1
CASR	Applied Biosystems	Hs00173436_m1
CDH11	Applied Biosystems	Hs00156438_m1
COL1A1	Applied Biosystems	Hs00164004_m1
COMP	Applied Biosystems	Hs00164359_m1
Desmin	Applied Biosystems	Hs00157258_m1
DMP1	Applied Biosystems	Hs00189368_m1
DSPP	Applied Biosystems	Hs00171962_m1
FGFR1	Applied Biosystems	Hs00241111_m1
FGFR2	Applied Biosystems	Hs00240796_m1
FGFR3	Applied Biosystems	Hs00179829_m1
FLT1	Applied Biosystems	Hs00176573_m1
GAPDH	Applied Biosystems	Hs99999905_m1
GDF10	Applied Biosystems	Hs00192033_m1
MMP13	Applied Biosystems	Hs00233992_m1
MMP2	Applied Biosystems	Hs00234422_m1

MSX1	Applied Biosystems	Hs00427183_m1
Myogenin	Applied Biosystems	Hs00231157_m1
OP	Applied Biosystems	Hs00959010_m1
Osterix	Applied Biosystems	Hs00541729_m1
PPAR-γ2	Applied Biosystems	Hs00234592_m1
PTHR1	Applied Biosystems	Hs00174895_m1
RUNX2	Applied Biosystems	Hs00231692_m1
SMAD1	Applied Biosystems	Hs00195432_m1
SMAD2	Applied Biosystems	Hs00183425_m1
SMAD3	Applied Biosystems	Hs00232222_m1
SMAD4	Applied Biosystems	Hs00232068_m1
SMAD7	Applied Biosystems	Hs00178696_m1
SMAD9	Applied Biosystems	Hs00195441_m1
SOX9	Applied Biosystems	Hs00165814_m1
SPARC	Applied Biosystems	Hs00277762_m1
TGFβ1	Applied Biosystems	Hs99999918_m1
TGFβ3	Applied Biosystems	Hs00234245_m1
TGFBR1	Applied Biosystems	Hs00610319_m1
TGFBR2	Applied Biosystems	Hs00559661_m1
TUFT1	Applied Biosystems	Hs00360629_m1
TWIST1	Applied Biosystems	Hs00361186_m1
TWIST2	Applied Biosystems	Hs00382379_m1
VDR	Applied Biosystems	Hs01045840_m1
VEGFA	Applied Biosystems	Hs00900054_m1
VEGFB	Applied Biosystems	Hs00173634_m1
WNT5A	Applied Biosystems	Hs00180103_m1
18S	Applied Biosystems	Hs99999901_s1

Table A9.3. Description of osteogenic genes analysed in chapter 5, result section 3.

GENE	DESCRIPTION OF CODED PROTEIN	ROLE IN OSTEOGENIC DIFFERENTIATION
ALP	- Enzyme	- Bone ALP is used as an osteogenic marker (Weiss *et al*, 1986); however its specific role in osteogenesis is unknown (Goseki-Sone *et al*, 1998). - Deficiency of ALP leads to defects in skeletal mineralization in mice (Gosike-Sone *et al*, 1998).
AMBN	- Enamel matrix glycoprotein (Hatakeyama *et al*, 2009)	- AMBN is secreted by ameloblasts and is involved in the mineralization of enamel (Hatakeyama *et al*, 2009).
AMELY	- Enamel matrix protein (Hatakeyama *et al*, 2009)	- AMBN is secreted by ameloblasts and is involved in the mineralization of enamel (Hatakeyama *et al*, 2009).
ARSE	- Enzyme	- ARSE catalyzes the hydrolysis of sulphate ester bonds but its role in osteogenesis is unknown (Parenti *et al*, 1997).

BMP2	- Growth factor - Belong to TGF-β family (Chen *et al*, 2004)	- BMP2 induces bone formation (Chen *et al*, 2004).
BMP4	- Growth factor - Belong to TGF-β family (Chen *et al*, 2004)	- BMP4 induces bone formation (Chen *et al*, 2004).
BMP7	- Growth factor - Belong to TGF-β family (Chen *et al*, 2004)	- BMP7 induce bone formation (Chen *et al*, 2004), and is timely expressed in fraction healing, *i.e.* after 14 days (Marsell *et al*, 2009).
BSP	- Glycoprotein	- BSP is expressed by fully differentiated osteoblast and function as structural protein in the bone matrix *i.e.* can bind to hydroxyapatite (Kim *et al*, 1994).
CALCR	- Receptor	- CALCR regulates bone formation but is only expressed on osteoclasts, not osteoblasts (Dacquin *et al*, 2004).

CASR	- G protein-coupled receptor (Theman & Collins, 2009)	- Expressed on the parathyroid glands and regulates PTH on the basis of Ca^{2+} (Theman & Collins, 2009).
CDH11	- Cell adhesion molecule (Bourne *et al*, 2004)	- CDH11 is upregulated during early stage of differentiation (Bourne *et al*, 2004).
COL1A1	- Part of type 1 collagen, *i.e.* abundant ECM protein (Uttering *et al*, 2006)	- Type 1 collagen forms the template for mineralisation of bone (Pace *et al*, 2001).
COMP	- Matrix protein - Member of thrombospondin gene family (Newton *et al*, 1994)	- COMP is secreted by chondrocytes (Newton *et al*, 1994).
DMP1	- Acidic phosphoprotein - Member of SIBLING family (Ling *et al*, 2005)	- ECM protein expressed by osteocytes (Khosla *et al*, 2008) and is involved in mineralization by binding Ca^{2+} and apatite (Ling *et al*, 2005).

DSPP	- Sialophosphoprotein (Thyagarajan *et al*, 2001)	- Odontoblast specific expression (Thyagarajan *et al*, 2001).
FGFR1	- Tyrosin kinase resceptor (White *et al*, 2005)	- FGFR1 is involved in the growth of long bones (White *et al*, 2005).
FGFR2	- Tyrosin kinase resceptor (White *et al*, 2005)	- FGFR2 is involved in the growth of long bones (White *et al*, 2005) and mutations can cause various skeletal abnormalities (Katoh, 2008). - Is regulated by TWIST1 (Katoh, 2008).
FGFR3	- Tyrosin kinase resceptor (White *et al*, 2005)	- Involved in the growth of long bones (White *et al*, 2005). - Function as a negative regulator (Deng *et al*, 1996).
FLT1	- Tyrosin kinase resceptor (Niida *et al*, 2005)	- Involved in osteoclastogenesis (Niida *et al*, 2005).

GDF10	- Closely related to BMP3 - Belongs to TGF-β family (Hino *et al*, 1996)	- Believed to have a role in the chondrogenic phase in endochondral bone formation (Marsell & Einhorn, 2009).
MMP13	- Enzyme	- MMP13 catalyzes the degradation of ECM and release factors stored in ECM *e.g.* VEGFA (Laush *et al*, 2009). - Is expressed by hypertrophic chondrocytes or osteoblasts (Laush *et al*, 2009) and
MMP2	- Enzyme	- MMP2 is expressed by MSCs (Adhalaq & Mao, 2004).
MSX1	- Homeobox gene (Blin-Wakkach, 2001)	- MSX1 is involved in the terminal differentiation of tooth and craniofacial skeleton and downregulates Runx2 (Blin-Wakkach, 2001).
OP	- Matrix protein	- Serves as an attachment protein linking cells to the bone mineral and is involved in bone remodelling (Kazanecki *et al*, 2007).

OSTERIX	- Zinc finger transcription factor - Member of the SP family (Gao *et al*, 2004)	- Only detected in embryonic human tissue not in adult human tissue (Gao *et al*, 2004).
PTHR1	- G protein–coupled receptors (Mannstadt *et al*, 1999)	- PTH1R is a part of the calcium ion homeostasis *in vivo* together with PTH (Pioszak & Xu, 2008).
RUNX2	- Transcription factor (Khosla *et al*, 2008) - Belongs to Runx family (Jonason *et al*, 2009)	- Runx2 is considered to be one of the earliest marker of osteogenic commitment and essential for osteogenic differentiation (Khosla *et al*, 2008).
SMAD1	- Glycoprotein (Farhadien *et al*, 2004)	- Smad 1 is an immediate downstream molecule of BMP receptors (Chen *et al*, 2004; Farhadien *et al*, 2004) and signal through Smad4 (Farhadien *et al*, 2004).
SMAD2	- Glycoprotein (Farhadien *et al*, 2004)	- TGF-β stimulation leads to Smad-2 activation (Inman *et al*, 2002). - Smad-2 forms complexes with Smad-4 that regulates transcription of target genes (Inman *et al*, 2002).

SMAD3	- Glycoprotein (Frahadien *et al*, 2004)	- Smad-3 is mainly responsible for TGF-β1-induced migration of MSCs (Tang *et al*, 2009). - Smad-3 forms complexes with Smad-4 that regulates transcription of target genes (Inman *et al*, 2002).
SMAD4	- Glycoprotein (Frahadien *et al*, 2004)	- Smad-2 or-3 forms complexes with Smad-4 to regulate transcription of target genes (Inman *et al*, 2002).
SMAD7	- Glycoprotein (Frahadien *et al*, 2004)	- Regulates TGF-β and BMPs by inhibiting Smad pathways in chondrocytes (Iwai *et al*, 2008).
SMAD9	- Glycoprotein (Frahadien *et al*, 2004)	- Immediate downstream molecule of BMP receptors and is a part of BMP signaling (Chen *et al*, 2004).
SOX9	- Transcription factor (Huang *et al*, 2001)	- Required for chondrocyte differentiation and cartilage formation (Huang *et al*, 2001).

SPARC	- Bone tissue specific protein (Termine *et al*, 1981)	- Initiate the mineralisation process in normal skeletal tissues and binds to both hydroxyapatite and collagen (Termine *et al*, 1981).
TGF-β1	- Belongs to the TGF-β superfamily (Thyagarajan *et al*, 2001)	- TGF-β1 recruits MSCs to bone remodelling sites *in vivo* and stimulate proliferation of progenitors and inhibit osteoblastic differentiation (Tang *et al*, 2009).
TGF-β3	- Belongs to the TGF-β superfamily (Hao *et al*, 2008)	- Inhibit osteogenesis of MSCs (Hao *et al*, 2008).
TGF-BRI	- Receptor (Hao *et al*, 2008)	- TGF-BRI is recruited by TGF-BRII and activates Smad (Hao *et al*, 2008).
TGF-BRII	- Receptor (Hao *et al*, 2008)	- TGF-BRII activate TGF-BRI (Hao *et al*, 2008).

TUFT1	- Tuftelin belongs to the enamelin group of proteins (Huang *et al*, 2001)	- Codes the enamel protein tuftelin (Deutsch *et al*, 1991).
TWIST1	- Transcription factors - Member of TWIST family (Isenmann *et al*, 2009)	- TWIST 1regulates the bone remodelling by decreasing Runx2 and OP (Isenmann *et al*, 2009).
TWIST2	- Transcription factors - Member of TWIST family (Isenmann *et al*, 2009)	- TWIST2 regulates the bone remodelling by decreasing Runx2 and OP (Isenmann *et al*, 2009).
VDR	- Receptor (St-Arnaud, 2008)	- VDR regulate mineral ion homeostasis by binding to 1,25-dihydroxyviatmin D (St-Arnaud, 2008).
VEGFA	- Growth factor (Shonmeyr *et al*, 2010)	- VEGFA inhibits BMP2 mRNA expression (Shonmeyr *et al*, 2010).

VEGFB	- Growth factor (Fischer *et al*, 2008)	- Anti-VEGFB inhibits arthritis (Fischer *et al*, 2008).
WNT5A	- Glycoprotein (Khosla *et al*, 2008)	- Wnt5a promotes osteogenesis in adult MSCs (Marie & Fromigue, 2006).

Table A9.4. List of antibodies.

PRODUCT	COMPANY	CAT# NO
1° Antibodies		
Anti-hα-sarcomeric actin Ms monoclonal IgM Clone 5C5	Sigma-Aldrich	A2172
Anti-hdesmin Ms monoclonal IgG_1 Clone D33	DAKO	M0760
Anti-hCD56 Ms monoclonal IgG_1 Clone 123C3	Santa Cruz	Sc-7326
hStro-1 Ms monoclonal IgM Clone Stro-1	R&D Systems	MAB1038
2° Antibodies		
Cy3 conjugated Goat Anti-Ms IgM specific	Jackson ImmunoResearch Laboratories, Inc	115-165-075
FITC-conjugated Goat Anti-Ms IgG specific	Jackson ImmunoResearch Laboratories, Inc	115-095-164
AlexaFluor conjugated Goat Anti-Ms IgG specific	Invitrogen	A11001
R-PE-conjugated Goat Anti-Mouse IgM specific	Jackson ImmunoResearch Laboratories, Inc	115-116-075

Table A9.5. List of assays or kits.

PRODUCT	COMPANY	CAT# NO
Annexin V-FITC Apoptosis Detection kit	Sigma-Aldrich	APOAF
FAST ™ p-Nitrophenyl Phosphate Tablets	Sigma-Aldrich	N1891
High capacity cDNA Reverse Transcription kit	Applied Biosystems	4368813

Table A9.6. List of reagents or chemicals.

PRODUCT	COMPANY	CAT# NO
β-glycerophosphate	Calbiochem	35675
α-MEM	GIBCO	22571
Accutase	Sigma-Aldrich	A6964
Alamar Blue	AbD Serotec	BUF012B
Alizarin Red S	Sigma-Aldrich	A5533
Cetylpyridium Chloride	Sigma-Aldrich	C0732
Chloroform-isoamyl alcohol mixture, -- DNase, RNase free	Fluka	25668
DAPI	Sigma-Aldrich	D9542
Dex	Sigma-Aldrich	D2915
Direct Red 80	Fluka	43665
DMEM-high glucose	PAA	E15-843
DMEM-low glucose	PAA	E15-806
Ethanol -DNAse, RNase free	Sigma-Aldrich	51976

Fast Red Violet LB Salt	Sigma-Aldrich	F3381
FBS	GIBCO/PAA	10270/ A15-151
Fn, from bovine plasma	Sigma-Aldrich	F4759
Gel	Sigma-Aldrich	G1393
Glycogen, DNase & RNase free	Invitrogen	10814-10
HCl	BDH Laboratory Supplies	20252.420
Indomethacin	Sigma-Aldrich	I7378
Insulin-like Growth Factor-1(E3R)	Sigma-Aldrich	I2656
Iso-propyl alcohol -DNase RNAse free	Acros Organics	327270010
L-ascorbic acid 2-phosphate	Sigma-Aldrich	A8960
Magnesium Chloride	Sigma-Aldrich	M-8266
Methanol	BDH Laboratory Supplies	10252
Methyl-Thiazolyl Blue Tetrazolium Bromide	Sigma-Aldrich	M5655
N,N-DMF	Sigma-Aldrich	D4551
NaCl	BDH Laboratory Supplies	10241AP
NaN_3	Sigma-Aldrich	71289
NaOH	BDH Laboratory Supplies	10252
Naphtanol	Sigma-Aldrich	N5000
Paraformaldehyde	Sigma-Aldrich	158127
PBS - Ca 2^+ & $Mg2^+$ free	PAA	H15-002

PBS tablets	Sigma-Aldrich	D4551
Penicillin/Streptomycin	PAA	P11-010
SDS solution (20%)	Fluka	05030
Sodium phosphate	Sigma-Aldrich	342483
TaqMan Universal PCR Master Mix	Applied Biosystems	4364340
Ti	Straumann	N/A
Triton-X	Sigma-Aldrich	101586B
TRIZOL®Reagent	Invitrogen	15596-018
Trypsin	PAA	L11-004
Water -RNAase/DNAse free	5 Prime	2900136

A9.1.7 APPARTUS AND SOFTWARE

Table A9.7. List of apparatus.

APPARATUS	MODEL	COMPANY
Confocal microscopy	Radiance 2100	Bio-Rad
CoolSnap-Pro camera	Roper Scientific Photometrics	MediaCybernetic
Flow cytometry	FACScanTM	Becton Dickinson
Fluoroscan	Ascent	Labsystems
Fluorescent microscope	Leica FW4000	Leica
Bright field microscope	Olympus BX50	MediaCybernetic
PCM	Olympus CK	MediaCybernetic
pH-meter	HI8520	Hanna Instruments
Plate reader	MRX-TC	Dynex Technologies
qPCR	ABI 7300 Real Time PCR machine in 96well format.	Applied Biosystems
Spectrophotometer	Ultrospec2000 UV/Visible	spectrophotometer, Pharmacia Biotech
Thermal cycler	PTC-100	Genetic Research Instrumentation Ltd
UV Sterilizer	2537å	Steristrom Coast-Air

Table A9.8. List of software.

SOFTWARE	FUNCTION
7300 System SDS Software	Run qPCR
Cell Quest	Run flow data
Flouroscan software	Measuring fluorescent
FWLeica 4300	Capture images
G*Power version 3.1	Sample size estimation
Image-Pro Plus 4.5, MediaCybernetic	Analysing images
Revelation	Measure absorbance
WinMDI 2.9	Analyse flow data